ACTIVATION OF INNATE IMMUNITY BY RIBONUCLEIC ACIDS

DISSERTATION

submitted to the Combined Faculties for the
Natural Sciences and for Mathematics
of the Ruprecht-Karls University of Heidelberg, Germany
for the degree of
Doctor of Natural Sciences

presented by
Dipl.-Biochem. Florian Eberle
born in Tübingen

DISSERTATION

submitted to the Combined Faculties for the
Natural Sciences and for Mathematics
of the Ruprecht-Karls University of Heidelberg, Germany
for the degree of
Doctor of Natural Sciences

presented by
Dipl. Biochem. Florian Eberle
born in Tübingen

Oral examination: …….

ACTIVATION OF INNATE IMMUNITY BY RIBONUCLEIC ACIDS

Referees: Prof. Dr. Ralf Bartenschlager

Prof. Dr. med. Alexander Dalpke

MEINEN ELTERN

List of abbreviations

APC	antigen presenting cell
APS	ammonium persulfate
Aqua dest	aqua destillata
β-gal/BG	β-galactosidase
BMDC	bone marrow-derived dendritic cell
bp	basepair(s)
Cardif	Caspase activation recruitment domain inducing IFN-β
CD	cluster of differentiation
cDNA	complementary DNA
CLR	C-type lectin receptor
c_t	threshold cycle
DAI	DNA-dependent activator of IFN-regulatory factors
DEPC	diethylpyrocarbonate
DC	dendritic cell
DMSO	dimethylsulfoxide
DNA	deoxyribonucleicacid
DNase	Deoxyribonuclease
dNTP	deoxynucleoside triphosphate
DOTAP	N-[1-(2,3-Dioleoyloxy)]-N,N,N-trimethylammonium propan methyl-sulfate
ds	double-stranded
DTT	dithiothreitol
E.coli	*Escherichia coli*
ECD	extracellular domain
EDTA	ethylene diamine tetraacetic acid
EGTA	ethylene glycol tetraacetic acid
EGFP	Enhanced green fluorescent protein
EIF2A	eukaryotic translation initiation factor 2A
ELISA	Enzyme-linked immunosorbent assay
FACS	Fluorescence activated cell sorting
FCS	Fetal calf serum
FITC	Fluoresceinisothiocyanat
FLT3L	FMS-like tyrosine kinase 3 ligand
fw	forward
GAPDH	Glycerinaldehyd-3-phosphate-dehydrogenase
GM-CSF	Granulocyte macrophage-colony stimulating factor

h	hour(s)
HCV	hepatitis C virus
HEK293	human embryonal kidney cells
Huh	human hepatocyte cell line
IFN	interferon
IL	interleukin
IPS-1	Interferon-β promoter stimulator 1
IRF	Interferon regulatory factor
ISG	interferon stimulated gene
ISRE	interferon stimulated response element
K_{50}	concentration required for half-maximal signalling
kDa	kilo-dalton
LB	Luria Bertani
LF	Lipofectamine
LGP2	Laboratory of genetics and physiology 2
LPS	Lipopolysaccharide
LRR	Leucine rich repeat
LTA	Lipoteichoic acid
MAPK	Mitogen-activated kinase
MAVS	Mitochondrial antiviral signalling
MDA5	Melanoma differentiation-associated gene 5
mDC	myeloid dendritic cell
min	Minute
mRNA	messenger RNA
MTT	3-(4,5-Dimethyl-2-thiazolyl)-2,5-diphenyl-2H-tetrazoliumbromide
MyD88	Myeloid differentiation primary response protein
NALP	NACHT-, LRR- and PYRIN-domain containing protein
n.d.	not detected
NFκB	Nuclear factor κB
NK cell	Natural killer cell
NLR	NOD (nucleotide-binding and oligomerization domain)-like receptor
n.t.	not tested
nt	nucleotide(s)
ODN	Oligodeoxynucleotide
PAGE	Polyacrylamide gel electrophoresis
PAMP	Pathogen-associated molecular pattern
PBMC	Peripheral blood mononuclear cell
PBS	Phosphate buffered saline

PCR	Polymerase chain reaction
pDC	plasmycytoid dendritic cell
PE	R-Phycoerythrin
Poly(C)	Polycytidylic acid
Poly(I)	Polyinosinic acid
Poly(IC)	Polyinosinic-polycytidylic acid
PRR	Pattern recognition receptor
PTO	Phosphothioate
PVDF	Polyvinylidene fluoride
qPCR	quantitative real time polymerase chain reaction
rE	relative expression
RIG-I	retinoic acid inducible gene I
RLR	RIG-I-like receptors
RNase	ribonuclease
rNTP	ribonucleoside triphosphate
rRNA	ribosomal RNA
RNA	ribonucleic acid
rpm	rotations per minute
rv	reverse
SDS	Sodiumdodecyl sulfate
SPF	specific pathogen free
ss	single-stranded
TEMED	Tetramethylethylendiamine
TIR	Toll/Interleukin 1 receptor
TLR	Toll-like receptor
TNF-α	Tumor necrosis factor-α
TRIF	TIr domain containing protein inducing IFN-β
U	Unit
v/v	volume per volume
VISA	virus induced signalling adaptor
w/v	weight per volume
WT	wild type

1 Summary

RNA provides a stimulus for innate immunity either by activating the endosomal Toll-like receptors (TLRs) 3, 7 and 8 or by triggering cytosolic RNA sensors of the RIG-I-like family (RLRs) or the NALP3-containing inflammasome. RNA recognition results in the secretion of type-I interferons or proinflammatory cytokines. Recognition of RNA is supposed to occur due to the presence of non-self structures, such as the abundance of nucleotide modifications, guanosine-uridine-rich sequences, double-stranded conformation or the presence of a terminal 5'-triphosphate. However, the exact structural requirements for RNA recognition are still largely unknown. Within this work the functional and structural interplay between RNA and different receptors within cells of the innate immune system was analyzed. In detail, bacterial RNA, synthetic siRNA and *in vitro* transcribed RNA was characterized.

It can be shown that TLR7 is the responsible receptor for the recognition of siRNA in plasmacytoid dendritic cells resulting in induction of type-I interferons which mediate unwanted off-target effects. Besides a minor sequence-dependent influence, introduction of nucleotide modifications identified the 2'-position of the ribose to be crucial for TLR7-mediated immunorecognition. Further, hyperchromicity assays and structure prediction give strong evidence that stimulating RNA adopts a duplex structure. These findings suggest that immunorecognition takes place within the minor groove of a given RNA duplex, thus revealing a possible mechanism of receptor ligand interaction. Confirming this notion, the introduction of different nucleotide modifications altering major groove recognition showed no effect on immunorecognition. Of note, incorporation of thymidine substitutions was demonstrated to reduce immunostimulation without any effect on gene knockdown. These results identify modifications that dissect unwanted immunostimulation from RNA interference in siRNA, thus paving the way for more precise therapeutic applications.

Next, the immunostimulatory potential of different prokaryotic RNAs was tested. It could be shown that recognition of bacterial RNA differs from all principles described so far. Whereas TLR7 mediated recognition in plasmacytoid dendritic cells and NALP3 was responsible for IL-1β secretion, prokaryotic RNA was shown to additionally trigger a cytosolic receptor system resulting in the activation of the transcription factor NFκB and interleukin-12p40 secretion. Using cells from various knockout mice and performing siRNA approaches, all described RNA receptors could be ruled out to be responsible for this activation. Immunostimulation by prokaryotic RNA thus mirrors findings previously described for cytosolic DNA recognition.

Finally, ligand specificity of RIG-I was investigated. It could be demonstrated that the 5'-triphosphate moiety is not the only target structure for RIG-I but that RNA in double-stranded conformation represents a second independent structural feature that activates RIG-I. The sensitivity of RIG-I to double-stranded RNA of increasing size was significantly enhanced, indicating that the biological role of RIG-I is rather the sensing of long dsRNA instead of recognizing the terminal 5'-end. Further, there is strong evidence that RIG-I might bind in a cooperative manner to double-stranded RNA structures explaining the significant length-dependency.

1 Zusammenfassung

RNA stellt über die Aktivierung der endosomalen Toll-like Rezeptoren (TLRs) 3, 7 und 8 sowie der zytosolischen RNA Sensoren aus der Familie der RIG-I-like Rezeptoren oder des NALP3 Inflammasoms einen Stimulus für das angeborene Immunsystem dar. Die Erkennung von RNA führt zur Sekretion von Typ-I Interferonen oder proinflammatorischen Zytokinen. Die Erkennung von RNA erfolgt dabei über das Vorhandensein von „Nicht-Selbst" Strukturen, wie Guanosin-Uridin-reiche Sequenzmotive, doppelsträngige Konformation, eine terminale 5'-Triposphatgruppe oder die Art und Häufigkeit von Nukleotidmodifikationen. Über die strukturellen Einzelheiten der RNA Erkennung ist aber nach wie vor wenig bekannt. In dieser Arbeit wurden die funktionellen und strukturellen Wechselwirkungen zwischen RNA und verschiedenen Rezeptoren im angeborenen Immunsystem genauer analysiert. Im Einzelnen wurden bakterielle RNA, synthetische siRNA und *in vitro* transkribierte RNA untersucht.

Es konnte gezeigt werden, dass TLR7 der Rezeptor für siRNA in plasmazytoiden dendritischen Zellen ist und dass siRNA über die TLR7 Stimulation zur Ausschüttung von Typ-I Interferonen führen kann, welche ungewollte Nebenwirkungen bei siRNA Applikationen bedingen. Neben einem geringen sequenzspezifischen Beitrag wurde durch die Einführung entsprechender Modifikationen die 2'-Position der Ribose als entscheidende Struktur für die Erkennung durch TLR7 identifiziert. Hyperchromizitätsanalysen und Strukturvorhersagen wiesen außerdem daraufhin, dass stimulative RNA Moleküle doppelsträngige Strukturen annehmen. Der Mechanismus der Erkennung von RNA durch TLR7 könnte damit über eine Interaktion des Rezeptors mit der kleinen Furche einer RNA Duplex erklärt werden. Unterstützend zu diesen Befunden zeigten Modifikationen der grossen Furche keinen Effekt auf die Immunstimulation. Des Weiteren wurde gezeigt, dass die Substitution von Uracil durch Thymidin die Immunstimulation durch siRNA deutlich reduzierte, während die gensuppressive Funktion unverändert blieb. Die Ergebnisse ermöglichen somit die Synthese von siRNA Molekülen, die eine gezielte Applikation ohne Immunaktivierung erlauben.

Als nächstes wurde die Immunstimulation durch prokaryotische RNA analysiert. Es konnte gezeigt werden, dass die Erkennung prokaryotischer RNA von den bisher beschriebenen RNA-Erkennungsmechanismen abweicht. Neben der Erkennung durch TLR7 in plasmazytoiden dendritischen Zellen und der NALP3-vermittelten Interleukin-1β Sekretion, aktivierte prokaryotische RNA zusätzlich ein zytosolisches Rezeptorsystem, das zur Aktivierung des Transkriptionsfaktors NFκB und zur Sekretion von Interleukin-12p40 führt. Durch Verwendung von knockout Mausmodellen sowie durch den Einsatz von siRNA konnten alle bisher beschriebenen RNA Rezeptoren ausgeschlossen werden. Die Erkennung prokaryotischer RNA zeigt damit Parallelen zu der kürzlich beschriebenen zytosolischen Erkennung von prokaryotischer DNA.

In einem dritten Teil der Arbeit wurde die Ligandenspezifität von RIG-I charakterisiert. Es konnte gezeigt werden, dass eine terminale 5'-Triphosphatgruppe nicht die einzige Erkennungsstruktur in viraler RNA darstellt, sondern dass auch die Dopplestrangkonformation von RNA als unabhängiger Stimulus für RIG-I fungiert. Die Sensitivität von RIG-I stieg dabei signifikant mit der Länge des doppelsträngigen RNA Liganden an. Dies deutet daraufhin, dass die biologische Funktion von RIG-I vielmehr die Erkennung doppelsträngiger Strukturen als die Erkennung der 5'-Triphosphatgruppe ist. Zudem weist die stark längenabhängige Erkennung auf eine kooperative Bindung von RIG-I an Doppelstrangstrukturen hin.

2 Introduction

The physiological function of the immune system is defence against infectious microbes. Therefore, it has to detect a wide variety of pathogens, ranging from bacteria to viruses. Common concepts in immunology imply that a very important feature of the immune system is to distinguish between self and non-self structures. In general the immune system can be divided into innate and adaptive immunity. Innate immunity represents the first line of defence and consists of cellular and humoral defence mechanisms that are in place even before infection. It further activates adaptive immunity. In contrast to the innate immune system, adaptive immunity relies on the clonal selection of lymphocytes with recombined highly affine receptors as postulated by Burnet. This second response is more specific and adapts to an infection, which leads to an increase in defence capabilities with every further exposure to the same infectious pathogen.

2.1 Innate immunity

Innate immunity represents the phylogenetically oldest way of defence and can be found in all classes of animals and plants. The major function of the innate immune system is the initial response to microbes which prevents infection and often results in elimination before adaptive immunity develops. This response is of generic and rather non-specific manner and does not provide long-lasting or protective immunity to the host. The epithelium serves as a physical barrier to invading microbes and also secrets soluble cytokines and antimicrobial peptides like defensins. The cellular fraction of the innate immune system is composed of circulating cells like neutrophils and natural killer cells that recognize microbes that have breached the epithelial barrier and entered host tissues and circulation. Upon recognition of microbes, secretion of cytokines and chemokines leads to the recruitment of further immune cells. Cells of the innate immune system combat infections by phagocytic destruction and secreted antimicrobial factors. Moreover, macrophages and dendritic cells are able to present detected microbial components on their surface, thereby activating the adaptive immune system. The latter cells have an important interface function bridging innate and adaptive immunity.

2.2 Recognition principles within the innate immune system

Conserved microbial components, termed pathogen associated molecular patterns (PAMPs) act as ligands for the innate immune system[1]. These patterns represent molecules vital for microbial survival which therefore are unlikely to mutate during evolution. Moreover, PAMPs represent molecules that share common building principles but differ in detected structural elements. PAMPs are detected by pattern recognition receptors (PRRs) which are present in the cytosol or on the surface of cells like macrophages and dendritic cells. In contrast to the receptors of adaptive immunity which undergo somatic recombination, PRRs are germline encoded and can detect only a limited number of different molecular structures. The concept that PRR-mediated detection is restricted to non-self structures[2,3] had to be expanded since it became evident that PRRs are also able to detect host structures under certain conditions[4]. Thus, it has been shown that rather the localization of the ligand (e.g. cytosol) is of importance for receptor interaction.

2.2.1 Pattern recognition receptors

PRRs are either attached to the surface, localized in intracellular compartments (e.g. endosomes) or present in the cytosol. Due to their molecular structure they can be subdivided into Toll-like receptors (TLRs), Retinoic acid inducible gene-I (RIG-I)-like receptors (RLRs) and NOD (nucleotide-binding and oligomerization domain)-like receptors (NLRs)[5-8]. Further proteins with C-type lectin-binding domains (CLRs) have various functions but also serve as pattern recognition receptors in innate immunity[9]. All of these receptors are composed of modular domain architecture with a ligand binding domain and signalling domains, the latter being regulated either through dimerization and oligomerization or conformational changes by enzymatic activities. Subsequently, singalling domains recruit adaptor proteins that initiate intracellular signalling (e.g. NFκB or IRF3 activation).

2.2.1.1 Toll-like receptors

The Toll protein was first described to play a pivotal role in the development and axis formation of *Drosophila melanogaster*[10]. However it was demonstrated that loss-of-function mutations within the Toll protein result in a higher susceptibility of *Drosophila melanogaster* to fungal infections, indicating a second function, namely as an immune receptor for sensing infections with fungi and gram-positive bacteria[11,12]. The TLRs represent the human homologs to the Toll protein. They are either expressed on the cell surface (TLR 1, 2, 4, 5, 6 and 10) or in intracellular compartments, namely endosomes (TLR 3, 7, 8 and 9)[13-16]. TLRs represent the best-described class of PRRs[17]. To date, in human 10 TLRs (TLR1-10) and in mouse 12 TLRs (TLR1-9 and 11-13) have been described. They consist of a leucine-rich repeat-containing extracellular domain (ECD) which mediates ligand binding, a transmenbrane domain connecting the ECD to the cytoplasmic Toll/interleukin-1 receptor (TIR) domain required for the initiation of intracellular signalling[18]. The proximal events of TLR-mediated signalling are initiated by TIR-domain-containing adaptor molecules. The endosomally located TLR7, 8 and 9 utilize the myeloid differentiation primary response protein 88 (MyD88), TLR3 the TIR domain-containing adaptor inducing IFN-β (TRIF) (also known as TICAM1) as proximal adaptor molecules[19,20]. TLR-mediated MyD88 recruitment activates a conserved inflammatory pathway resulting in the activation of mitogen-activated protein (MAP)-kinases and translocalization of NFκB into the nucleus[21-23]. TLR3 signalling by means of TRIF activates IRF3 in a MyD88-independent manner. Plasmacytoid dendritic cells (pDCs) represent a subset of immune cells that is specialized on the detection of viruses and which is responsible for the exclusive secretion of IFN-α in the peripheral blood[24]. Importantly, pDCs express TLR7 and TLR9 and produce large amounts of type-I interferons upon stimulation with the corresponding ligands what contrasts findings in other cell-types[25,26]. In pDCs both, TLR7 and 9, signal via the adaptor molecule MyD88 and activate the constitutively expressed transcription factor IRF7 linking MyD88-dependent signalling to IRF7 activation and subsequent IFN-α induction in this cell-type[24,27]. As shown for CpG deoxynucleotides which are recognized by TLR9, TLR-mediated recognition in pDCs is enhanced by an increased endosomal trafficking compared to myeloid dendritic cells (mDCs)[28].

2.2.1.2 Cytoplasmic receptors

Whereas TLRs detect ligands in specific cells such as dendritic cells and macrophages, RLRs and NLRs reside in the cytosol and are expressed in a broad range of somatic cells. The RLR family is composed of the three members retinoic acid inducible gene-I (RIG-I), melanoma-differentiation-associated gene 5 (MDA5) and laboratory of physiology and genetics 2 (LGP2) which were originally described as RNA helicases[29]. Besides this function it has been shown that RIG-I and MDA5 recognize viral components and are able to initiate an immune response[30-33]. The amino termini of RIG-I and MDA5 contain two regions similar to the caspase activation and recruitment domain (CARD) and acts as a protein interaction motif to facilitate associations with downstream components. LGP2 does not harbor this amino-terminal domain and has therefore been reported to be a negative regulator for RLR-mediated signalling by ligand sequestration[34-36], especially important for RIG-I-mediated signalling[37,38]. The central portion of all three family members shows homologies with the DexD/H box RNA helicase family and is implicated in double-stranded RNA binding and ATP-dependent unwinding[39]. The carboxy-terminus harbors a regulatory or repression domain that interacts with the helicase domain and inhibits signalling by the amino-terminal CARDs[6,29,37]. RLRs are thought to undergo a conformational change upon ligand binding which exposes the CARDs and allows multimerization and cell signalling[37]. Signalling initiation is mediated by the adaptor molecule IPS-1 (also known as MAVS, VISA or CARDIF)[40-43]. The IPS-1 molecule is attached with the carboxy-terminus to the mitochondrial membrane[41]. At its amino-terminus IPS-1 also contains a CARD, which is recognized by the activated RIG-I and MDA5 proteins. CARD interactions lead to the activation of cytoplasmic kinase complexes and finally to the phosphorylation-mediated activation of IRF-3 and NFκB, respectively[44].

With 23 members NLRs represent the largest family of PRRs in humans[45]. NLRs also show a tripartite domain structure that shares high structural and functional similarities to plant resistance genes (R-genes)[8,46,47]. All NLRs harbor a central NACHT domain which is responsible for oligomerization and activation of the respective NLR. The phylogenetic history of the respective NACHT domains is used for classification of the 23 NLRs[8]. The NLRs are further grouped in NODs and NALPs (also known as PANs or PYPAFs)[8,47,48]. NODs mediate signalling by an amino-terminal CARD which activates NFκB in a similar way to TLRs and RLRs[7,46,49] but shows no influence on caspase activation[50,51]. NALPs on the other hand, possess an amino-terminal pyrin (PYR) effector domain and have been shown to activate caspase-1 and caspase-5. The carboxy-terminus of all NLRs owns an LRR domain which is, similar to TLRs, responsible for ligand binding[8]. Like RLRs, NALPs reside in the cytosol in an inactive and repressed form. Ligand binding promotes a conformational change which leads to oligomerization and activation[52]. Upon activation, NALPs form multimeric protein complexes which are termed inflammasomes[52-54]. Besides NALP3 the inflammasome consists of the apoptosis-associated speck-like protein (ASC), Cardinal, NALP2 and pro-caspase-1[55]. ASC represents an essential adaptor molecule for inflammasome signalling[53,54]. ASC acts by PYR-PYR domain interaction with the respective NALP and subsequently activates pro-caspase-1 leading to the processing of pro-IL-1β and pro-IL-18[56,57]. Although most of the ligands are unknown so far, NLRs are regarded as sensors for intracellular PAMPs in general. Mutations and polymorphisms of NLR genes are associated with a higher susceptibility to inflammatory disorders (e.g. Muckle-Wells syndrome),

underlining the importance of this receptor class for proper immune function[58-61]. Additionally, NALP3 mutations can lead to the excessive secretion of IL-1β and induce necrosis-like death in monocytes by a process dependent on ASC[62].

2.2.2 Cooperative recognition in innate immunity

Although the different receptor classes trigger conserved inflammatory pathways, there is strong evidence that PRRs rather complement each other than functioning apart from each other[63]. NALP-mediated IL-1β and IL-18 secretion requires induction of pro-IL-1β and pro-IL-18, which is induced by stimulation of TLRs[52,64-66]. TLRs therefore serve as key inducers for inflammasome activation[67]. On the other hand, processed IL-1β and IL-18 recruit MyD88 upon binding to their respective receptors, linking cytosolic pathogen sensing to TLR signalling pathways. Further, ASC also activates NFκB besides the activation of caspase-1 and caspase-5[68] leading to the secretion of proinflammatory cytokines, similar to TLR-mediated signalling. PAMP-mediated IL-1β and IL-18 secretion therefore requires the coordination of the TLR and NLR receptor systems. It has also been shown that adenoviral DNA triggers type-I interferons but also induces the secretion of IL-1β in a NALP3 and ASC-dependent manner[69], linking NLRs to the cytosolic virus recognition which is mainly mediated by RLRs. Additionally, the simultaneous triggering of TLRs and NLRs shows rather synergistic than additive effects on cytokine secretion indicating cooperation of the different signalling pathways[70]. PAMP recognition gains additional complexity by cell-type-specific expression of different sets of PRRs. Virus protection is mediated by the cytosolic residing RLRs as shown in conventional DCs and fibroblasts[34,71]. In contrast, virus recognition in plasmacytoid dendritic cells (pDCs) is mediated exclusively by the TLR system instead of the RLRs[71]. Therefore, TLRs and RLRs, similar to TLRs and NLRs, function cooperatively to provide ubiquitous immune protection.

2.3 Ligands of pattern recognition receptors

The broad classes of pathogens (e.g. bacteria, viruses and fungi) express molecules that are shared across subclasses of pathogens but are ‘foreign’ to the host organism. Most recognized molecular structures are expressed on the pathogen’s surface such as lipoteichoic acids which are part of gram-positive bacterial cell walls and lipopolysaccharides (LPS) of gram-negative bacterial cell walls which are sensed by the surface expressed TLR2 and 4, respectively[72-75]. Besides ‘non-self’ structures innate immunity is triggered also by viral structures although all their components are derived from the infected host cell and therefore do not represent ‘foreign’ structures. In addition, it becomes evident that even endogenous molecules represent triggers for immunorecognition if their intracellular distribution is altered due to infectious or inflammatory processes[76,77].

2.3.1 Nucleic acids: pathogen associated molecular patterns

Besides surface located PAMPs, endogenous molecular structures such as bacterial- or viral-derived nucleic acids are recognized by innate immunity. First, unmethylated CpG-rich DNA as it occurs in bacteria and is rare in eukaryotic DNA due to extensive cytosine-methylation of CpG dinucleotides has been shown to trigger the endosomally located TLR9[78]. The frequency of CpG dinucleotides within bacterial DNA correlates thereby with the potential to stimulate TLR9[79]. This reveals a sequence-

specific recognition by TLR9. Further, non-self DNA is also capable of triggering cytosolic receptors like the inflammasome or the recently discovered DNA sensor DNA-dependent activator of IFN-regulatory factors (DAI)[69,80]. Besides DNA, it has been shown that also RNA displays a target for immunorecognition principles[81]. Figure 1-1 provides a schematic overview of the major RNA recognition pathways leading to the transcription of proinflammatory cytokines or type-I interferons.

2.3.2 Recognition of RNA

2.3.2.1 RNA recognition by TLR7/8

The recognition of RNA-oligonucleotides has been shown by several groups to be mediated by TLR7 and TLR8 in human and by TLR7 in mouse[81]. Murine TLR8 has been regarded to be non-functional in mice although recent reports show that the receptor can be triggered by cotransfection with dT-deoxynucleotides[82]. RNA recognition by TLR7 and 8 is dependent on the size of the respective RNA oligonucleotide and it has been shown that a minimum of 19 nucleotides is required for an efficient recognition[83]. TLR7 and TLR8 are exclusively expressed in endosomal compartments, therefore the differentiation between endogenous and non-self RNA molecules has been linked to the localization of the respective ligands within the cell. Endogenous RNA molecules (e.g. messenger RNA) reside either in the cytosol or in the nucleus and do not enter compartments like endosomes that participate in the uptake of exogenous substances. Inhibitors of endosomal maturation or acidification (e.g. chloroquine) have been shown to abrogate TLR7 and TLR8-mediated signalling, indicating that these receptors require an intact endosomal compartment for functionality[84]. Sequence analysis revealed several possible immunostimulatory sequences, characterized by a high content of guanosine (G) and uridine (U) residues, to play a role for recognition. Several studies were performed to identify a specific sequence motif which triggers these receptors[83-86]. All studies revealed that the content of uridine residues seems to play an important role for the signalling strength[86]. The two GU-rich sequence motifs 5'-GUCCUUCAA-3' and 5'-UGUGU-3' have been identified to possess a high potential for immunorecognition[83,85]. Differences in the responsivness of TLR7 and TLR8 to the synthetic ligands resiquimod (R848) and imiquimod (R837) revealed different ligand requirements for these two receptors[87]. Further characterization of immunostimulatory sequences of RNA oligonucleotides showed that TLR7 and TLR8 indeed recognize different sequence motifs although sharing a high homology in sequence and structure. In contrast to the recognition of GU-motifs by TLR7, TLR8 has been shown to detect AU-rich sequence motifs[88]. However, unlike DNA recognition by TLR9, the recognition of a specific sequence seems not sufficient to explain immunorecognition. Transfection with eukaryotic RNA containing high amounts of uridine residues and GU-dinucleotides resulted in a significant lower cytokine secretion compared to synthetic RNA oligonucleotides. TLR7 and 8-mediated recognition has therefore additionally been linked to the frequency of nucleotide modifications[89,90]. Some nucleotide modifications (e.g. 2'-*O*-methyl-modification) which naturally occur only in eukaryotes but are absent or show a comparatively low frequency in prokaryotes limit the extent of cytokine secretion, whereas other modifications seem to play a minor role for recognition (e.g. 5'-methyl-cytosine)[89]. Studying various modification patterns it was shown that the 2'-position of the ribose is critical for immunorecognition principles. Methylation or addition of other chemical modifications (e.g. fluoride-addition) led to an abrogation of cytokine secretion in general[91-93]. TLR7

and 8-mediated recognition was not restricted to RNA oligonucleotides but also occured with viral RNA[94]. Bacterial RNA has also been linked to recognition by TLR7 and TLR8 due to its lower content of nucleotide modifications[89]. Small interfering RNA (siRNA) is composed of a double-stranded RNA molecule with a length of approximately 21-23 basepairs to avoid non-specific effects on the cellular protein metabolism that arise from inducing the double-stranded RNA (dsRNA)-dependent protein kinase (PKR)[95]. However, siRNA has now been discussed as a target structure for TLR-mediated recognition. Although siRNA recognition was initially discussed controversially[96], it is now clear that synthetic siRNA duplexes induce the upregulation on IFN-stimulated genes[97-99], potentially leading to severe side effects. Harboring stimulatory sequences or immunological relevant nucleotide modifications corresponds with immunostimulation in a similar way as described for single-stranded RNA oligonucleotides. In most cases immunostimulatory motifs are more effectively recognized by innate immunity in the context of single-stranded conformation compared to duplex-structures[100]. Therefore, it is not clear whether siRNA is recognized in a single- or double-stranded conformation. However, the intracellular integrity of siRNA has been shown to be not affected during cell access indicating that short double-stranded RNA is recognized in a double-stranded conformation[101]. The expression of TLR7 and TLR8 is restricted to professional immune cells linking their respective activation rather to the immune system than to a general response to RNA entry. Especially pDCs show strong expression levels of TLR7 and TLR9 and are known to produce vast amounts of type-I interferons upon viral infections[102]. Endosomal recognition in pDCs is increased by enhanced endosomal trafficking and longer presence in the endosomal compartments[28] indicating that mainly pDCs are responsible for TLR7-mediated type-I interferon secretion. Ligand receptor interactions have not been studied in detail for TLR7 and TLR8 so far, mainly due to a missing crystal structure. However, it has been shown that the amino-terminus of TLR9 is cleaved off for receptor activation and ligand recognition[103,104]. Due to the high homology between TLR7, 8 and 9, this has also been proposed for RNA sensing[103,105].

2.3.2.2 RNA recognition by TLR3

Besides the above described TLR7, 8 and 9, TLR3 is also expressed in the endosomal compartments of immune cells[13]. However, in some cell-types (e.g. fibroblasts) TLR3 is also expressed on the cell surface[106]. The expression pattern of TLR3 thus comprises a much broader range of cell-types compared to TLR7 and 8. Additionally TLR3 seems to play a role in immunorecognition of non-immune cells (e.g. keratinocytes)[107]. The first ligand structure described for TLR3 was long double-stranded RNA which was demonstrated by a high sensitivity to Poly(IC) representing a synthetic analog to double-stranded RNA leading to the activation of NFκB[108,109]. Long double-stranded RNAs are naturally absent in eukaryotic cells but viral RNA has been described to form long double-stranded RNA intermediates during the process of replication. Although the recognition of viral RNA by TLR3 has been discussed controversially[110-112], it is now clear that TLR3 participates in the recognition of at least some viral RNAs (e.g. west nile virus)[69,113]. Eukaryotic messenger RNA which tends to form of intermolecular duplex-structures has been described as a further target structure for TLR3 if entering the endosomal compartments as described for messenger RNA of necrotic or apoptotic cells[114]. The recognition of siRNA has been shown to depend on TLR7 and TLR8; however, a recent study showed that also TLR3 participates in siRNA recognition. Activation of TLR3 requires at least 19 nucleotides

long dsRNA for activation and shows no signalling by binding to shorter dsRNA molecules. A required minimum length of the RNA ligand and additional structure predictions gave strong evidence that TLR3 forms dimeric structures upon ligand binding which are essential for activation[115,116]. Further, CD14, a well described PRR in innate immunity, has been shown to enhance TLR3-mediated signalling[117]. The excessive glycosylation of TLR3 plays a pivotal role for ligand recognition. Deglycosylation studies and mutational approaches revealed the requirement of N-linked glycosylation for the bioactivity of TLR3[118].

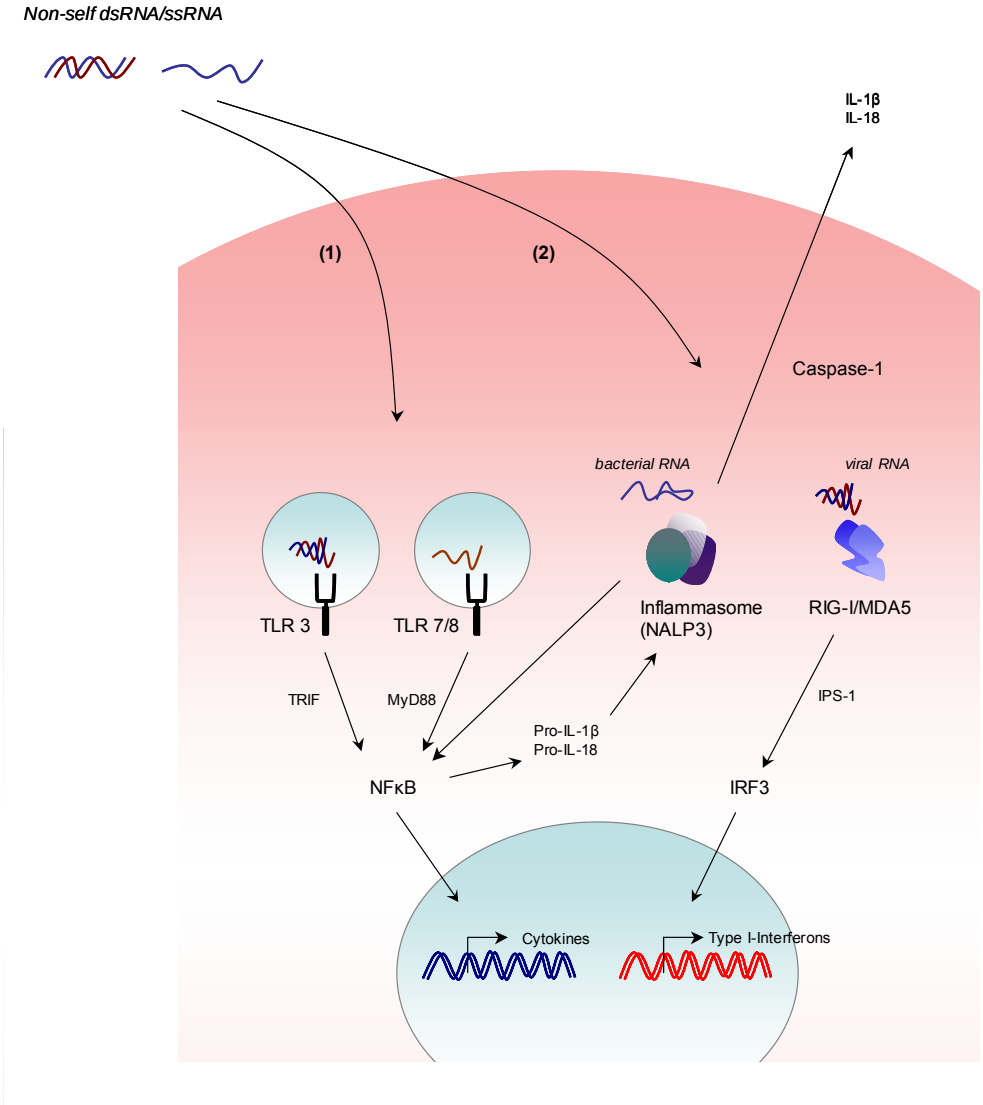

Fig. 2-1 Principles of cellular RNA recognition.
Simplified schematic representation of the major pathways leading to the expression of cytokines and type-I interferons upon stimulation with non-self RNA. For the sake of simplicity this illustration shows only the participating receptors and adaptor molecules, further NFkB activation by RIG-I and MDA5 and IRF3 activation by TRIF are omitted. **(1)** Endocytotic pathway: Double-stranded (dsRNA) and single-stranded RNA (ssRNA) are recognized by the endosomally located TLR3 and TLR7 and TLR8, respectively. Receptor binding leads to the recruitment of the TRIF and MyD88 adaptor molecules and finally to the activation of NFκB. NFκB induces both, the secretion of proinflammatory cytokines and the expression of pro-IL-1β and pro-IL-18. **(2)** Bacterial RNA binds to NALP3 which is a part of the inflammasome. Inflammasome activation leads to the processing of TLR-induced pro-IL-1β and pro-IL-18 by activated caspase-1 as well as to the activation of NFκB. Viral RNAs are recognized by RIG-I and MDA5, respectively, depending on the type of virus. Signalling is mediated by the mitochondrial-associated adaptor molecule IPS-1 leading to the activation of IRF3 and subsequent type-I interferon secretion.

In contrast to other TLRs, the strucure of the ECD of TLR3 has been resolved by crystallization[119,120]. The ECD shows a horseshoe-shaped overall structure composed of 23 LRRs motifs. LRR motifs have

been described firstly 1985 and are characterized by a 24 amino acid long sequence with conserved hydrophobic residues that tend to form β-sheets[121]. Within the regular LRR-structure also irregular LRRs (LRR12 and LRR20 in TLR3) have been identified that deviate in terms of length and sequence from the LRR-consensus sequence[122]. These LRRs are characterized by the presence of insertions after position 10 or 15 that do not fit in the overall LRR structure and are exposed from the receptor surface. The irregular LRR20 has been shown to be important for ligand binding whereas LRR12 is not essential for receptor signalling[123]. The recently published structure of TLR3 with bound double-stranded RNA ligand confirmed the findings described above[116].

2.3.2.3 RNA recognition by RLRs

Whereas TLRs detect viral components in specific cells such as dendritic cells and macrophages, RLRs sense viral infection in the cytoplasm of most cell-types. RLRs sense viral RNA and their activation results in immunological responses including the secretion of type-I interferons and proinflammatory cytokines[6,29,124]. A common feature of antiviral responses to dsRNA in general is the induction of type-I interferons[125]. Studies with knockout mice revealed that RIG-I and MDA5 detect specific types of viruses. Interestingly, RLRs induce an interferon response also in somatic cells (e.g. fibroblasts)[44,71,126]. MDA5 has been shown to be activated by picornaviruses whereas RIG-I senses many other viruses, including influenza A virus, Sendai virus, vesicular stomatitis virus and Japanese encephalitis virus[44]. This differential recognition is thought to be based on the distinct nonself RNA patterns generated by the respective viruses. The molecular mechanisms of the differential recognition are not fully understood by now, but several studies uncovered differences in the ligand requirement between RIG-I and MDA5. It was observed that RIG-I is selectively activated by transfection with *in vitro* transcribed RNA harboring a 5'-triphosphorylated terminus which is also present in various viral RNAs[127,128]. Once an RNA ligand contains such a terminal triphosphate, a double-stranded conformation of the RNA is not required anymore, identifiying the 5'-triphosphate as a target structure sufficient to activate RIG-I[128]. Although the requirement of a 5'-triphosphate for ssRNA recognition by RIG-I has been demonstrated for short *in vitro* transcripts (58 nt or shorter) as well as for single-stranded viral RNAs (e.g. influenza), the biological relevance of 5'-triphosphate recognition is not fully understood[127-129]. The 5'-end of endogenous (self) RNA is either removed or masked by the addition of a cap structure before leaving the nucleus and entering the cytosol. The accessible 5'-triphosphorylated terminus therefore represents a nonself structure which could indeed display a target for immunorecognition. MDA5 is not activated by triphosphorylated structures but has been shown to sense selectively Poly(IC)[44,130]. However, other reports showed that also RIG-I is activated by Poly(IC)[131]. Additionally the requirement of specific stimulatory sequences within viral RNA, analogous to TLR-mediated RNA recognition, has been suggested[132]. Further studies with time-dependent RNase treatment of Poly(IC) gave strong evidence that in fact the length of the respective dsRNA ligand is of importance for the differential recognition of RIG-I and MDA5. Using the respective knockout mice models it has been shown that MDA5 binds long dsRNA molecules with a length of approximately 2000 basepairs or longer whereas RIG-I senses shorter double-stranded RNA molecules up to a length of approximately 2000 basepairs[131]. These observations separate the ligand requirements of RIG-I and MDA5 giving each a distinct role in cytosolic viral RNA sensing. However, the molecular mechanism underlying the sensing of nucleotide length is unknown.

Further, it is not well understood how nonself double-stranded RNA is physically recognized since neither of these helicases contains a known RNA binding motif. Recent biochemical studies revealed that the carboxy-terminal domain (CTD) of RIG-I binds to 5'-triphosphorylated RNA whereas binding of double-stranded RNA by the CTD has been studied with discriminative results[129,130]. Crystallization of the CTD of RIG-I uncovered a basic cleft which shows a high affinity to 5'-triphosphorylated and double-stranded RNA[129]. Size exclusion chromatography and NMR-based ligand binding studies revealed that the CTD is responsible for ligand binding. These results were further supported by mutational approaches within the CTD identifying important amino acid residues to be essential for RIG-I signalling. As predicted from its primary structure, RIG-I is a ligand-dependent ATPase[129,130,133]. Mutation of the ATP-binding site (K270A) inactivates the ability of RIG-I to trigger antiviral signalling[6,133]. However, RIG-I K270A was still able to bind 5'-triphosphorylated and dsRNA. *In vitro* helicase assays revealed that RIG-I is able to unwind efficiently either dsRNA or RNA/DNA duplexes but not dsDNA. For duplex unwinding, a 3'-terminal single-stranded overhang is required[129]. Interestingly, blunt-ended dsRNA, which therefore is resistant to helicase activity, efficiently induced type-I interferons. On the other hand, dsRNA harboring a 3'-terminal overhang (>5nt), which are susceptible to being unwound, failed to activate interferon associated genes[134]. These observations indicate that unwinding of the dsRNA ligand is not the critical step for triggering an immune response. This raises questions about the role of ATP hydrolysis for RIG-I activation. To date, the current opinion is that the RNA ligand binds to the CTD and ATPase activity results in a switch of this precomplex into its active conformation. This idea is further supported by the identification of a repressor domain overlapping with the CTD of RIG-I which is able to interact with the CARD and helicase domain of RIG-I and thereby keeping RIG-I in an inactive status[37]. In addition it has been shown that RIG-I and LGP2 form dimers and multimers upon activation, similar to reported dimerization of TLR3 upon ligand binding[36,116,130]. Although the CTD of MDA5 shares high homology to the extensively studied CTDs of RIG-I and LGP2, molecular differences responsible for the different ligand requirements have not been investigated yet.

2.3.2.4 RNA recognition by NALP3

Among the 14 described NALPs, NALP3 has been identified as a further cytosolic RNA sensor. NALP3 binds bacterial RNA and promotes the processing of pro-IL-1β and pro-IL-18 by caspase-1 activation[8,55,64,135]. Importantly, inflammasome activation by bacterial RNA requires priming with a TLR-specific stimulus. In contrast to the already described TLRs and RLRs, the ligand spectrum of NLRs is more ambiguous. This is demonstrated by the fact that NALP3 is additionally activated by bacterial toxins and uric acid[65,66]. Compared to TLRs and RLRs, RNA recognition by NALP3 follows different mechanisms since neither viral RNA nor RNA oligonucleotides have been described as ligands for NALP3. Intracellular bacteria (e.g. *Francisella tularensis*) have been reported to activate the inflammasome in a manner dependent on type-I interferon signalling[136]. Similar findings have been made for bacterial DNA which is sensed in a CpG-dependent manner by TLR9 in the endosome. However, independent of a specific sequence, bacterial DNA also triggers a cytosolic receptor[78,137]. Additionally silica crystal-induced lysosomal damage induces inflammasome activation by the release of self-components, restricted in healthy cells to the endosome (e.g. cathepsins) indicating that the ligands for NALP3 might include host-derived structures[76]. To date, the molecular mechanism of

NALP3-mediated ligand recognition is not fully understood but it is evident that the role of NALP3 is the sensing of ligands within the cytosol leading to a proinflammatory response. Table 2-1 summarizes the RNA receptors described above, their respective ligands and the responsible target structures.

Table 2-1 Overview of cellular RNA receptors and their respective ligands

Receptor	Described ligands	Target structure	Activation
TLR3	dsRNA, Poly(IC)	Double-strandness	NFκB, IRF3
TLR7	ssRNA, siRNA, R837, R848	GU-rich RNA sequences	NFκB, (IRF7 in pDCs)
TLR8	ssRNA, siRNA, R848	AU-rich RNA sequences	NFκB
RIG-I	Viral RNA, Poly(IC)	Double-strandness (up to 2 kbp in length), 5'-triphosphate	NFκB, IRF3
MDA5	Viral RNA, Poly(IC)	Double-strandness (longer than 2 kbp)	NFκB, IRF3
NALP3	Bacterial RNA	unknown	NFκB, Caspase-1

2.4 RNA interference

RNA interference (RNAi) is a pathway involved in cellular defence against viral invasion, transposon expansion, and post-transcriptional regulation[138-140]. This evolutionarily conserved phenomenon is observed in nearly all eukaryotes and represents a unique form of post-transcriptional gene silencing. The original phenotypic observations of RNAi were made by researchers working on plant and fungal genetics[141]. However, major strides in the underlying mechanisms of RNAi were performed by Andrew Fire, Craig Mellow and colleagues working with *Caenorhabditis elegans*[142]. They observed that injection of double-stranded RNA (dsRNA) induced sequence-specific reduction of messenger RNA with complementary sequence to the injected dsRNA. In further studies the RNAi pathway was also described for mammalian cells[143,144]. Since these observations, several groups have contributed to elucidating the RNAi pathway, depicted in Figure 1-2.

In nature, RNAi is initiated when the host cell encounters a long dsRNA transcribed from a virus, mobilized transposons or an inappropriately transcribed sequence. Additionally, a newly identified class of regulatory, non-coding microRNAs (miRNAs) induce RNA interference[145,146]. The miRNAs are synthesized in the nucleus as large precursor forms. An enzyme known as Drosha mediates processing of the primary miRNA transcripts into pre-miRNAs which size approximately 70 nt[147]. After being exported to the cytoplasm, the RNase III-like enzyme DICER is responsible for cleavage of the pre-miRNA into small interfering RNA duplexes (siRNA) of 19-25 bp in length with characteristic 3'-dinucleotide overhangs[148-150]. The siRNA is incorporated into the RNA-induced silencing complex (RISC). An RISC-associated helicase activity unwinds the duplex, thus enabling either of the two strands to independently guide target mRNA recognition[151,152]. The degree of complementarity between the guide strand and the target mRNA determines whether mRNA silencing is achieved by siRNA-mediated specific cleavage of the mRNA[153] or is mediated by translational repression[154,155]

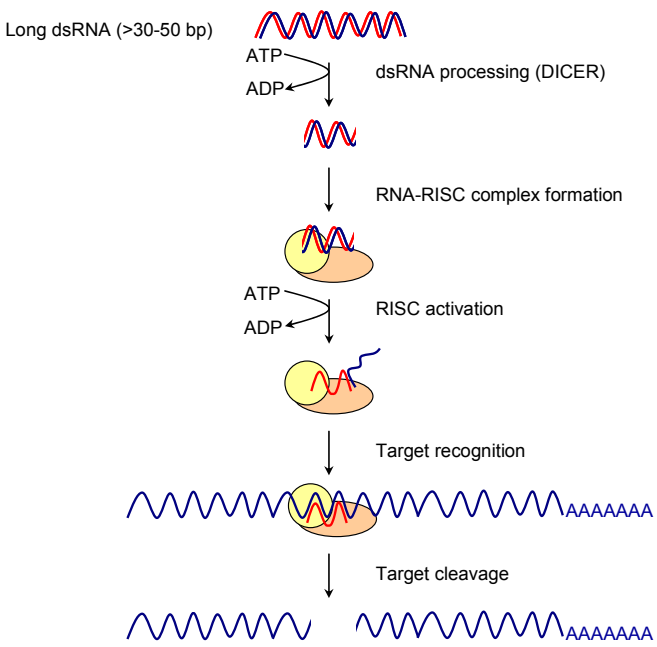

Fig. 2-2 The RNAi pathway
The pathway is triggered by dsRNA which share a sequence-specific homology with an mRNA. The dsRNA molecule is cleaved by the RNase III-like enzyme DICER resulting in the generation of 21-25 nt long siRNA duplexes. The siRNAs are incorporated into RISC. RISC is activated by ATP and probes the target mRNA for complementary sequences. Upon recognition RISC mediates mRNA cleavage and subsequently gene silencing.

2.4.1 Small interfering RNA as molecular tool for gene-suppression

While RNAi was commonly used for functional gene studies in plants, *Caenorhabditis elegans* and *Drosophila melanogaster*, attempts to induce RNAi in mammalian cell lines using long dsRNA had only limited success[156,157]. This was due to the induction of an interferon response which resulted in a general inhibition of protein synthesis and eventual cell death[158,159]. It was shown that long dsRNA activates 2'-5'-oligoadenylate synthetase (OAS1) which induces sequence-independent RNA degradation by activating RNaseL[159]. The dsRNA-dependent protein kinase (PKR) is also involved in dsRNA sensing. PKR phosphorylates the eukaryotic translation initiation factor EIF2A upon activation by long dsRNA leading to translational repression. Further, PKR was shown to activate NFκB[160].

Tuschl's group was the first to demonstrate that short synthetic duplexes mimicking natural 19-25 nt siRNAs could be introduced into mammalian cells eliciting sequence-specific mRNA degradation. The new concept in their work was the observation that these 21mer siRNA molecules were short enough to bypass PKR- and OAS-mediated recognition and therefore did not lead to the general shutdown of protein synthesis[149,161]. Additional studies showed that the silencing effect is relatively stable, persisting through several cell divisions and up to 10 days in mammalian cells. Due to higher efficiency of siRNAs compared to traditional methods like antisense oligonucleotides or ribozymes[162-164] and the ease of usage, siRNA applications have rapidly become a standard technique in life sciences. Furthermore, siRNAs hold the potential for therapeutic gene inhibition in various diseases[165,166].

2.5 Objectives of this work

As outlined in the chapters above, RNA represents a ligand for various immunorecognition principles. TLRs as well as cytoplasmic receptors have been described to be triggered by RNA molecules, which harbor different features that are recognized as non-self structures. Although some receptor ligand interactions could be identified already, essential parts of RNA immunorecognition remain unclear so far. This study aimed to characterize the interaction of different RNA ligands with the respective immunoreceptors.

The first part of the work should be the design of siRNA molecules which avoid the activation of innate immunity. The immunostimulatory portential of siRNA was to be assessed by measuring the induction of IFN-α in human PBMCs. In parallel RNAi efficiency should be determined by gene-suppression of different reporter genes in HEK293T cells. Focus should be laid on possible immunostimulatory sequences as well as the influence of nucleotide modifications. Moreover, the formation of intra- and intermolecular structures and their contribution to immunorecognition, as already described for DNA immunorecognition principles, should be investigated.

In a second part, immunorecognition of prokaryotic RNA should be analyzed. Therefore it should be assessed whether bacterial RNA stimulates innate immunity. Furthermore, responsiveness to bacterial RNA should be examined in different cells. Differences in the immunostimulatory potential of RNA purified from different bacterial species should be investigated. It was intended to identify structures which are responsible for the recogniton by the immune system, paralleling recognition principles for bacterial DNA.

Finally, using different *in vitro* tanscribed RNA ligands as analogs for viral RNA the precise ligand specificity of the cytosolic RNA sensor RIG-I should be examined. The influence of the terminal 5'-triphosphate as well as the presence of double-stranded conformation of the ligand on RIG-I-mediated signalling should be investigated. Single- or double-stranded-, *in vitro* transcribed RNA bearing either a 5'-triphosphate or not should be used for transfection of Huh7.5 cells overexpressing functional RIG-I and therefore being sensitive to RIG-I activation. Increasing the size of the RNA ligands should clarify the relevance of double-strand recognition compared to the recognition of the 5'-structure which in turn might help to elucidate differences to the homologous molecule MDA5.

Clarifying of these issues should help to advance the understanding of the immunorecognition of RNA and probably disclose the interplay of TLR and cytosolic receptor systems.

3 Materials and Methods

3.1 Materials

3.1.1 Chemicals and enzymes

3.1.1.1 Chemicals and reagents

If not stated otherwise, all solvents and chemicals were purchased from the following companies: Merck (Darmstadt) and Sigma-Aldrich (Taufkirchen) with a purity of "pro analysi". Specific reagents are listed in Table 3-1.

Table 3-1 List of essential materials and suppliers used in this study

32-[P]-GTP [10 µCi/µl]	Perkin Elmer, Walham, USA
Biocoll (1.09 g/ml)	Biochrom AG, Berlin
Coelenterazine	PJK, Kleinblittersdorf
DEPC	Sigma-Aldrich, Taufkirchen
DNA loading dye (6x)	MBI Fermentas, St. Leon-Rot
dNTPs	MBI Fermentas, St. Leon-Rot
DOTAP transfection reagent	Roth, Karlsruhe
Effectene transfection reagent	Qiagen, Hilden
EDTA	Sigma-Aldrich, Taufkirchen
EGTA	Sigma-Aldrich, Taufkirchen
FCS[a]	Biowest, Nuaillé, France
Lipofectamine™ 2000	Invitrogen, Karlsruhe
Luciferine	PJK, Kleinblittersdorf
S-LPS (*Salmonella minnesota*)	Ulrich Seydel, Forschungszentrum Borstel
Methylthiazoltetrazolium (MTT)	Sigma-Aldrich, Taufkirchen
Poly(C)	Sigma-Aldrich, Taufkirchen
Poly(I)	Sigma-Aldrich, Taufkirchen
Poly(IC)	Sigma-Aldrich, Taufkirchen
R837 (imiquimod)	Invivogen, Toulouse, France
R848 (resiquimod)	Invivogen, Toulouse, France
RiboLock™ RNase Inhibitor	MBI Fermentas, St. Leon-Rot
RNA loading dye (2x)	MBI Fermentas, St. Leon-Rot
rNTPs	MBI Fermentas, St. Leon-Rot

3.1.1.2 Enzymes

Enzymes used throughout this study are listed in Table 3-2.

Table 3-2 List of essential enzymes and suppliers used for this study

AccuTaq™ LA DNA Polymerase	Sigma-Aldrich, Taufkirchen
Agarase	MBI Fermentas, St. Leon-Rot
DNase I	MBI Fermentas, St. Leon-Rot
Lysozyme (chicken egg white)	Sigma-Aldrich, Taufkirchen
Lyticase (*Arthrobacter luteus*)	Sigma-Aldrich, Taufkirchen
Restriction endonucleases (div.)	MBI Fermentas, St. Leon-Rot
RNase A	Sigma-Aldrich, Taufkirchen
Shrimp Alkaline Phosphatase (SAP)	MBI Fermentas, St. Leon-Rot
T4 DNA Ligase	MBI Fermentas, St. Leon-Rot
T7 RNA polymerase	MBI Fermentas, St. Leon-Rot

[a] FCS batch number: S04224S1810, Endotoxin content: 0.2 EU/ml

3.1.2 Kits

Purchased kits used for this study are listed in Table 3-3.

Table 3-3 List of purchased kits and suppliers

Absolute SYBR Green RoxMix	ABgene House, Epsom, UK
BD OptEIA™ Human ELISA Set (IL-8, IL-6, TNF-α)	BD Biosciences Pharmingen, Heidelberg
BD OptEIA™ Mouse ELISA Set (IL-12p40, IL-1β)	BD Biosciences Pharmingen, Heidelberg
Dual-Luciferase Reporter Assay System	Promega, Madison, USA
High Pure RNA Isolation Kit	Roche, Mannheim
JETSTAR / LFU Plasmid Mini/Maxiprep Kit	Genomed GmbH, Löhne
JETQUICK PCR Purification Spin Kit	Genomed GmbH, Löhne
JETQUICK Gel Extraction Spin Kit	Genomed GmbH, Löhne
Matched Antibodies (Module Set)(human IFN-α)	Bender MedSytems, Vienna, Austria
µMACS Streptavidin Kit	Miltenyi Biotech, Bergisch Gladbach
QIAxcelRNA control kit	Qiagen, Hilden
QuantiChrom™ ATPase/GTPase Assay Kit	Bioassay systems, Hayward, USA
Quant-iT RNA Assay Kit	Invitrogen, Karlsruhe
RevertAid™ First Strand cDNA Synthesis Kit	MBI Fermentas, St. Leon-Rot
RNeasy Mini/Maxi Kit	Qiagen, Hilden
One Shot™ Top Ten chemically competent *E.coli*	Invitrogen, Karlsruhe

3.1.3 Buffers and solutions

Selected buffers and solutions for cell culture, nucleic acid, protein and ELISA work are listed in Table 3-4, Table 3-5, Table 3-6 and Table 3-7, respectively.

3.1.3.1 Cell culture

Table 3-4 List of commonly used buffers and solutions

β-galactosidase lysis buffer	100 mM β-mercaptoethanol; 9 mM $MgCl_2$; 0.125% NP40; 0.15 mM CPRG
β-galactosidase stop solution	300 mM glycin; 15mM EDTA
Luciferase assay buffer phosphate	25 mM glycyl-glycin (pH 7.8); 15 mM potassium-buffer (pH 7.8); 15 mM magnesiumsulfate; 4 mM EGTA;1 mM DTT; 2 mM ATP
Luciferase lysis buffer	1% (v/v) Triton X-100; 25 mM glycyl-glycin (pH 7.8); 15 mM magnesiumsulfate; 4 mM EGTA; 1mM DTT
Luciferase substrate solution	1:5 dilution of 1 mM luciferine solution with 25 mM glycyl-glycin (pH 7.8)
Renilla substrate solution	Luciferase assay buffer without DTT and ATP; 1.5 µM coelenterazine
Trypsin solution	0.05% trypsin; 0.02% EDTA
Trypan blue solution	2 mg/ml trypan blue in 1x PBS
Penicillin/Streptomycin (100x)	10.000 U/ml penicillin G; 10 mg/ml streptomycin; 0.9% (w/v) NaCl
Water	To avoid microbial contaminations, all buffers, solutions and media for cell culture were prepared with pyrogen-free water
10x PBS	80 mM di-sodiumhydrogenphosphate; 20 mM sodium-di-hydrogenphosphate; 1.4 M NaCl; pH 7.4

3.1.3.2 Nucleic acid work

Table 3-5 List of commonly used buffers and solutions

TAE (50x)	2 M Tris-OH; 1 M acetic acid; 0.05 M EDTA
TBE (10x)	0,89 M Tris-OH; 0.89 M boric acid; 0.02 M EDTA
TE	10 mM Tris-HCl (pH 8.0); 1 mM EDTA
PCR reaction buffer (5x)	750 mM Tris-HCl (pH 8.8); 200 mM $(NH_4)_2SO_4$; 0.1% (v/v) Tween 20
In vitro transcription buffer (5x)	200 mM Tris-HCl (pH 7.9); 30 mM $MgCl_2$; 50 mM DTT; 50 mM NaCl; 10 mM spermidine
Ethidium bromide solution	10 mg/ml ethidium bromide in H_2O
Water	Buffers and solutions used in conjunction with RNA were prepared with DEPC-treated water (3.2.2.1).
Y1 buffer	70% (v/v) ethanol ; 1 M saccharose ; 0.1 M EDTA; pH 7.4; supplemented with 0.1% (v/v) β-mercaptoethanol and 100 U/ml lyticase

3.1.3.3 Protein work

Table 3-6 List of commonly used buffers and solutions

Acrylamid stock solution	30% acrylamid and bisacrylamid solved 29:1
ATPase assay buffer (2x)	100 mM Tris-HCl (pH 7.4); 6 mM magnesiumchloride; 6 mM DTT; 2 mM EGTA; 1 mM ATP
Blocking buffer (western blot)	1x PBS; 0.5% (w/v) Tween20; 3% milk powder
Coomassie staining solution	0.25% (w/v) coomassie brilliant blue R-250; 50% (v/v) methanol; 10% (v/v) acetic acid
Destain solution	5% (v/v) methanol; 5% (v/v) acetic acid
SDS PAGE sample buffer (6x)	600 mM Tris-HCl (pH 8.8); 15 mM EDTA ; 0.3% (w/v) bromophenolblue; 30% (w/v) sucrose; 9% (w/v) SDS; 6% (v/v) β-mercaptoethanol
Semidry blotting buffer	48 mM Tris; 39 mM glycin; 0.00375% (w/v) SDS; 20% (v/v) methanol
Separating gel buffer	1.5 M Tris-HCl (pH 8.8); 0.4% (w/v) SDS
Stacking gel buffer	1 M Tris-HCl (pH 6.8); 0.8% (w/v) SDS
Running buffer	25 mM Tris-OH (pH 8.3); 192 mM glycin; 10% (v/v) methanol

3.1.3.4 ELISA

Table 3-7 List of commonly used buffers and solutions

Coating buffer (pH 9.5)	0.1 M Sodiumcarbonate: 8.4 g $NaHCO_3$; 3.6 g Na_2CO_3; adjusted to pH 9.5; ad 1000 ml H_2O
Coating buffer (pH 6.5)	0.2 M Sodiumphosphate: 11.8 g Na_2HPO_4; 16.1 g NaH_2PO_4; adjusted to pH 6.5; ad 1000 ml H_2O
Blocking buffer	1x PBS; 10% (v/v) FCS
Wash buffer	1x PBS; 0.05% (v/v) Tween20

3.1.4 Primer for quantitative real-time RT-PCR

Primers were designed with the software Primer3 (http://frodo.wi.mit.edu). If possible primers were placed on exon/intron boundaries to avoid amplification of genomic DNA. For this reason, only monoexonic genes were sensitive to amplification from genomic DNA (Table 3-8, Table 3-9).

Table 3-8 Primer sequences for the amplification of human transcripts

Gene		Sequence 5'-3'	Product (cDNA)	Product (genomic DNA)[b]	Amplicon position	Data base[c]
β-Actin	fw	AGAGCTACGAGCTGCCTGAC	183 bp	-	786	NM_001101
	rv	AGCACTGTGTTGGCGTACAG			969	
MDA5	fw	CTGCTGCAGAAAACAATGGA	201 bp	-	680	NM_022168
	rv	TTGAGGACCATCAACTTGTGA			879	
NALP3	fw	CCGAAGTGGGGTTCAGATAA	183 bp	-	1020	NM_004895.3
	rv	TTCAATGCACTGGAATCTGC			1202	
NOD1	fw	CTCCTTCGTCCTGCATCACT	172 bp	-	2510	NM_006092
	rv	CAGCTCTTCGCTTAGCACCT			2682	
NOD2	fw	ATCTTCACACCGTCCCAGAG	189 bp	-	624	NM_0022162
	rv	GAAGCGAGACTGAGCAGACA			913	
RIG-I	fw	CCCTGGTTTAGGGAGGAAGA	188 bp	-	249	NM_014314.2
	rv	TCCCAACTTTCAATGGCTTC			436	
TLR3	fw	GTGCCAGAAACTTCCCATGT	173 bp	-	383	NM_003265
	rv	ATGTGATTAAATTCTTCTGCTTGA			555	
TLR7	fw	AATGTCACAGCCGTCCCTAC	185 bp	185 bp	782	NM_016562
	rv	TTATTTTTACACGGCGCACA			966	
TLR8	fw	TCCTTCAGTCGTCAATGCTG	167 bp	167 bp	219	NM_016610
	rv	CGTTTGGGGAACTTCCTGTA			385	

Table 3-9 Primer sequences for the amplification of murine transcripts

Gene		Sequence 5'-3'	Product (cDNA)	Product (genomic DNA)[b]	Amplicon position	Data base[c]
β-Actin	fw	CCCTGTGCTGCTCACCGA	186 bp	-	383	NM_007393
	rv	ACAGTGTGGGTGACCCCGTC			568	
MDA5	fw	TGCTGAGAAGGATTGTGCAG	183 bp	-	734	NM_027835
	rv	CAGCAGGCAGAAGACACTCA			916	
NALP3	fw	ACCAGCCAGAGTGGAATGAC	167 bp	-	489	NM_145827
	rv	CCTGCTTCTCACATGTCGTC			655	
RIG I	fw	AGGATGAGGAGGTGCAGTACA	165 bp	-	106	NM_172689
	rv	TGGCTTCACAAAGTCCACAG			270	
TLR3	fw	CTGCACGAACCTGACAGAAC	198 bp	198 bp	728	NM_126166
	rv	CGCAACGCAAGGATTTTATT			925	
TLR7	fw	CCTGTTCTACTGGGGTCCAA	167 bp	167 bp	493	NM_133211
	rv	GCCTCAAGGCTCAGAAGATG			659	

[b] No amplifcation of genomic DNA due to extended size by exon/intron structure

[c] National Center for Biotechnology Information (NCBI: www.ncbi.nlm.nih.gov)

3.1.5 Primer for *in vitro* transcription

In order to generate *in vitro* transcripts of increasing length with similar sequences, one forward primer for all transcripts was designed to bind at position 1271 of TLR3 within pcDNA3-hTLR3. The forward primer contained a 5'-overhang with the promoter site for T7 polymerase. The respective reverse primer bind with increasing distances. The reverse primer contained a 3'-overhang with the final 6 nucleotides of the T7 RNA polymerase promoter sequence, which is part of every transcription product. Primer for complementary transcripts were designed the same way *vice versa*. For 40 bp *in vitro* transcripts, sense 5'-GGG AGA TAG GTG GCC CAA CCA AGA GAA AGC ATC ATC TCC CTA TAG TGA GTC GTA TTA-3' and antisense 5'-GGG AGA TGA TGC TTT CTC TTG GTT GGG CCA CCT ATC TCC CTA TAG TGA GTC GTA TTA-3' DNA oligonucleotides, containing the T7 RNA polymerase promoter site on each respective 5'-end, were purchased in HPLC purity from MWG-Biotech (Ebersberg) and annealed as described (3.2.2.14), resulting in the template DNA for *in vitro* transcription. Strategy for *in vitro* transcription reaction is summarized in Fig. 3-1. Primer used for *in vitro* transcription are listed in Table 3-10.

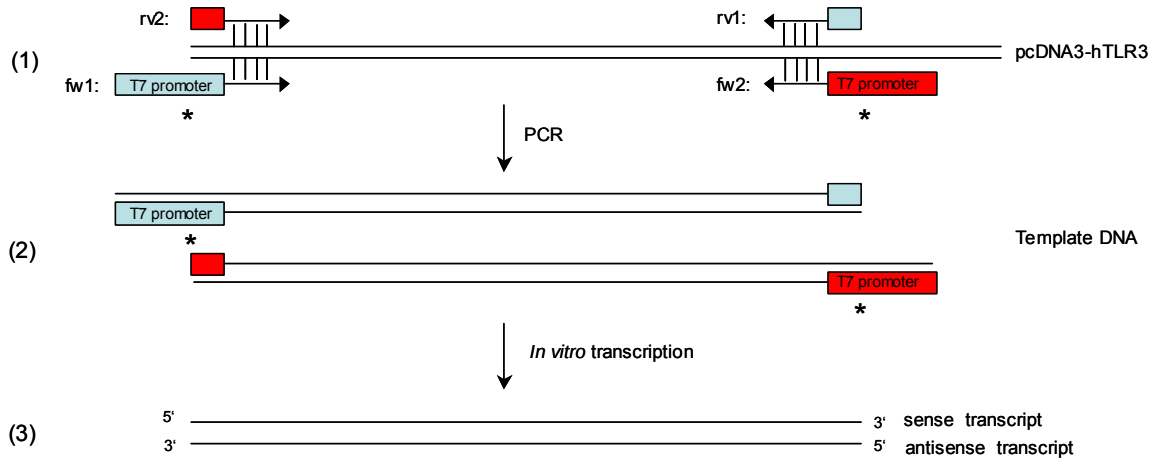

Fig. 3-1 Summary of *in vitro* transcription
PCR was performed either with fw1/rv1 primer or with fw2/rv2 using pcDNA3-hTLR3 as template (1). PCR products representing templates for *in vitro* transcription contain each a T7 promoter sequence (2). *In vitro* transcription results in transcripts of exclusively complementary sequences depicted as sense and antisense transcripts, respectively (3). *, depicts the starting point of transcription. To obtain transcripts of increasing length rv1 and fw2 primer were designed to bind further downstream of pcDNA3-hTLR3.

Table 3-10 Primer sequences for in vitro transcription

In vitro transcript	Orientation	Product size	5'-3' Sequence[d]
fw1	sense	-	TAATACGACTCACTATAGGGAGATGATGCTTTCTCTTGGTTGGGC
rv1-100	sense	100	**GGGAGA**TCTCCATTCCTGGCCTGTGA
rv1-200	sense	200	**GGGAGA**GCATCAGTCGTTGAAGGCTTG
rv1-400	sense	400	**GGGAGA**ACCACCAGGGTTTGCGTGTTT
rv-1600	sense	1600	**GGGAGA**GAACTTCAGGGTCAGCTTGC
rv2	antisense	-	**GGGAGA**TGATGCTTTCTCTTGGTTGGGC
fw2-100	antisense	100	TAATACGACTCACTATAGGGAGATCTCCATTCCTGGCCTGTGA
fw2-200	antisense	200	TAATACGACTCACTATAGGGAGAGCATCAGTCGTTGAAGGCTTG
fw2-400	antisense	400	TAATACGACTCACTATAGGGAGAACCACCAGGGTTTGCGTGTTT
fw2-1600	antisense	1600	TAATACGACTCACTATAGGGAGAGAACTTCAGGGTCAGCTTGC

[d] T7 promoter sequences is underlined, transcription start position is depicted in red; transcribed T7 promoter sequence depicted in bold letters

3.1.6 Plasmids

Plasmids for reconstitution experiments and reporter assays are listed in Table 3-11.

Table 3-11 List of relevant recombinant plasmids and source used in this study

Plasmid name	Basic vector	Insert	Source
pEF-SEM	pcDNA3	Neomycin resistance, EF1α promotor	H. Häcker, TU Munich
pEGFP-N1	pEGFP	Enhanced green fluorescent protein (eGFP), CMV promoter	BD, Heidelberg
pSV-β-gal control vector	pSV	*LacZ* gene, SV40 promoter/enhancer	Promega, Madison, USA
pCDNA3-hTLR3	pcDNA3	Human TLR3-YFP, CMV promotor	T. Espevik, NTNU, Trondheim, Norway
pCDNA3.1-hTLR7	pcDNA3.1	Human TLR7, CMV promotor	S. Bauer, University Marburg
pCDNA3.1-hTLR8	pcDNA3.1	Human TLR8, CMV promotor	S. Bauer, University Marburg
pCDNA3.1-mTLR7	pcDNA3.1	Murine TLR7, CMV promotor	S. Bauer, University Marburg
pISRE-Luc	pLuc	Firefly luciferase reporter, ISRE promotor	Stratagene, La Jolla, USA
p6NFκB-Luc	pGL3	Firefly-luciferase reporter, 6xNFκB promotor	C. Kirschning, TU Munich
pGL3B/561	pISG56	Firefly-luciferase reporter, ISG56 promoter	G.Sen, Lerner Research Institute, Cleveland, USA
pRL-SV40	pRL	Renilla-luciferase, SV40 enhancer, CMV promoter	Promega, Madison, USA

3.1.7 Markers

Molecular markers used for electrophoresis are listed in Table 3-12.

Table 3-12 Molecular markers used for this study

RiboRuler RNA Ladder (100-1000 bp)	MBI Fermentas, St. Leon-Rot
RiboRuler RNA Ladder (200-6000 bp)	MBI Fermentas, St. Leon-Rot
GeneRuler DNA Ladder #323 (100-3000 bp)	MBI Fermentas, St. Leon-Rot
GeneRuler DNA Ladder #333 (100-10000 bp)	MBI Fermentas, St. Leon-Rot
Page Ruler Prestained Protein Ladder plus	MBI Fermentas, St. Leon-Rot

3.1.8 Oligonucleotides

3.1.8.1 Deoxynucleotides

As RNA-independent control ligand, unmethylated CpG DNA oligonucleotides were used, which have been shown to trigger exclusively TLR9. All deoxynucleotides were purchased with HPLC purity from MWG-Biotech (Ebersberg) and are listed in Table 3-13

Table 3-13 List of CpG deoxynucleotides relevant in this study

Name	5'-3' Sequence[e]
CpG D19	GGtgcatcgatgcaGGGGGG
CpG 1668	TCCATGACGTTCCTGATGCT
CpG 2216	GGgggacgatcgtcGGGGGG

[e] PTO modified oligonucleotides are depicted in capital letters; unmodified oligonucleotides in small letters.

3.1.8.2 Ribonucleotides

Ribonucleotides were either in-house synthesized and HPLC purified by a) Kerstin Giessler (Department of Organic Chemistry, University Karlsruhe) as described in[167] or b) purchased in HPLC purity at IBA (Göttingen). RNA oligonucleotide sequences are listed in Table 3-14.

Table 3-14 List of ribonucleotides relevant for this study

Name	5'-3' Sequence[f]	Source[g]
RNA40	GCCCGUCUCUGUGUGACUC	b)
EGFP1s	GCAAGCUGACCCUGAAGUUCAU	a) b)
EGFP1s (dT)	GCAAGC**dT**GACCC**dT**GAAG**dTdT**CA**dT**	a)
EGFP1as	GAACUUCAGGGUCAGCUUGCCG	a) b)
EGFP1as (dA)	G**dAdA**CUUC**dA**GGGUC**dA**GCUUGCCG	a)
EGFP1as (dC)	GAA**dC**UU**dC**AGGGU**dC**AG**dC**UUG**dCdC**G	a)
EGFP1as (dG)	**dG**AACUUCA**dGdGdG**UCA**dG**CUU**dG**CC**dG**	a)
EGFP1as (dU)	GAAC**dUdU**CAGGG**dU**CAGC**dUdU**GCCG	a)
EGFP1as (mA)	G**mAmA**CUUC**mA**GGGUC**mA**GCUUGCCG	a)
EGFP1as (mC)	GAA**mC**UUCAGGGU**mC**AGmCUUGmCmCG	a)
EGFP1as (mU)	GAAC**mUmU**CAGGG**mU**CAGC**mUmU**GCCG	b)
EGFP1as (nG)	**nG**AACUUCA**nGnGnG**UCA**nG**CUU**nG**CC**nG**	a)
EGFP1as (m5C)	GAA**m5C**UUCAGGGU**m5C**AG**m5C**UUG**m5Cm5C**G	a)
EGFP1as (dT)	GAAC**dTdT**CAGGG**dT**CAGC**dTdT**GCCG	a)
EGFP1as (dT-A)	GAAC**dTdT**CAGGGUCAGCUUGCCG	a)
EGFP1as (dT-B)	GAACUUCAGGG**dT**CAGC**dTdT**GCCG	a)
EGFP1as (dT-C)	GAACUUCAGGGUCAGC**dTdT**GCCG	a)
EGFP2s	ACUACAACAGCCACAACGUCUA	b)
EGFP2as	GACGUUGUGGCUGUUGUAGUUG	a) b)
EGFP2as (dT-A)	GACG**dTdT**G**dT**GGCUGUUGUAGUUG	a)
EGFP2as (dT-B)	GACGUUGUGGC**dT**G**dTdT**G**dT**AG**dTdT**G	a)
EGFP2as (dT)	GACGdTdTGdTGGCdTGdTdTGdTAGdTdTG	a)
EGFP3s	GAGCAAAGACCCCAACGAGAAG	b)
EGFP3as	UCUCGUUGGGGUCUUUGCUCUG	b)
BGs	CUACACAAAUCAGCGAUUUU	a) b)
BGas	AAAUCGCUGAUUUGUGUAGUU	a) b)
BGas (dT)	AAAdTCGCdTGAdTdTdTGdTGdTAGdTdT	a)

3.1.8.3 siRNAs

All siRNAs were purchased in HPLC purity from MWG-Biotech (Ebersberg). Sequences shown in Table 3-15 confer to the respective passenger-strand of the siRNA. The siRNAs, targeting the reporter genes enhanced green fluorescent protein (EGFP) or β-galactosidase (BG) (siEGFP1-3, siBG) as well as the control siRNA (siCon) were designed, regarding published siRNA-efficiency rules[168-170]. All other siRNAs were validated by MWG-Biotech. Sequences of the respective passenger-strands are listed in Table 3-15.

[f] Bold letters indicate modified oligonucleotides; d: deoxynucleotides; m: 2'-O-methylation; m5C: 5'-methylcytosine; nG: 7'-deaza-guanosine

[g] a) In-house synthesized by Kerstin Giessler, University Karlsruhe; b) purchased at IBA, Göttingen

Table 3-15 List of relevant siRNAs used in this study

Name	5'-3' Sequence	Target gene
siEGFP1	GCAAGCUGACCCUGAAGUUCAU	EGFP
siEGFP2	ACUACAACAGCCACAACGUCUA	EGFP
siEGFP3	GAGCAAAGACCCCAACGAGAAG	EGFP
siBG	CUACACAAAUCAGCGAUUUU	BG
siCon	GCAAGCUGACCCUGAAGUUCAU	No target
siRIG-I	ACGGAUUAGCGACAAAUUUAA	Human RIG-I protein
siTLR3	ACUUAAAUGUGGUUGGUAAUU	Human Toll-like-receptor 3

3.1.9 Antibodies

Antibodies used for the indicated applications are listed in Table 3-16, Table 3-17 and Table 3-18.

Table 3-16 List of antibodies for flow-cytometry

Species	Source	Fluorescent-label	Antigen	Clone
Anti-mouse	BD (Heidelberg)	PE	B220/CD45R	RA3-6B2
Anti-mouse	BD (Heidelberg)	FITC	CD11c	HL3

Table 3-17 Antibodies used for murine interferon-α ELISA

Species	Source	Antigen	Final concentration
Anti-mouse	PBL (Piscataway, USA)	Interferon-α	2 ng/ml
Anti-mouse	PBL (Piscataway, USA)	Interferon-α	2 ng/ml
Anti-rabbit	Cell signalling (Boston, USA)	Rabbit IgG	4 ng/ml

Table 3-18 Antibodies used for western blot analysis

Species	Source	Antigen	Final concentration
Rabbit	Acris (Herford)	human RIG-I	0.5 µg/ml
Anti-rabbit	Acris (Herford)	Rabbit IgG	0.5 µg/ml

3.1.10 Bacteria and cell culture

3.1.10.1 Prokaryotic cells

NEB-5α high efficiency competent *E.coli* were used for plasmid transformations (genotype: *fhuA2*Δ*(argF-lacZ)U169 phoA glnV44 Φ80* Δ*(lacZ)M15 gyrA96 recA1 relA1 endA1 thi-1 hsdR17*) (New England Biolabs, Ipswich, USA). Bacteria used for RNA isolation are listed in Table 3-19.

Table 3-19 List of bacterial species and sources

Bacterial species	Source	Culture media[h]
Escherichia coli	ATCC 25922	a)
Moraxella catarrhalis	Isolate from patient	b)
Proteus mirabilis	Isolate from patient	a)
Pseudomonas aeruginosa	ATCC 27853	a)
Bacillus subtilis	ATCC 6051	b)
Enterococcus faecalis	ATCC 29212	a)
Listeria monocytogenes	ATCC 15313	b)
Staphylococcus aureus	ATCC 25923	a)
Staphylococcus epidermidis	ATCC 14990	a)
Streptococcus pneumoniae	ATCC 49619	b)

[h] a) Bacterial species were grown in LB media (3.1.10.3) b) Bacterial species were grown in BHI media (3.1.10.3).

3.1.10.2 Eukaryotic cells

HEK293T

Human embryonic kidney[171] cells expressing the SV40 large T-antigen. Cells were cultured in DMEM (3.1.10.3) and passaged approximately twice a week.

Huh7-clone Huh7.5

Human hepatoma cell line Huh7 derived clone Huh7.5 was received from M.Binder, University Heidelberg[172]. Huh7.5 cells expressing functional RIG-I protein were generated and described by M.Binder previously[173].

PBMC

Peripheral blood mononuclear cells were isolated from voluntary healthy donors as described in 3.2.1.1.

FLT3L-derived dendritic cells[174-176]

Bone marrow-derived plasmacytoid dendritic cells ($CD11c^+$; $B220^+$) were generated as described in 3.2.1.1. The used mouse strains are described in 3.1.11.

GMCSF-derived dendritic cells[177]

Bone marrow-derived myeloid dendritic cells ($CD11c^+$; $B220^-$) were generated as described at 3.2.1.1. The used mouse strains are described in 3.1.11.

Yeast

Candida albicans (ATCC 90028) was received from the Department of Medical Microbiology and Hygiene, University Heidelberg and cultured in LB-medium.

3.1.10.3 Media

Bacteria

LB: 10 g/l tryptone, 5 g/l yeast extract, 5 g/l NaCl; 1.5% agar-agar added for solid media.

BHI: 6 g/l brain-heart infusion, 6 g/l cattle tissue, 5 g/l NaCl, 3 g/l glucose, 2.5 g/l Na_2HPO_4, 14.5 g/l gelatine.

SOC: 20 g/l tryptone, 5 g/l yeast extract, 8.56 mM NaCl, 2.5 mM KCl, 10 mM $MgCl_2$, 20 mM glucose

Mammalian cells

DMEM (Dulbecco's modified eagle media): supplemented with 10% (v/v) heat-inactivated FCS; penicillin G (100 IU/ml); streptomycin sulfate (100 IU/ml).

RPMI 1640 (Rosswell Park Memorial Institute): for murine dendritic cells, supplemented with 10% (v/v) heat inactivated FCS; 50 mM β-mercaptoethanol; penicillin G (100 IU/ml); streptomycin sulfate (100 IU/ml).

Differentiation media: For culturing of human PBMCs, RPMI 1640 was supplemented with 2% (v/v) autologous serum. Medium was supplemented with 5% (v/v) GM-CSF or 0.1% (v/v) FLT3L-containing supernatant for the generation of GM-CSF-derived dendritic cells and FLT3L-derived-dendritic cells, respectively.

OptiMEM: defined medium formulation with reduced serum (GIBCO #31985).

3.1.11 Mouse strains

C57BL/6 mice were purchased from Charles River Laboratories (Wilmington, MA USA), TLR7 and TLR9-deficient mice ($TLR7^{-/-}$, $TLR9^{-/-}$) were obtained from Stefan Bauer (University Marburg), Interferon-α/β receptor-deficient mice ($IFNAR1^{-/-}$) were obtained from Heike Weighardt (University Düsseldorf), Apoptosis-associated speck-like protein-deficient mice ($ASC^{-/-}$) were obtained from Vishva Dixit (Genentech, San Francisco, USA), *lps2* mice carrying a mutation in the TRIF adaptor protein were obtained from Marina Freudenberg (University Freiburg). Mice were breeded under specific pathogen free (SPF) conditions. Breeding and monthly control for infections were performed according to the list of GV-SOLAS 1995. Killing and dissection of mice were approved and experiments were properly recorded and reported to the regional commission Tübingen.

3.2 Methods

3.2.1 Cell biology

3.2.1.1 Cell culture of mammalian cells

Cells were grown as monolayers in cell culture dishes or in cell culture flasks (Greiner Bio-One, Frickenhausen) in fully supplemented DMEM culture media. Cells were split twice a week by washing with 1x PBS and detaching by 5 minutes incubation with trypsin solution. Pipetting the cell suspension up and down sheared the cells and a single cell suspension was yielded. Cells were split dependent on cell type and actual growth conditions, usually a ratio between 1:5 and 1:8 was chosen. All mammalian cells were incubated at 37°C and 5% CO_2 in humidified atmosphere. To determine the cell number of a cell suspension, 10 µl of cell suspension was mixed with 90 µl trypan blue solution which stains exclusively dead cells. Cell numbers were determined with a Neubauer cell counting chamber.

Isolation of human PBMCs (peripheral blood mononuclear cells)

Human peripheral blood mononuclear cells (PBMCs) were isolated from whole blood of young healthy voluntary donors. Isolation was performed by standard Ficoll-Hypaque density centrifugation. Blood was diluted 1:2 with PBS, underlaid by Biocoll (Biochrom, Berlin) and centrifuged at 485x g for 20 minutes. PBMCs were washed twice with PBS and resuspended in complete medium (RPMI1640, supplemented with 2% heat-inactivated autologous serum). PBMCs were plated at $4x10^5$ cells/well in a 96-well flat bottom plate for stimulation assays.

Generation of primary bone marrow-derived dendritic cells

GM-CSF-derived dendritic cells were prepared from female, 4- to 10-week-old mice as described by Inaba[177] with minor modifications. Briefly, bone marrow was collected from femurs and tibiae. Cells were placed in 70 cm^2 tissue-culture flasks in differentiation medium (3.1.10.3). After 24 h non-adherent cells were collected, washed and counted. 10^7 of these cells were seeded into 175 cm^2 tissue-culture flasks in differentiation medium. At day 5 fresh differentiation medium was added and at day 9 non-adherent, immature dendritic cells ($CD11c^+$, $B220^-$) were harvested. Culture supernatant of the plasmacytoma X63 cell line which produces murine GM-CSF was used as a source of GM-CSF (supplied by M.Lutz, University Würzburg). FLT3L-derived dendritic cells were prepared the same way as described above. $1.5x10^7$ cells were seeded into 75 cm^2 tissue-culture flasks and supplemented with 10 µl FMS-like tyrosine kinase 3 ligand (Flt3L)-containing supernatant (supplied by S.Bauer, University Marburg). The same volume of Flt3L was added again after four days. Eight days after dissection of the mouse, immature pDC-like dendritic cells ($CD11c^+$, $B220^+$) cells were harvested. Dendritic cells were plated at $2x10^5$ cells/well in a 96-well flat bottom plate for further stimulation assays.

3.2.1.2 Cell culture of prokaryotic cells and yeast

Bacteria and yeast were grown in specific media (Table 3-19) in a shaker (225 rpm) at 37°C. For quantitative RNA isolation (3.2.2.7) cells were cultured in 100 ml culture media and harvested within the mid log-phase growth. The number of colony forming units was determined by detecting the absorption at 600 nm (McFarland, 1 McF = 3 x 10^8 CFU/ml)[178]. The average time to reach mid-log growth for the used microorganisms is listed in Table 3-20.

Table 3-20 List of used species and time to reach mid log-phase growth

Species	mid log-phase reached after [h]
Candida albicans	12-15h
Bacillus subtilis	3-4h
Escherichia coli	3-5h
Enterococcus faecalis	7-8h
Listeria monocytogenes	12-15h
Moraxella catarrhalis	9-14h
Proteus mirabilis	3-5h
Pseudomonas aeruginosa	4-6h
Staphylococcus aureus	3-5h
Staphylococcus epidermidis	12-15h
Streptococcus pneumoniae	14-17h

For plasmid preparation cells were grown overnight in culture media supplemented with the appropriate antibiotics. Cells were centrifuged at 4500 rpm (Multifuge 3 S-R, Heraeus Instruments, Hanau) at 4°C. Plasmid preparations were performed with the JETSTAR kit (3.1.2) according to the manufacturer's protocol.

3.2.1.3 Liposome based transfection of eukaryotic cells

Lipofectamine2000

Transfection of cells with Lipofectamine2000 transfection reagent was performed according to the manufacturer's protocol. Cells were seeded 24 h prior transfection and transfected at a confluence of approximately 70%. Culture medium was exchanged 4 h post transfection procedure.

Effectene

Cells were transfected with Effectene transfection reagent according to the manufacturer's protocol. Cells were seeded 24 h prior transfection and transfected at a confluence of 80%. Culture media was not changed for the experiments.

3.2.1.4 Luciferase reporter assays

For all reporter assays Firefly luciferase activity was normalized to *Renilla* luciferase activity on a per well basis. Values are typically expressed as fold-induction over mock treated or Poly(C) treated cells, alternatively luciferase activity is expressed in relative light units (RLU). Values are given as the mean of duplicate measurements. Error bars are presented as the SD.

ISG56 reporter assay

Huh7.5 cells were seeded in a 24 well format ($1x10^5$ cells/well). 24 h later, cells were cotransfected with pGL3/B561 and pRL-SV40 (3.1.6) in a ratio of 3:1 using Effectene transfection reagent. 6 h post transfection cells were stimulated by transfection of defined *in vitro* transcribed RNAs using Lipofectamine2000 according to the manufacturer's recommendations. All RNAs were filled up to 1 µg with Poly(C) to ensure similar total RNA:Lipofectamine2000 ratios. 16 h after stimulation, medium was removed and cells were lysed with ice-cold luciferase lysis buffer in the plate (200 µl/well). Firefly luciferase activity was measured for 20 s in a Lumat LB9507 luminometer (Berthold, Freiburg) after injection of 200 µl luciferase substrate solution. *Renilla* luciferase activity was determined by injection of 100 µl *Renilla* substrate solution and subsequent measuring for 10 s in the same luminometer.

NFκB reporter assay

HEK293T cells were seeded in a 24 well format ($1.5x10^5$ cells/well). After 24 h cells were cotransfected with p6xNFκB-Luc and pRL-SV40 (3.1.6) in a ratio of 1:2 using Lipofectamine2000. 6-8 h after transfection cells were stimulated with variable amounts of RNA oligonucleotides or bacterial RNA using DOTAP as transfection reagent (3.2.1.5). 16 h after stimulation cells were lysed and Firefly and Renilla luciferase activities were measured using the Dual Luciferase Reporter Assay System (3.1.2).

3.2.1.5 Cell stimulation

Stimulation with RNA oligonucleotides or bacterial RNA was performed using DOTAP transfection reagent according to the manufacturer's protocol. RNAs were encapsulated with DOTAP in a 1:2.5 (w/v) ratio. 16 h after transfection either cell free supernatants were analyzed for cytokine and

interferon secretion using sandwich ELISA or cells were lysed and luciferase activity was measured as described above. For ISG56 reporter assays RNAs were encapsulated with Lipofectamine instead of DOTAP.

3.2.1.6 Enzyme-linked immunosorbent assay (ELISA)

To determine the quantities of secreted cytokines or interferons cell free supernatants were removed and analyzed by sandwich ELISA. Supernatants were diluted with 1x PBS, supplemented with 10% (v/v) FCS. Assays were performed according to the manufacturer's protocols. Detection of murine Interferon-α was adapted to the protocol of murine IL-12p40 ELISA using separately purchased antibodies specific for murine interferon-α (PBL, Piscataway, USA) (3.1.9) in the same concentrations as recommended in commercially available ELISA kits (3.1.2). Buffers used for human interferon-α ELISA were also used for the analysis of murine interferon-α. Analysis was performed in duplicates and all experiments were performed at least three times if not indicated otherwise. Cytokines were detected by measuring the absorbance at 490 nm with a 650 nm reference in a photometer (SUNRISE Absorbance reader, Tecan, Salzburg, Austria). Cytokine concentrations were calculated using a standard dilution of the respective recombinant cytokines. Finally, concentrations were calculated with the Magellan V 5.0 software (TECAN, Salzburg, Austria).

3.2.1.7 MTT-assay

Viability of stimulated cells was determined by MTT-assay. MTT substrate is reduced by various mitochondrial dehydrogenases resulting in a change of substrate colour. After removing cell free supernatants for cytokine detection, MTT solution was prepared according to the manufacturer's recommendations and added to culture medium in a ratio of 1:20 (v/v). Cells were incubated for 1 h at 37^{o}C and absorbance at 550 nm with 650 nm reference wave length was measured in a photometer (SUNRISE Absorbance reader, Tecan, Salzburg, Austria) adapting a 4 parameter fit regression analysis.

3.2.1.8 Flow cytometry (FACS)

Staining of surface molecules

To determine the purity of bone marrow-derived dendritic cells characteristic surface molecules were stained with fluorescence-labelled antibodies (3.1.9). Approximately 2.5x10^{5} cells were washed with 1x PBS, supplemented with 2% (v/v) FCS. Cell suspension was adjusted to a volume of 100 µl and incubated with the respective antibody for 20 minutes on ice. After washing twice with 1x PBS, cells were analyzed in a flow cytometer (FACS Canto, BD, Heidelberg). Cells were identified and gated by size and granularity according to forward/sideward scatter characteristics. Mean fluorescence intensity (MFI) of the respective 20x10^{3} living cells was analyzed for expression of the respective fluorochrome (expressed as percentage of positive cells). Unstained and isotype stained cell controls were used to gate for the respective fluorochrome.

Determination of gene-silencing activity

$1.5x10^5$ HEK293T cells were plated in DMEM supplemented with 10% (v/v) FCS per well of a 24-well culture plate. The following day cells were cotransfected either with 400 ng pEGFP-N1 encoding enhanced green-fluorescent-protein (EGFP) or with 500 ng pSV-β-galactosidase control vector encoding β-galactosidase together with the respective siRNA in the indicated concentration according to the Lipofectamine2000 protocol for DNA siRNA cotransfections. After 24 h cells were washed with 1x PBS and reporter gene expression was analyzed. Expression of EGFP was determined by flow cytometry (FACS Canto, BD, Heidelberg) in the FITC channel (530/30 nm). Mean fluorescence intensity (MFI) of 20,000 live cells gated according to forward/side scatter characteristics was detected. The β-galactosidase activity was determined by incubation of the cells for 4 hours at 37°C in β-galactosidase lysis buffer. Reaction was stopped by addition of β-galactosidase stop solution and optical density was measured at 570 nm with 650 nm reference wave length.

3.2.1.9 siRNA transfection

For RNAi-mediated gene-silencing of endogenously expressed genes $1x10^5$ cells were seeded in a 24 well format. 24 h later cells were transfected with 10 nM of the respective siRNA using Lipofectamine2000 according to the manufacturer's protocol. After 72 h cells were transfected again the same way. Next day gene-silencing was validated by quantitative real-time RT-PCR.

3.2.2 Molecular biology

3.2.2.1 DEPC-treated water

Water used for RNA-related work was treated with DEPC to eliminate contaminations with RNases. Briefly, 1 ml DEPC was added to 1 l H_2O and stirred for 15 minutes. For RNase inactivation water was autoclaved by standard procedure.

3.2.2.2 Transformation of competent bacteria

For transformation 50 µl competent *E.coli* (3.1.10.1) were mixed with 5-10 µl of 100-200 ng/µl plasmid DNA and incubated at least 20 minutes on ice. After incubation of the bacteria at 42°C for 30 seconds, 1 ml SOC media was added and bacteria were incubated at 37°C on a shaker (225 rpm) for 1 h. Thereafter 50-100 µl cell suspension was pipetted on a agar plate containing the appropriate antibiotic. Colonies were grown overnight at 37°C.

3.2.2.3 Plasmid preparation

Preparation of plasmid DNA from bacteria was performed using silica membrane based spin column kits (mini) (3.1.2) according to the manufacturer's protocol. In general, approximately 5 ml of an overnight cell suspension were used for mini preparations. For larger plasmid DNA preparations ion-exchanger columns (maxi) (3.1.2) were used according to the manufacturer's protocol. Plasmid DNA was eluted in 200 and 500 µl water, respectively.

3.2.2.4 DNA sequencing

Sequencing was performed commercially by GATC (Konstanz). 2-3 µg plasmid DNA was analyzed with either standard or specifically designed primer. Results were validated by aligning with the theoretical sequences using the alignment program CLUTALW2 (www.ebi.ac.uk/Tools/clustalw2).

3.2.2.5 Quantitative RT-PCR

RNA preparation

Total RNA preparation was performed using the High Pure RNA Isolation kit (Roche, Mannheim) according to the manufacturer's protocol. RNA preparation included a DNase I digestion. The eluted RNA was either stored at –80^{o}C or directly used for cDNA synthesis.

cDNA synthesis

Synthesis of cDNA was performed with the RevertAid first strand cDNA synthesis kit using the RevertAid™ M-MuLV Reverse Transcriptase (Fermentas, St.Leon-Rot). Messenger RNA was amplified using Oligo(dT)$_{18}$ primers according to the manufacturer's protocol. The cDNA was finally diluted with H_2O in a ratio of 1:5.

SYBR green based quantitative RT-PCR (qRT-PCR)

The cyanid fluorescent dye SYBR-green which interferes with double-stranded DNA was used for DNA quantification. For qRT-PCR the Absolute SYBRgreen RoxMix kit (ABgene House, Epsom, UK) was used and gene specific primer pairs were ordered from Operon (Cologne) (3.1.4). 2.5 µl template cDNA, 12.5 pmol forward and reverse primer, 12.5 µl SYBR Green Rox Mix were used for each 25 µl PCR reaction. Reactions and detection were performed in the 7900 HT Fast Real-Time PCR System (AB Applied Biosystems, Darmstadt) in a 96 well format (program: 95^{o}C 15 min; 40x [95^{o}C, 15sec; 60^{o}C, 1min]).

Each gene was typically measured in duplicates in each cDNA sample. Automatic detection of baseline and threshold values was used and the determined C_t values were substracted from the C_t values of an endogeneous constitutively expressed reference gene (β-actin) resulting in a ΔC_t for each target gene. Relative expression (rE) was calculated as $rE = 1/(2^{\Delta Ct})$ and PCR reactions were verified for similar efficiencies. For reaction specificity, "no reverse-transcriptase" and "no template" controls were performed with each reaction. Additionally the dissociation curves of each target gene were analyzed.

3.2.2.6 Gel electrophoresis

For DNA visualization standard agarose gel electrophoresis procedure was performed. DNA sample was mixed with 6x DNA loading dye and applied to 1-2% 1x TAE agarose gel electrophoresis (run at approximately 120 V). For RNA agarose gel electrophoresis it had to be ensured that no contaminating RNases were present, therefore all buffers and solutions were prepared with DEPC-treated water. The electrophoresis chamber was incubated with 3% (v/v) H_2O_2 for 30 minutes and washed with 100% ethanol before usage. 1-2 µg ethidiumbromide was added to the agarose gels for UV-based detection of the respective nucleic acids (infinity video documentation system 3000,

Peqlab, Erlangen). RNA samples were mixed with 2x RNA loading dye and preheated to 70°C for 10 minutes to avoid second stucture formation prior application to the gel electrophoresis.

3.2.2.7 Quantitative purification of RNA

All RNA purifications described below included an on-column DNase I digestion ensuring that no residual genomic DNA was present in the RNA preparations.

Eukaryotic RNA

Total RNA isolation from HEK293T cells was performed with the RNeasy mini kit according to the animal cell protocol of the manufacturer. $1.2x10^7$ HEK cells were taken for each purification. *Candida albicans* RNA isolation was performed the same way. Due to the cell wall $5x10^{10}$ cells from mid log-phase growth were incubated for 30 minutes at room temperature with Y1 buffer containing 100 U/ml lyticase. RNA from the resulting spheroblasts was purified with the animal cell protocol of the manufacturer.

Prokaryotic RNA

$1.5x10^{11}$ bacteria were taken from mid log-phase growth and lysozyme digested for 30 minuntes. Gram-positive bacteria were treated with 1x TE, supplemented with 40 mg/ml lysozyme, whereas gram-negative bacteria due to the thinner cell wall were treated with 1x TE, supplemented with 10 mg/ml lysozyme. After lysozyme digestion RNA purification was performed with the RNeasy mini kit according to the bacterial RNA isolation protocol of the manufacturer.

Viral RNA

Viral RNA was prepared from supernatants of cultured Huh-7 cells infected with vesicular stomatitis virus (VSV). Briefly, superantant was cleared by table-top centrifugation and filtration through a 0.45 µm syringe tip filter. Virus particles were then pelleted by ultracentrifugation for 2 h at 100.000x g (RCF max) through a 25% sucrose cushion and viral RNA was extracted using the NucleoSpin RNA II kit (Macherey-Nagel, Düren) according to the manufacturer‘s recommendations. Hepatitis C virus (HCV) genome length positive and negative sense RNAs were prepared by *in vitro* transcription of the construct Con1ΔGDD, referring to the full-length Con1 genome (AJ238799) bearing the inactivating GDD deletion, and annealed to form a double-stranded hybrid as described[173].

3.2.2.8 Isolation of *E.coli* 16S ribosomal RNA

Isolation of *E.coli* 16S rRNA from total *E.coli* RNA preparations was performed using a 3’-biotinylated capture DNA, containing a 15 nucleotide long spacer between the complementary sequence and the 3’-end (5’-CGT TTA CGG CGT GGA CTA CCA GGG TAT CTA ATC C*AC AGA CAC AGA GTA C*-biotin-3[i]). 40 µg of total RNA was denaturated for 5 minutes at 75°C, incubated with the capture DNA in a molar ratio of 1.5:1 and slowly cooled down to the calculated annealing temperature of 62°C. Annealing was performed for 10 minutes in TEN buffer (TE buffer supplemented with 100 mM NaCl).

[i] Capture DNA: consisting of a 34 nucleotide sequence complementary to 16S rRNA of *E.coli,* a 15 nucleotide spacer sequence depicted in italic and a 3’-Biotin.

Subsequently, the RNA/DNA duplex was incubated with µMACS Streptavidin beads (Miltenyi, Bergisch Gladbach, Germany) according to the manufacturer's recommendations and purified using a µMACS magnet-attached column. After 3 times washing with 1x TE, RNA was eluted by denaturation of the DNA/RNA duplexes with preheated RNase-free water (approximately 90°C).

3.2.2.9 Polymerase chain reaction (PCR)

PCR was performed according to general protocols using Accu Taq LA DNA polymerase. Annealing temperatures for standard cloning purposes was 5°C under calculated annealing temperatures, elongation times were 60 sec per 1000 bp. PCR products were directly purified using the JETQUICK PCR Purification Spin Kit.

3.2.2.10 *In vitro* transcription

For generation of *in vitro* transcripts of defined length standard PCR using pcDNA3-hTLR3 as template DNA was performed with primers containing the T7 RNA polymerase promoter site (3.1.5). PCR products were purified as described above and annealed (3.2.2.14).

The *in vitro* transcription had a final reaction volume of 100 µl, containing 20 µl *in vitro* transcription buffer, 6.25 µl rNTPs (25 mM each), 50 U RiboLock, 5-10 µg template PCR product and 60 U T7 RNA polymerase. After 2 h incubation at 37°C additional 60 U T7 RNA polymerase were added and reaction was continued for another 2 h. Transcription reaction was terminated by adding 1 U RNase-free DNase/µg template DNA and further 30 minutes incubation at 37°C. For *in vitro* transcripts of 200 bp or shorter transcription reaction was extended for another 2 h.

To label the 5'-triphosphate of *in vitro* transcripts, γ^{32}[P]-GTP was added to the *in vitro* transcription reaction in a γ^{32}[P]-GTP: GTP ratio of 1:100 – 1:500. Since the triphosphate group is cleaved off during RNA extension the radiolabel remains only at the free 5'-end of each molecule. Afterwards, the sample was cleared from non-incorporated radioactive nucleotides by using a microspin 25 column-based gel filtration (GE Health Care, Munich) according to the manufacturer's protocol.

3.2.2.11 Purification of *in vitro* transcripts

In vitro transcripts were purified to avoid protein contaminations and to ensure the absence of side products of varying lengths. *In vitro* transcription products were therefore separated by gel electrophoresis using 1-3% low-melting agarose dependent on the expected product size. Transcripts of the expected size were excised with a scalpel from the gel. Gel slices were melted for 10 minutes at 70°C, cooled down to 42°C and agarose was degraded by incubation with 1 U agarase/100 mg gel for 30 minutes. Ammoniumacetate was added to a final concentration of 2.5 M and residual agarose was precipitated by centrifugation at 13000 rpm for 10 minutes. Then 2/3 volumes of acidic water saturated phenol (Roth, Karlsruhe) were added to the supernatant and incubated for 10 minutes on ice. After 10 minutes of centrifugation (10000 rpm) at 4°C, the supernatant was extracted with 1 volume chloroform. RNA–containing supernatant was mixed with 10% (v/v) ammoniumacetate and 2 volumes ice-cold ethanol, following incubation for 2 h at –80°C and final precipitation by centrifugation (13000 rpm) at 4°C for 45 minutes. Finally RNA was dissolved in RNase-free water.

Due to their small size 40 nucleotide transcripts were purified by gel filtration using NAP-5 spin-columns (GE Healthcare, Munich) according to the manufacturer's protocol.

3.2.2.12 RNA digestion

RNA was denatuated for 5 minutes at 95°C to ensure single-stranded conformation and primary structure formation of the respective RNA sample. For digestion RNA samples were incubated with 10 µg RNaseA/µg RNA for 3 h at 65°C.

3.2.2.13 RNA dephosphorylation

Bacterial messenger RNA and *in vitro* transcribed RNA contain a triphosphorylated nucleotide at the very 5'-end. To remove the terminal 5'-triphosphate RNA samples were dephosphorylated using shrimp alkaline phosphatase (SAP). RNA samples were incubated for 30 minutes at 37°C with 0.5 U SAP/pmol 5'-end of the RNA samples. After 30 minutes another 0.5 U SAP/pmol 5'-end RNA was added and incubated for another 30 minutes. Reaction was terminated by heating the reaction mixture for 10 minutes at 65°C. The amount of 5'-ends in pmol was calculated as:
Amount of 5'-ends [pmol] = (RNA [g] x [nt]/ (RNA length x 330 g/mol x nt)) x 10^{12} pmoles/mol.
The efficiency of triphosphate removal was controlled by dephosphorylation of 5'-^{32}[P]-radiolabelled *in vitro* transcripts (3.2.2.10). *In vitro* transcripts were therefore cleared from non-incorporated nucleotides by using a microspin 25 column-based gel filtration (GE Health Care, Munich) according to the manufacturer's recommendations. Samples were further either SAP- or mock-treated, respectively. After a second gel filtration, the remaining radiolabeled nucleotides were detected in a liquid scintillation counter (Beckman Coulter LS6500, Krefeld).

3.2.2.14 Annealing to duplexes

To generate double-stranded RNA or DNA duplexes, sense and complementary antisense strand were mixed at equimolar concentrations in annealing buffer (20 mM HEPES, 50 mM NaCl, pH 7.4), heated to 90°C for 5 minutes, followed by slowly cooling down to room temperature.

3.2.2.15 Quantification and validation of RNA samples

All RNA preparations were quantified with the Qubit Fluorometer (Invitrogen, Karlsruhe) using the Quant-iT RNA Assay Kit. This method is based on an RNA-specific fluorescent dye and allows quantification of concentrations as low as 1 ng/ml. Quality and integrity of the RNA preparations were determined by QIAxcel capillary gel electrophoresis (Qiagen, Hilden, Germany) according to the manufacturer's protocol.

3.2.3 Biochemistry

3.2.3.1 Recombinant expression of human RIG-I protein

Recombinant protein expression and purification was performed by M.Binder (Department of molecular Virology, University Heidelberg) using the Bac-to-Bac Baculovirus expression system (Invitrogen, Karlsruhe). Briefly, human RIG-I protein was cloned in the pFastBac-DualGFP vector

under the control of a polyhedron (PH) promoter, whereas the GFP protein was controlled by the p10 promoter. The glutathione-S-transferase tag (GST) was cloned from pGEX 6p1 to the N-terminus of the RIG-I protein and a cleavage site for Prescission protease (Invitrogen, Karlsruhe) was introduced between the GST-tag and the RIG-I protein by PCR method. Next, the pFasBac-DualGFP vector containing the GST-tagged RIG-I protein was transformed in a DH10Bac *E.coli* strain, where the vector is recombined to a bacmid. Once the recombinant bacmid was isolated, it was transfected into the oocyte insect cell line *Sf9*. Baculovirus containing supernatant was collected after Sf9 cells showed strong GFP expression which was reached approximately after 72 h. Supernatant was passaged 3 times, thereby increasing the number of infected Sf9 cells constantly. Finally, 3 times passaged supernatant was used to infect 20x 15 cm^2 cell culture plates of confluent Sf9 cells (1.5 ml supernatant/15 cm^2 cell culture plate).

3.2.3.2 Purification of recombinant expressed human RIG-I protein

Cells were centrifuged and cell pellets were taken up and resuspended in 4x 10 ml binding buffer (150 mM NaCl, 50 mM Tris, 1 mM DTT, 1 mM $MgCl_2$, supplemented with 1 Complete Protease Inhibitor Cocktail tablet (Roche, Mannheim). Cell pellets were lysed by freeze/thawing for 3 times by switching between 20^oC water bath and liquid nitrogen, resulting in the complete lysis of the cells. Cell suspension was centrifuged at 14000 rpm, 15 minutes, 4^oC, and cleared supernatant was mixed with 2 ml of Glutathione 4B Sepharose Beads (GE Health Care, Krefeld). Additionally 0.1 U/µl *Micrococcus* S7 Nuclease was added to eliminate possible DNA or RNA contaminations. The sepharose beads were incubated for 3 h, 4^oC on a rotating shaker and separated by centrifugation with 500x g for 5 minutes. Next, sepharose beads were washed 3 times with binding buffer and resuspended in 500 µl binding buffer, supplemented with 20 U GST-tagged Prescission protease. Protease cleavage was performed overnight at 4^oC. Finally, RIG-I containing supernatant was separated from the sepharose beads by filter spin columns (GE Health Care, Krefeld). Protein concentration was determined by the Qubit fluorometer, using the Quant-IT protein assay kit (Invitrogen, Karlsruhe). RIG-I containing supernantant was mixed with 50% (v/v) glycerol, aliqoted and stored at -70^oC.

3.2.3.3 SDS-PAGE

For protein analysis cell pellets were lysed in SDS-PAGE sample buffer and denaturated at 98^oC for 10 minutes. The samples were loaded on a 10% polyacrylamide gel and run at constant current for approximately 4 hours (30 mA for a 15x 15 cm gel). For PAGE a vertical gel chamber was used. As a reference a prestained protein marker (3.1.7) was used. Proteins from the gel were either visualized by Coomassie staining or further analyzed by Western Blotting (3.2.3.4). For staining the gel was incubated for 30 minutes in Coomassie staining solution and directly incubated with destain solution at 37^oC until the staining intensity seemed appropriate.

3.2.3.4 Western blot analysis

Proteins from SDS-PAGE (3.2.3.3) were blotted to methanol-activated PVDF membranes (Millipore, Billerica, USA) by semidry blotting procedure with 1 mA/cm^2 for at least 1 hour. Membranes were incubated overnight in blocking buffer, and then membranes were incubated with primary antibody

(3.1.9). After washing three times with 1x PBS supplemented with 0.05% (v/v) Tween, the membrane was incubated with horseradish peroxidase-conjugated secondary antibody (3.1.9). After three further washing steps with 1x PBS supplemented with 0.05% (v/v) Tween bound antibodies were detected by chemoluminescence using enhanced luminol (ECL plus, Amersham, Freiburg). Chemoluminescence was detected with a cooled CCD-camera device (Chemi-Smart 2000, Peqlab, Erlangen) and analyzed with the Chemi-Capt software (Vilber Lomat, Eberhardzell).

3.2.3.5 ATPase Assay

Functionality of recombinant human RIG-I protein was analyzed by detection of ATPase activity. Therefore the QuantiChrom™ ATPase/GTPase Assay Kit (Bioassay systems, Hayward, USA) was used according to the manufacturer's protocol. The reaction mixture had a final volume of 20 µl. First, 2 µl human RIG-I [110 ng/µl], which corresponds to 2 pmol recombinant protein, was mixed with varying concentrations of ligand RNA and 2x ATPase reaction buffer, either containing 1 mM ATP or not. Mixture was incubated for 20 minutes at 37^{o}C. Finally 180 µl detection solution was added and freed pyrophosphate was detected by absorbance at 620 nm in a photometer (SUNRISE Absorbance reader, Tecan, Salzburg, Austria).

3.2.4 Statistical analysis, data transformations and structure predictions

Data were analyzed by GraphPad Prism 4.03 program (GraphPad Software, San Diego, USA). Significant differences were assessed by analysis of variance (ANOVA) to compare three or more groups followed by Dunnett's test to compare selected groups. In all figures * represents p-values <0.05. Means of triplicates were used for linear regression analysis with GraphPad Prism 4.03 program.

Structure predictions for RNA oligonucleotides in monomeric and dimeric conformation were calculated with the *Mfold* program (www.mfold.bioinfo.rpi.edu)[179].

4 Results

4.1 Characterization of siRNA-mediated immunostimulation

It had been shown that single-stranded RNA oligomers induce a type-I interferon response in a TLR7- and TLR8-dependent manner[81,180] . Results from several further groups showed that also short, synthetic, double-stranded RNAs such as siRNAs are able to mount a type-I interferon response in human PBMCs[97-99] which was mediated by the activation of human pDCs. A general aim of this work was to identify these immunorecognition principles and to try to separate siRNA-mediated RNA interference from immunostimulation. This would allow the generation of more specific siRNAs for therapeutic applications.

4.1.1 RNA oligonucleotide mediated immunostimulation

As a starting point, RNA-mediated immunostimulation had to be confirmed and characterized. Therefore we analyzed interferon-α (IFN-α) secretion by a recently published immunostimulatory single-stranded RNA oligonucleotide (RNA40) of 20 nucleotides in length[81]. RNA40 was either encapsulated with the transfection reagent DOTAP in order to facilitate cellular uptake and endosomal delivery or was directly applied to the cells. Upon transfection of isolated human PBMCs with RNA40 encapsulated RNA40 showed a robust and dose-dependent secretion of interferon-α (IFN-α). In contrast, application of RNA40 to the cells without transfection reagent did not result in any detectable IFN-α secretion (Fig. 4-1 [A]). To further address the question of cellular delivery of RNA, oligonucleotide RNA40 containing a phosphothioate-modified sugar-phosphate backbone (PTO) was designed and used to transfect human PBMCs. For DNA oligonucleotides it had been shown earlier that introduction of phosphothioate into the sugar-phosphate backbone (PTO) was sufficient to increase cellular delivery and to activate immunorecognition principles[181] thereby avoiding the need of any transfection reagent formulation. We assumed that this mechanism could also be assigned to RNA mediated immunostimulation. DOTAP complexed RNA40, carrying a PTO-modified backbone, resulted in a dose-dependent IFN-α secretion in human PBMCs. However, RNA40-PTO showed a slightly reduced immunostimulatory potential compared to the unmodified RNA40 oligonucleotide. Transfection of RNA40-PTO without DOTAP did not result in any detectable IFN-α secretion. This suggested that the mechanisms of RNA and DNA uptake as well as the induced immunostimulation are different. TLR7-dependent recognition of single-stranded RNA oligonucleotides had been demonstrated earlier[81], however, profound characterization of siRNA recognition had not yet been done. We therefore generated murine GM-CSF-derived dendritic cells (mDCs) from wild type and TLR7$^{-/-}$ mice. As an activation marker for murine dendritic cells secretion of interleukin-12p40 (IL-12p40) was analyzed.

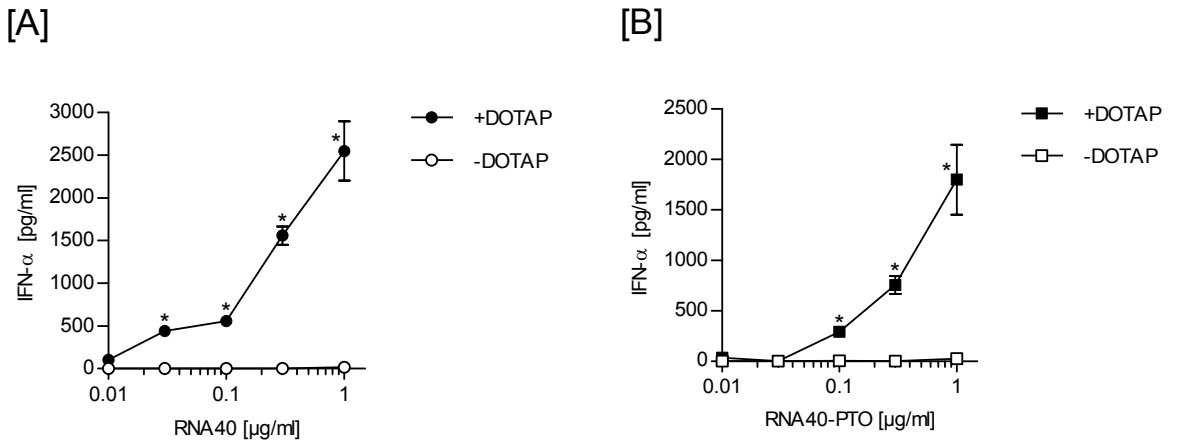

Fig. 4-1 Influence of transfection agent and PTO-backbone modification on RNA-mediated IFN-α secretion in PBMCs
Human PBMCs were transfected with single-stranded RNA oligonucleotide RNA40 either complexed with DOTAP or not. [A] Unmodified RNA40 or [B] PTO-backbone modified RNA40 was used. IFN-α secretion was detected by ELISA (n=3, mean ±SD), (*, p<0.05 as compared to the RNA oligonucleotide without DOTAP).

Upon transfection of equal concentrations of encapsulated siRNA and the thereof derived single-stranded RNA oligonucleotides, strong induction of IL-12p40 secretion was detected in wild type DCs (Fig. 4-2). The single-stranded RNAs displayed a higher induction of IL-12p40 compared to the annealed siRNA duplex. To compare the cytokine secretion of cells derived from wild type and TLR7$^{-/-}$ mice, IL-12p40 secretion was normalized to the strictly TLR4-dependent ligand LPS. In TLR7$^{-/-}$ mDCs IL-12p40 secretion upon transfection with single-stranded and annealed siRNA was significantly reduced. The TLR7-specific control resiquimod (R848) showed no IL-12p40 secretion in TLR7$^{-/-}$ cells as expected. The TLR3-specific control Poly(IC)[109] showed equal amounts of secreted IL-12p40 in wild type compared to TLR7$^{-/-}$ cells.

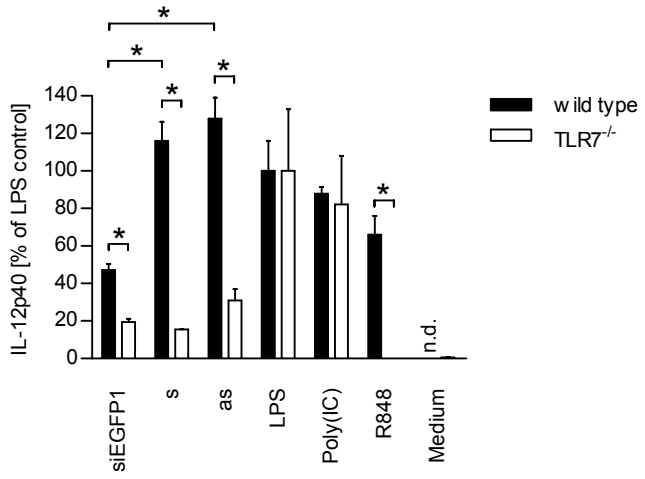

Fig. 4-2 Relevance of TLR7 for siRNA induced immunostimulation
Murine GM-CSF-derived dendritic cells of wild type and TLR7 knockout mice were prepared and stimulated with either 1 µg/ml siRNA targeting EGFP or with 1 µg/ml of the thereof derived sense (s) and antisense (as) strands. RNA molecules were encapsulated with DOTAP prior to transfection. 1 µg/ml R848 served as TLR7-specific control, 100 ng/ml LPS and 25 µg/ml Poly(IC) served as TLR4-specific and TLR3-specific controls, respectively. IL-12p40 secretion was detected by ELISA and values were normalized to LPS for better comparability (n=3, mean ±SD), (n.d., not detected, *, p<0.05 as compared to the wild type control).

4.1.2 Immunostimulation of fuctional siRNAs

To investigate the siRNA-mediated immunostimulation in more detail, it was necessary to establish a model system which enabled the study of siRNA-mediated immunostimulation and siRNA-mediated RNA interference. For this reason siRNAs were designed which targeted the two reporter genes

enhanced green-fluorescent protein (EGFP) and β-galactosidase (BG). For analysis of immunostimulation, human PBMCs were isolated from healthy donors and transfected with RNA oligonucleotides, encapsulated with the transfection reagent DOTAP. Upon transfection of these siRNAs and the corresponding sense (s) - and antisense (as) -strands human PBMCs secreted large amounts of IFN-α (Fig. 4-3 [A]). It could be observed that the transfected RNA molecules showed significant differences in their ability to induce IFN-α secretion. In contrast to RNA-induced IL-12p40 secretion in mDCs (Fig. 4-2) the amounts of secreted IFN-α in human PBMCs upon transfection with siRNA were comparable to single-stranded RNA. To confirm the gene-silencing activity of the tested siRNAs, HEK293T cells were cotransfected with either the EGFP-encoding reporter plasmid pEGFP-N1 or the β-galactosidase-encoding reporter plasmid pSV-β-gal control vector and the respective siRNAs. Gene-silencing activity of the siRNA targeting EGFP was determined by flow-cytometry and fluorescence microscopy, respectively. B-galactosidase activity was analyzed by β-galactosidase assay (Fig. 4-3 [B]+[C]). Both siRNA duplexes showed a silencing activity of approximately 90%, compared to cells which were only transfected with the respective reporter plasmids.

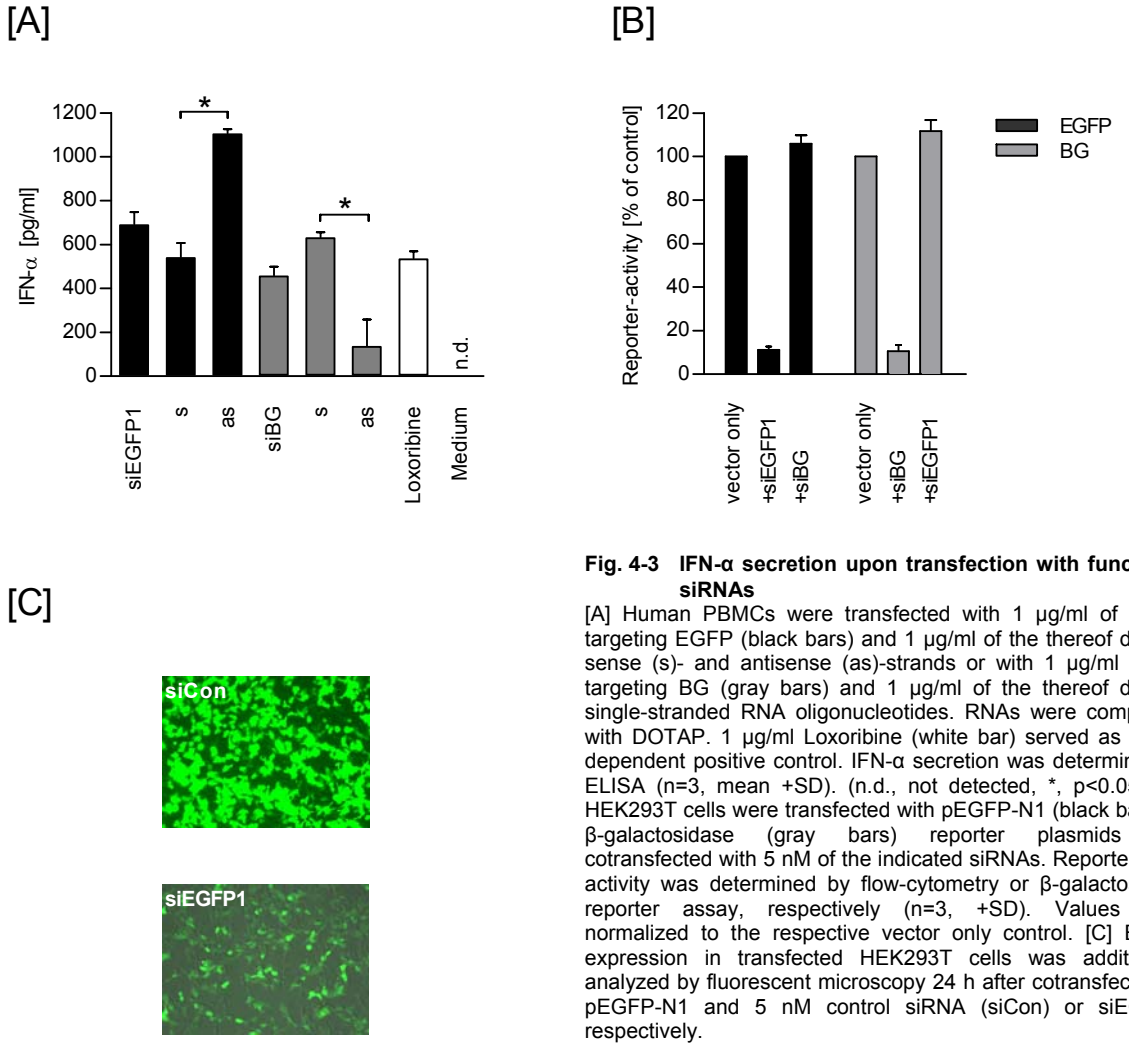

Fig. 4-3 IFN-α secretion upon transfection with functional siRNAs

[A] Human PBMCs were transfected with 1 µg/ml of siRNA targeting EGFP (black bars) and 1 µg/ml of the thereof derived sense (s)- and antisense (as)-strands or with 1 µg/ml siRNA targeting BG (gray bars) and 1 µg/ml of the thereof derived single-stranded RNA oligonucleotides. RNAs were complexed with DOTAP. 1 µg/ml Loxoribine (white bar) served as TLR7-dependent positive control. IFN-α secretion was determined by ELISA (n=3, mean +SD). (n.d., not detected, *, $p<0.05$). [B] HEK293T cells were transfected with pEGFP-N1 (black bars) or β-galactosidase (gray bars) reporter plasmids and cotransfected with 5 nM of the indicated siRNAs. Reporter gene activity was determined by flow-cytometry or β-galactosidase reporter assay, respectively (n=3, +SD). Values were normalized to the respective vector only control. [C] EGFP-expression in transfected HEK293T cells was additionally analyzed by fluorescent microscopy 24 h after cotransfection of pEGFP-N1 and 5 nM control siRNA (siCon) or siEGFP1, respectively.

4.1.3 Analysis of immunostimulatory sequence motifs

Previously, IFN-α secretion upon transfection with RNA oligonucleotides was linked to not precisely defined immunostimulatory sequence motifs. However, sequences with high amounts of uridine residues[86] or high numbers of guanosine-uridine dinucleotides[83] were identified as superior inducers of IFN-α secretion. To analyze the possible influence of these immunostimulatory sequence motifs on siRNA-mediated IFN-α secretion, three different siRNAs were designed, all of them targeting EGFP. Assuming that the presence of certain sequence motifs was responsible for IFN-α secretion, siRNAs were designed that contained either high or low amounts of uridine- or guanosine-uridine dinucleotides in either strand of the respective siRNA duplex. Transfection with the three passenger-strand and the three leading-strand RNA oligonucleotides derived of these siRNAs showed obvious differences in terms of IFN-α secretion (Fig. 4-4). RNA oligonucleotides with low amounts of either uridine residues or guanosine-uridine dinucleotide stretches (EGFP2s, EGFP3s) showed a low ability to induce IFN-α in human PBMCs. However, RNA sequence EGFP3as covered with 10 uridine residues over a total length of 22 nucleotides showed lower amounts of secreted IFN-α, compared to RNA oligonucleotides with equally distributed nucleotides (EGFP1s, EGFP1as). The presence of high numbers of guanosine-uridine dinucleotides did also not result in a higher IFN-α secretion. RNA with a total size of 22 nucleotides, containing 5 guanosine-uridine dinucleotides (EGFP2as) showed a rather moderate IFN-α induction compared to sequences containing only 1 dinucleotide within their sequences (EGFP1s and EGFP1as).

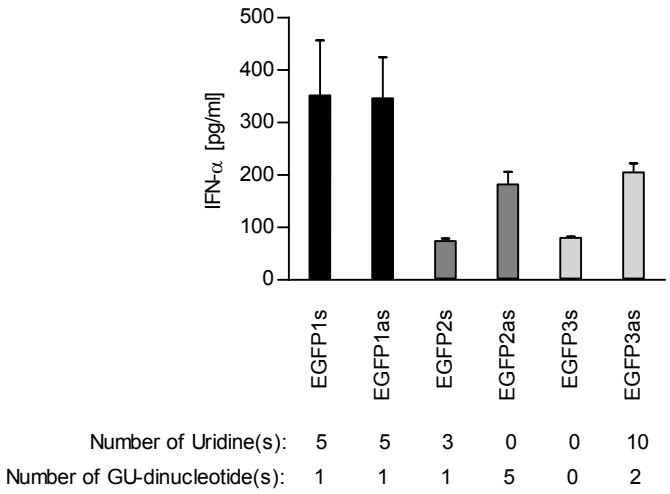

Fig. 4-4 RNA sequence-dependent IFN-α secretion
Human PBMCs were transfected with 1 µg/ml of the indicated single-stranded RNA oligonucleotides derived from siRNAs targeting EGFP. The number of uridine residues and guanosine-uridine (GU)-dinucleotides within the respective sequences is depicted below. IFN-α secretion was determined by ELISA (n=3, mean +SD).

4.1.4 Analysis of nucleotide modifications and their effects on immunostimulation

The presence of naturally occuring nucleotide modifications has been proposed to be relevant for RNA-mediated immunorecognition[89]. The 2'-position of the ribose is apparently not absolutely required for RNA interference activity[182] leading to the speculation that the introduction of non-canonical nucleotides could separate immunostimulation from gene-silencing activity[183]. We assumed that the recognition principles of the immune system causing the siRNA-mediated side effects are highly specific to discriminate between self and non-self RNA molecules. In contrast, the enzymatic system

of the RNAi machinery which targets a high number of different substrate RNAs of different origin might be less discriminating. The choice of modifications that we introduced was governed by the consideration that the modified RNA oligonucleotides were structurally changed at positions that were likely to play a role for immunorecognition but show only negligible effects on the propensity to form double-stranded duplexes necessary for RNA interference.

4.1.4.1 Influence of modifications at the 2'-position of the ribose

The 2'-position of the ribose was considered to be critical for immunorecognition as it is the position where DNA and RNA structurally differ. Two types of modifications were included at this position, those that lack the 2'-oxygen (deoxy derivates) and those that feature a methyl-group at this position (2'-*O*-methyl derivates). The former would miss a functional group, the latter would sterically be very demanding and thereby possibly preventing receptor binding. Based on the sequence EGFP1as which was both immunostimulatory and showed strong RNA interference activity (Fig. 4-3) modified derivates were synthesized. All ribonucleotides of one given nucleobase were replaced by their 2'-deoxy counterpart (dA, dU, dC and dG). Additionally, 2'-*O*-methyl derivates of adenosine (2mA), uridine (2mU) and cytosine (2mC) were prepared (Fig. 4-5).

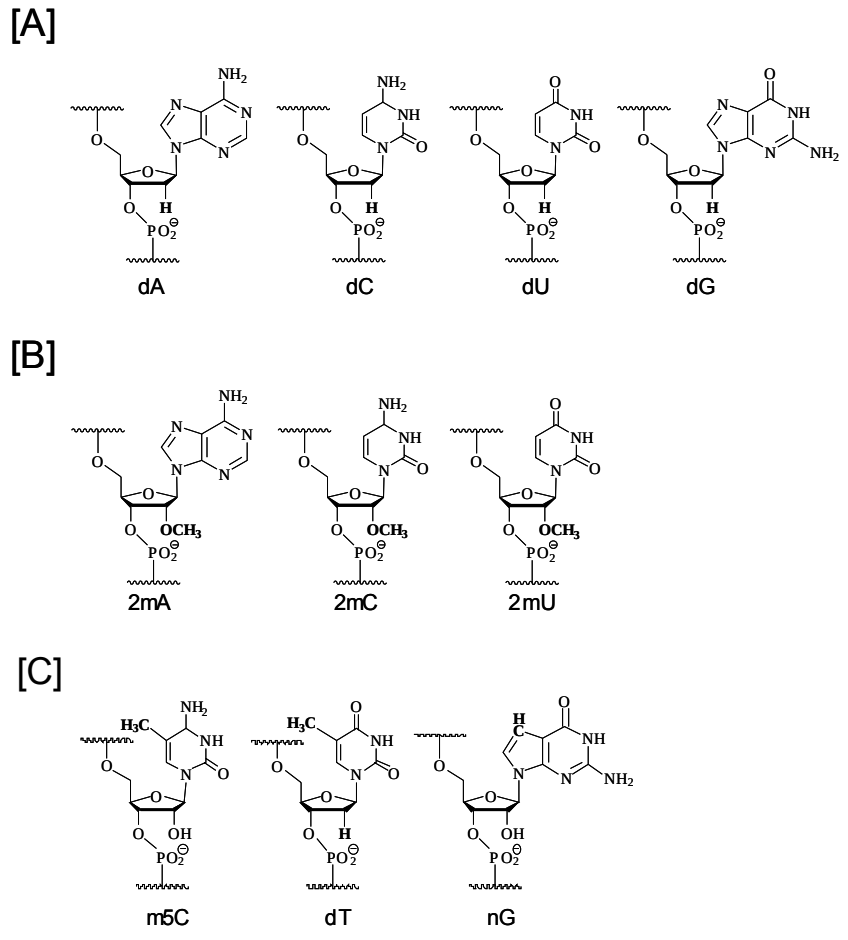

Fig. 4-5 Structures of modified ribonucleotides used in this study
[A] 2'-deoxy derivates of adenosine (dA), cytosine (dC), uridine (dU) and guanosine (dG). [B] 2'-*O*-methyl-derivates of adenosine (2mA), cytosine (2mC) and uridine (2mU). [C] Nucleobase modifications of cytosine: 5'-methyl-cytosine (m5C), uridine: thymidine (dT) and guanosine: 7'-deaza-guanosine (nG). Modifications are depicted in bold letters.

First, the 2'-deoxy derivates of the single-stranded sequence EGFP1as were tested. RNA oligonucleotides were formulated with DOTAP as before and tested for IFN-α secretion from human

PBMCs over a concentration range from 0.01 to 1 µg/ml (Fig. 4-6). Again a dose-dependent IFN-α secretion was observed which varied between 900 and 1400 pg/ml due to donor heterogenity. EGFP1as carrying dU modifications showed a significantly decreased immunostimulatory activity. Residual IFN-α was only detectable at the highest applied concentration of 1 µg/ml of RNA. Diminished IFN-α secretion was also detected for dC-modified EGFP1as, however, the reduction was far less than for dU-modified EGFP1as. Substitution of the other two nucleobases (dA, dG) showed no alteration in IFN-α secretion (Fig. 4-6 [A]).

Next, the 2'-*O*-methyl derivates of EGFP1as were tested. For derivates carrying 2mA or 2mU modified nucleotides IFN-α secretion was completely abrogated. Even at the highest concentration of 1 µg/ml no IFN-α was detectable, exceeding the inhibitory effect of the dU derivate. In contrast, 2mC-modified EGFP1as showed no significant alteration in immunostimulation (Fig. 4-6 [B]).

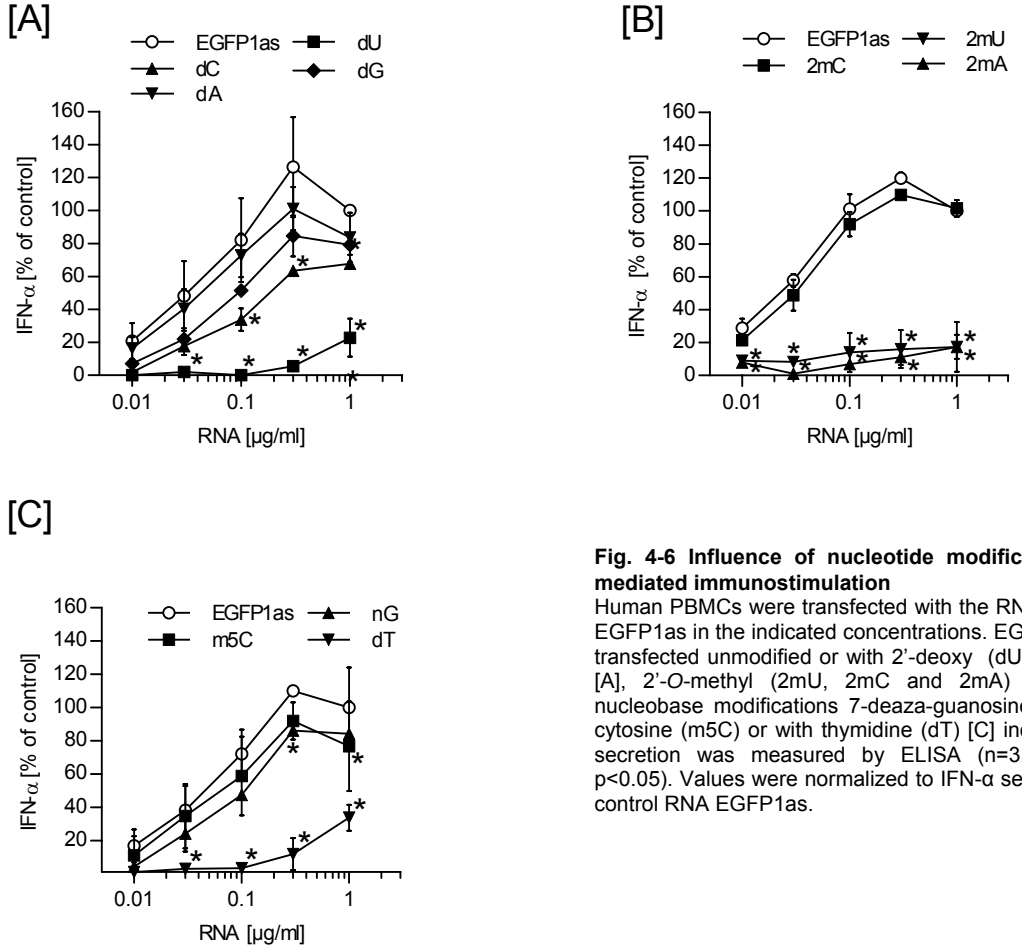

Fig. 4-6 Influence of nucleotide modifications on RNA-mediated immunostimulation
Human PBMCs were transfected with the RNA oligonucleotide EGFP1as in the indicated concentrations. EGFP1as was either transfected unmodified or with 2'-deoxy (dU, dC, dG and dA) [A], 2'-*O*-methyl (2mU, 2mC and 2mA) [B] or with the nucleobase modifications 7-deaza-guanosine (nG), 5'-methy-cytosine (m5C) or with thymidine (dT) [C] incorporated. IFN-α secretion was measured by ELISA (n=3, mean ±SD, *, $p<0.05$). Values were normalized to IFN-α secretion of 1 µg/ml control RNA EGFP1as.

4.1.4.2 Immunostimulation with base-modified derivates

In parallel to backbone modifications nucleobase modified EGFP1as were tested. In contrast to backbone modifications which mediate recognition within the minor groove of any given duplex nucleobase modifications affect the recognition within the major groove. The major groove is the site most frequently involved in sequence-specific interactions between DNA and proteins. Either thymidine (dT) was replaced for all uridine residues or 5'-methyl-cytosine (m5C) replaced the cytosine residues within EGFP1as. Both modifications possess an additional methyl-group at the nucleobase

and were therefore regarded as structurally more demanding. Additionally, guanosine residues were replaced by 7'-deaza-guanosine (nG) which lacks a nitrogen group at the nucleobase (Fig. 4-5 [C]).

Neither nG-modified nor m5C-modified EGFP1as oligonucleotides showed any alteration in IFN-α secretion upon transfection of human PBMCs compared to the unmodified EGFP1as. However, dT-modified EGFP1as showed reduced IFN-α secretion, comparable to the dU-derivate (Fig. 4-6 [C]).

4.1.5 Gene-silencing activity of modification-containing siRNAs

4.1.5.1 Thymidine-containing siRNAs show no alteration of gene-silencing activity

Next, it has to be assessed whether the immunostimulatory relevant modifications affect the activity of the corresponding siRNA duplex in terms of gene-silencing activity. EGFP1as and the four derivates (dU, 2mA, 2mU and dT) showing decreased immunostimulation were annealed to the unmodified complementary sequence (EGFP1s). HEK293T cells were cotransfected with the different siRNAs and pEGFP-N1 encoding the EGFP reporter gene. Additionally, a control siRNA (siCon) with a non-genomic sequence was used to control for sequence-specific RNA interference. The efficiency of siRNA was tested over a concentration range from 1.5 nM up to 15 nM. The unmodified siEGFP1 showed highly efficient gene-silencing activity. EGFP expression was not inhibited but even slightly increased upon cotransfection with the control siRNA (siCon), demonstrating that the detected gene-silencing effects were sequence-specific. Higher plasmid transfection efficiency by cotransfection with non-specific RNA might be the explanation for the observed increase of EGFP expression. Among the modified siRNAs only the dT-containing siRNA displayed silencing activity comparable to the unmodified siRNA. In contrast, dU- and 2mU-containing siRNAs suppressed EGFP expression much less with inhibition of 43% and 38% at 1.5 nM concentration, respectively. By increasing the siRNA concentration ten-fold gene-silencing activity was improved but still not as efficient as the unmodified siRNA. 2mA-modified siRNA showed even at the highest concentration low gene-silencing activity (Fig. 4-7).

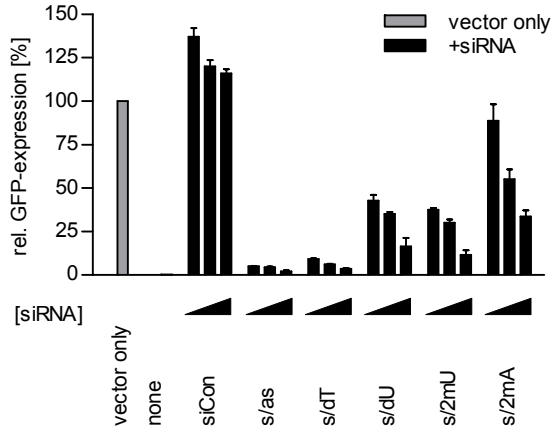

Fig. 4-7 Gene-silencing using 2'-deoxy- and 2'-*O*-methyl-modified siRNA duplexes
HEK293T cells were transfected with EGFP expressing vector pEGFP-N1 (gray bar). Additionally, annealed siRNA targeting EGFP composed of an unmodified strand in sense orientation and unmodified (s/as), thymidine (s/dT)-, deoxy-uridine (dU)-, 2'-*O*-methyl-uridine (s/2mU)- or 2'-*O*-methyl-adenosine (s/2mA)- modified antisense strand was added (black bars) in increasing concentrations of 1.5 nM, 7.5 nM and 15 nM. A control siRNA (siCon) was used to test for specificity of gene-silencing. Values are normalized to the EGFP expression of the vector control. EGFP expression was analyzed by flow cytometry (n=3, mean +SD) and mean fluorescence intensity is displayed as compared to the vector only control.

4.1.5.2 Thymidine residues separate immunostimulation from gene-silencing

Thymidine modification displayed the favorable residue to reduce IFN-α secretion in human PBMCs and additionally barely affected gene-silencing activity. To determine whether these observations were specific for the tested siRNA (siEGFP1) or hold true for siRNAs in general, two further siRNAs,

targeting either EGFP at another position (siEGFP2) or β-galactosidase (siBG), were included in the experiments. Leading-strands of these two siRNAs contained a high amount of uridine nucleotides and guanosine-uridine dinucleotides allowing for immunostimulation. Uridine residues in the respective leading-strands were again replaced by thymidine residues. The modified RNA oligonucleotides were applied to human PBMCs and IFN-α secretion was analyzed (Fig. 4-8 [A]-[C]). We observed a strong dose-dependent IFN-α secretion upon transfection with all unmodified RNA oligonucleotides. In all cases introduction of thymidine residues reduced

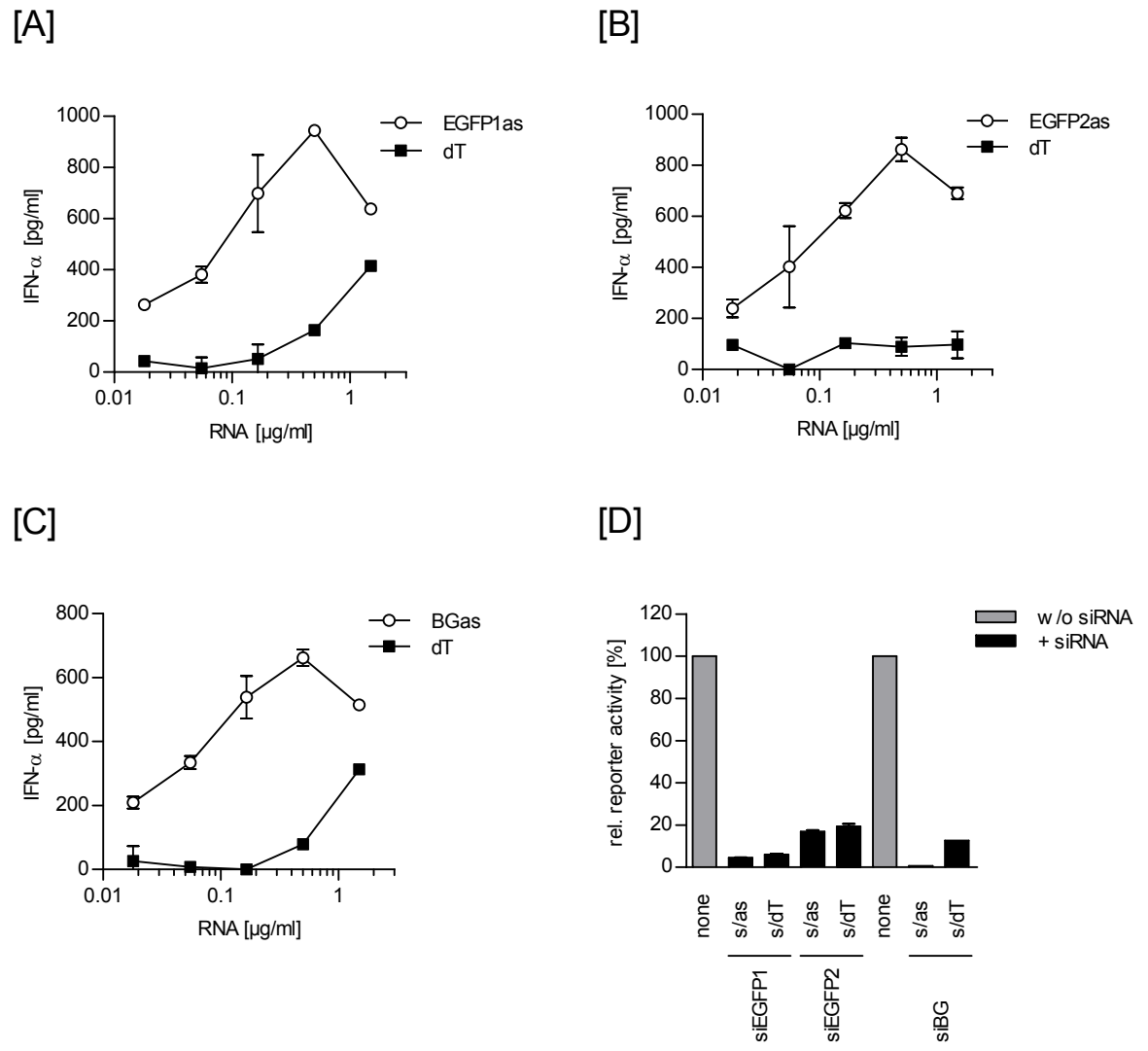

Fig. 4-8 Thymidine modified siRNAs separate immunostimulation from gene-silencing
[A]-[C], Human PBMCs were transfected with the single-stranded RNA oligonucleotides EGFP1as [A], EGFP2as [B] and BGas [C] either unmodified or dT-modified in the indicated concentrations. IFN-α secretion was determined by ELISA, (n=2, mean ±SD). [D], HEK293T cells were transfected with reporter plasmids encoding EGFP and β-galactosidase (gray bars). 5 nM annealed siRNA duplexes composed of unmodified sense strand (s/as) and thymidine-containing antisense strand (s/dT) and directed against EGFP (siEGFP1, siEGFP2) or β-galactosidase (siBG) were tested for gene-silencing activity. Values were normalized to the vector only control (n=3, mean +SD).

IFN-α secretion strongly, showing only for the highest concentration of 1.5 µg/ml a low IFN-α secretion. These results confirmed our hypothesis that thymidine residues display a modification that reduces IFN-α secretion in general. Next, siRNA duplexes, containing the modified leading-strand were generated by annealing to unmodified passenger-strand and gene-silencing activity was analyzed by reporter gene knockdown (Fig. 4-8 [D]). Reporter gene expression of EGFP and

β-galactosidase was suppressed in HEK293T cells by siRNAs carrying dT modifications comparable to unmodified siRNA. These results confirmed that thymidine modifications reduce IFN-α secretion but retain gene-silencing activity for more than one sequence implicating a general principle.

4.1.6 Effect of thymidine residues in both strands of the siRNA duplex

We clearly demonstrated that uridine replacement by thymidine residues reduced IFN-α secretion significantly and that residual IFN-α secretion was only observed at high concentrations. Moreover, thymidine residues in the leading-strand of a siRNA did not affect RNA interference. However, the passenger-strand of siEGFP1 by itself showed also strong IFN-α secretion upon transfection (Fig. 4-3). We therefore assumed that possibly the remaining immunostimulation was mediated by unmodified passenger-strand. To further decrease IFN-α secretion we generated a thymidine-containing passenger-strand for siEGFP1. Annealing of modified leading- and modified passenger-strand resulted in a siRNA containing thymidine modifications in both strands. Transfection of human PBMCs with siRNA carrying dT modifications in both strands reduced IFN-α secretion further as compared to the siRNA carrying dT modifications only in the leading-strand. IFN-α secretion was only detectable at concentrations above 0.3 µg/ml (Fig. 4-9 [A]). Next, we had to examine whether this siRNA was still as effective in terms of gene-silencing as the unmodified siRNA. Cotransfection of pEGFP-N1 reporter plasmid and the respective siRNAs in HEK293T cells showed no alteration of gene-suppression activity (Fig. 4-9 [B]). Concentrations necessary for efficient gene-silencing (0.03-0.1 µg/ml) were far below any concentration of residual IFN-α secretion.

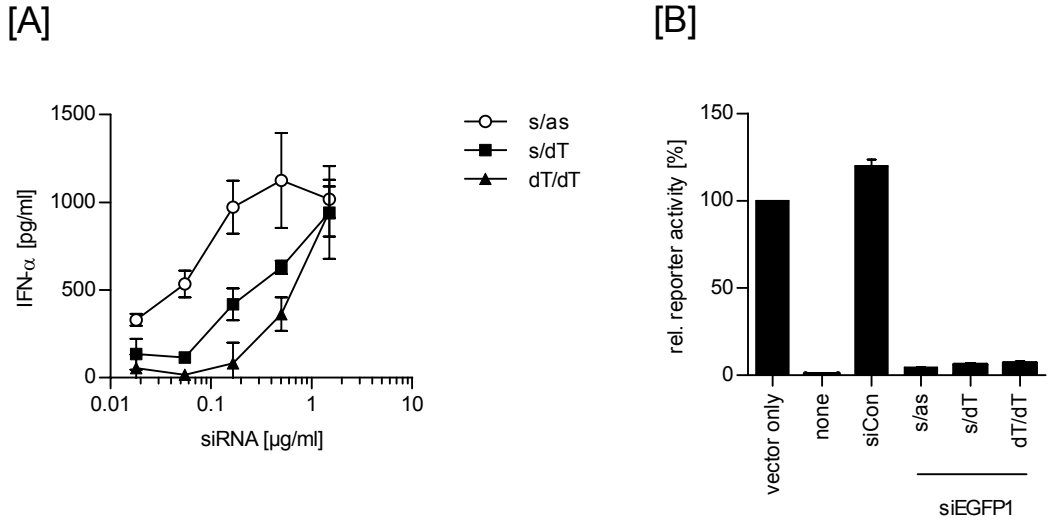

Fig. 4-9 Effect of thymidine modifications in sense- and antisense-strands of a siRNA duplex
Human PBMCs were transfected with annealed siRNA (siEGFP1) that was composed of unmodified strands (s/as) and thymidine modifications in the leading-strand (s/dT) or containing thymidine modifications in either strand (dT/dT) in the indicated concentrations. IFN-α secretion was measured by ELISA (n=3, mean ±SD) [A]. HEK293T cells were transfected with pEGFP-N1 reporter plasmid or cotransfected with 5 nM of the annealed siRNAs and tested for gene-silencing activity. Control siRNA (siCon) served as specificity control and untransfected HEK293T cells (none) were tested for autofluoresence. Gene-silencing activity was analyzed by flow cytometry (n=3, mean +SD).

4.1.7 Antagonistic effects on RNA-induced interferon-α secretion

It had been reported before that 2'-*O*-methyl derivates of RNA oligonucleotides act as TLR7-antagonists[184]. However, from the results above it seemed unlikely that thymidine modifications act in a dominant-negative manner on TLR7-signalling. To address this issue we repeated stimulation experiments with siRNA duplexes from above but also included the 2'-*O*-methyl-modified adenosine

and uridine residues in the leading-strand of siEGFP1. Again, we detected a reduced IFN-α induction by siRNA carrying thymidine residues in the leading-strand. The siRNA duplex containing 2'-*O*-methyladenosine in the leading-strand showed completely abrogated IFN-α secretion (Fig. 4-10 [A]). This indicated that the 2'-*O*-methyladenosine-modified RNA strand was able to suppress the signalling of the active unmodified passenger-strand of the siRNA duplex in contrast to thymidine-modified siRNA. Surprisingly, the abrogation of IFN-α secretion was not observed when transfecting a siRNA carrying 2'-*O*-methyluridine in the leading-strand. Although showing a decrease in IFN-α secretion immunostimulation was still higher than for thymidine-modified siRNA. To further investigate the dominant-negative behavior of 2'-*O*-methyladenosine-modified RNA oligonucleotides, human PBMCs were cotransfected with unmodified and modified EGFP1as strands both in the antisense conformation thus avoiding the formation of a double-stranded duplex. The presence of 2'-*O*-methyladenosine suppressed the activity of the otherwise stimulative unmodified EGFP1as completely (Fig. 4-10 [B]). In contrast, thymidine-modified EGFP1as did not alter the immunostimulatory potential of the cotransfected unmodified EGFP1as. Thymidine residues therefore represent a modification, which in contrast to 2'-*O*-methyladenosine, acts as an immunological silent but not dominant-negative modification.

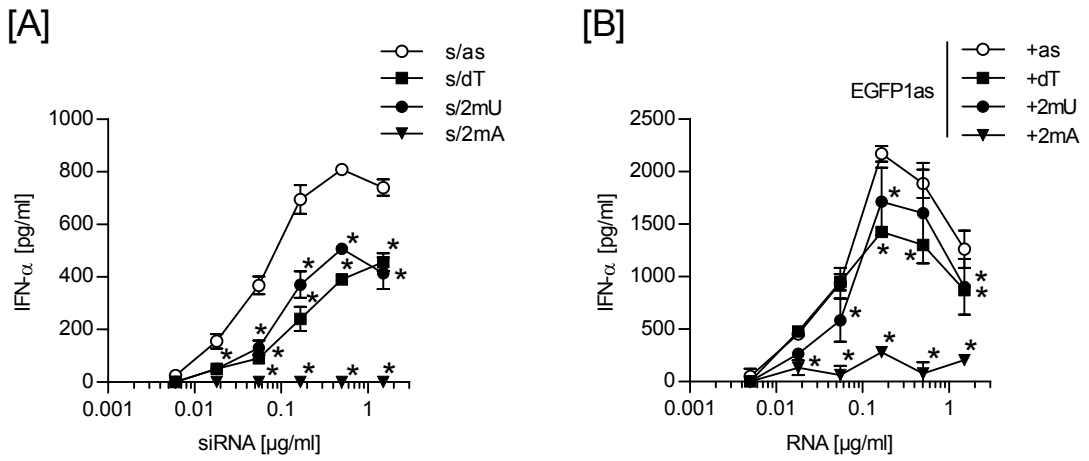

Fig. 4-10 2'-*O*-methyladenosine modified, but not thymidine modified RNA strands possess antagonistic activity
[A] Human PBMCs were transfected with annealed siRNA (siEGFP1) that was composed of unmodified strands (s/as), thymidine (s/dT), 2'-*O*-methyluridine (s/2mU) and 2'-*O*-methyladenosine (s/2mA) modifications in the leading (antisense) strand. IFN-α secretion was measured by ELISA (n=3, mean ±SD), (*, $p<0.05$ as compared to the unmodified siRNA). [B] Human PBMCs were transfected with unmodified RNA oligonucleotide EGFP1as (as). The indicated modified oligonucleotides also in antisense orientation were added in equal concentrations. IFN-α secretion was measured by ELISA (n=3, mean ±SD), (*, $p<0.05$ as compared to unmodified EGFP1as with addition of unmodified EGFP1as).

4.1.8 Secondary structure formation of RNA oligonucleotides

Our results as well as data from the literature[81,83,86] suggest that uridine residues are critical for TLR7-mediated immunorecognition. Furthermore, uridine plays a pivotal role in the formation of intramolecular duplexes since it can form hydrogen bonds with guanosine and adenosine residues[185]. We therefore investigated the secondary structure formation of the immunostimulatory RNA oligonucleotide EGFP1as. EGFP1as was subjected to UV monitored thermal denaturation. Indeed, the resulting melting curve exhibited two sigmoidal transition points. The first was observed just below room temperature the second at approximately 50°C. In contrast, thymidine-modified EGFP1as showed only the latter one. The altered propensity to form partial double-stranded structures might be

due to the additional, sterically demanding methyl-group of the thymidine residues (Fig. 4-11). To further validate the hypothesis of secondary structure formation for immunostimulation, we performed the same experiment with EGFP3s, an RNA oligonucleotide with very low immunostimulatory potential (Fig. 4-11). We obtained a much broader transition with reduced hyperchromicity, comparable to the control Poly(C), which is unable to form any secondary structures (Fig. 4-11).

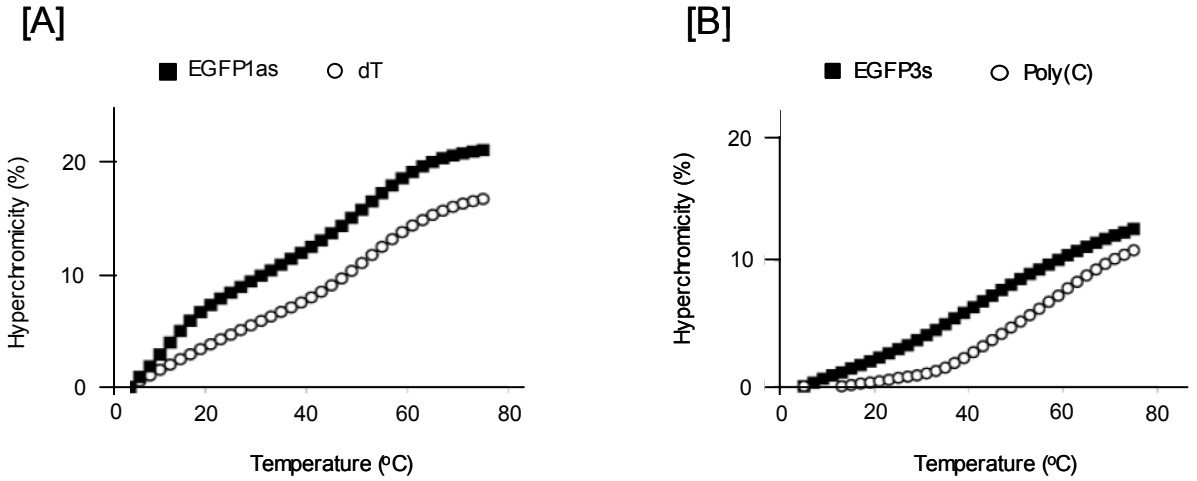

Fig. 4-11 UV-melting curves
Transition of EGFP1as and thymidine modified [A] and transition of EGFP3s and Poly(C) [B] was detected at 260 nm wavelength. Oligoribonucleotide concentration was 3.5 µM in 1x PBS. Concentration of Poly(C) was adjusted to the same molarity.

The results of the hyperchromicity experiments were further validated using the structure prediction program Mfold[179]. Structure prediction analysis was performed for RNA oligonucleotides regarding intramolecular secondary structures (unimolecular folding) and intermolecular secondary structures (dimerization). Structure predictions underlined that EGFP1as might form secondary structures. The predicted structures showed that the immunostimulatory RNA oligonucleotide EGFP1as bears the ability to form uridine-containing duplex structures in the monomeric and dimeric conformation (Fig. 4-12).

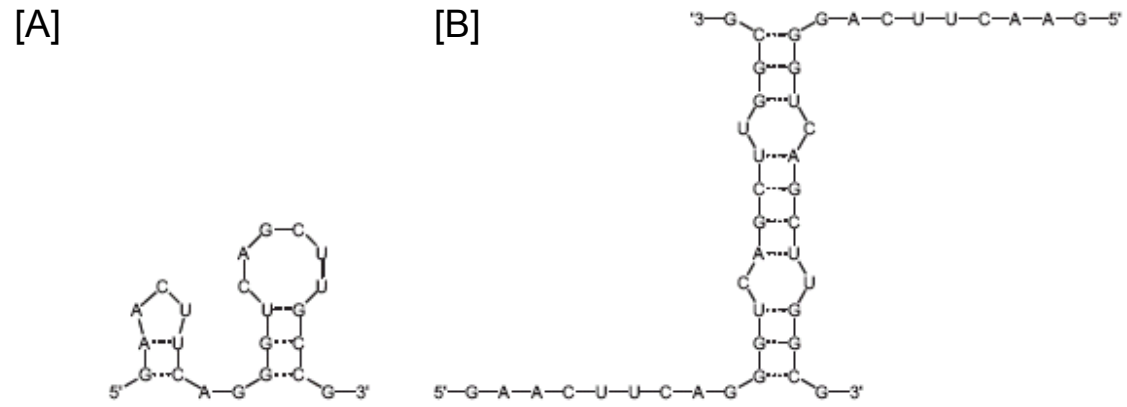

Fig. 4-12 Predicted secondary structure of EGFP1as
Predicted structure of unimolecular folding [A] and dimerization [B] of RNA oligonucleotide EGFP1as as calculated with Mfold software. Sequences were entered with or without the corresponding pairing partner together with the following conditions: 142 nM [1 µg/ml] of strand concentration and 150 mM NaCl.

In contrast, prediction for the non-immunostimulatory RNA oligonucleotide EGFP3s showed no tendency to form any significant duplex structures (data not shown). Structure predictions of eight further RNA oligonucleotides showed that sequences with high immunostimulatory activity always formed stem/duplex structures with incorporated uridine residues (structure predictions not shown).

4.1.9 Positional influence of thymidine modifications on immunostimulation

To address the issue whether immunostimulation is induced by uridine residues within stem/duplex structures uridine residues were replaced by thymidine residues in the immunostimulatory RNA oligonucleotides EGFP1as and EGFP2as at selected positions (Fig. 4-13). Modifications were either inserted in predicted duplex/stem structures (EGFP1as(dT-B), EGFP1as(dT-C), EGFP2as(dT-B)) or in sequence stretches with no predicted propensity for structure formation (EGFP1as(dT-A), EGFP2as (dT-A)), resulting in RNA oligonucleotides with partially substituted thymidine residues. Transfection of human PBMCs resulted in a dose-dependent IFN-α secretion upon transfection with the unmodified RNA oligonucleotides. IFN-α secretion was slightly reduced upon partial introduction of thymidine residues but was still elevated for all RNA oligonucleotides compared to the completely thymidine modified RNA oligonucleotides (Fig. 4-13). The most significant reduction for partial substitution with thymidine residues in IFN-α secretion for EGFP1as was detected for EGFP1as(dT-A), which carried thymidine residues in predicted single-stranded stretches, whereas the strongest reduction in IFN-α secretion for EGFP2as was obtained for EGFP2as(dT-B), containing thymidine residues exclusively in duplex/stem structures.

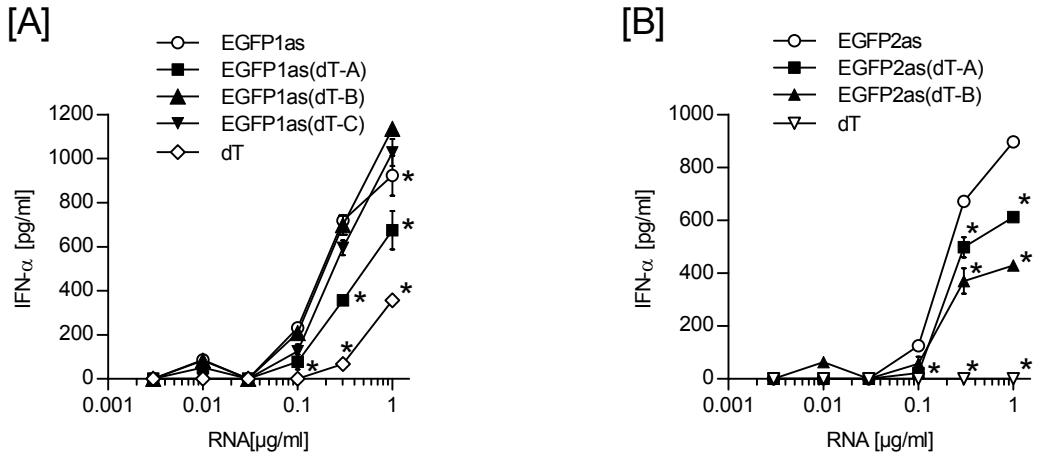

Fig. 4-13 Effect of partially thymidine-modified RNA oligonucleotides on IFN-α secretion
[A] Human PBMCs were transfected with unmodified RNA oligonucleotide EGFP1as, GAACdTdTCAGGGUCAGCUUGCCG (EGFP1as(dT-A)), GAACUUCAGGGdTCAGCdTdTGCCG (EGFP1as(dT-B)), GAACUUCAGGGUCAGCdTdTGCCG (EGFP1as(dT-C)) and totally thymidine-modified (dT). Positions of thymidine modifications are depicted as dT. IFN-α secretion was determined by ELISA (n=3, mean ±SD), (*, $p<0.05$ as compared to unmodified EGFP1as). [B] RNA oligonucleotide EGFP2as was used for transfection either unmodified, partially thymidine-modified GACGdTdTGdTGGCUGUUGUAGUUG (EGFP2as(dT-A)) or GACGUUGUGGCdTGdTdTGdTAGdTdTG (EGFP2as(dT-B)) or totally thymidine-modified (dT). Positions of thymidine modifications are depicted as dT in bold letters. IFN-α secretion was determined by ELISA (n=3, mean ±SD), (*, $p<0.05$ as compared to unmodified EGFP2as).

4.1.10 Summary

It could clearly be shown that thymidine-modified RNA oligonucleotides significantly reduced IFN-α secretion in human PBMCs. Annealed siRNA duplexes with thymidine-modified antisense strand also decreased IFN-α secretion without affecting gene-silencing activity. This can be regarded as a general principle since it was tested for three different functional siRNA sequences. Introducing thymidine modifications in either strand of a siRNA duplex reduced IFN-α secretion further without any detectable influence on RNA interference. In contrast 2'-*O*-methyladenosine-, 2'-*O*-methyluridine- and 2'-deoxyuridine-modified RNA oligonucleotides reduced IFN-α secretion but showed lower efficiency in gene-silencing. Further, 2'-*O*-methyladenosine-modified but not thymidine-modified RNA oligonucleotides possessed antagonistic activity. We further show strong evidence that secondary structure formation mediates RNA-mediated immunostimulation. However, the presence of uridine residues in stem/duplex displays not the only target structure for immunorecognition principles.

4.2 Immunorecognition of prokaryotic RNA

RNA of prokaryotic origin has been suggested to be recognized as a non-self structure[186]. In contrast to the recognition principles of RNA oligonucleotides such as siRNAs (4.1.2) and viral RNA only little is known about bacterial RNA recognition. TLRs could be involved due to (i) the decreased extent of nucleotide modifications in prokaryotic RNA as compared to eukaryotic RNA, (ii) positive sensing of nucleotide modifications that are absent in eukaryotic RNA or (iii) presence of sequence patterns specific for prokaryotic RNA. Furthermore, the cytosolic RNA-helicases RIG-I and MDA5 might detect bacterial RNA due to the fact that (i) prokaryotic messenger RNA is 5'-triphosphorylated thereby representing a possible target structure for RIG-I[187] or (ii) because ribosomal RNA forms secondary structures that display partial double-stranded conformation[188]. In this study we were interested to identify the mechanisms how bacterial RNA is recognized by the innate immune system. We addressed the question whether recognition of bacterial RNA is species-dependent and whether it follows the same recognition principles described for RNA oligonucleotides or viral RNA.

4.2.1 Purification and validation of prokaryotic RNA

Before transfecting cells with bacterial RNA, RNA was purified and controlled by capillary electrophoresis. For all experiments only RNA with an optical density quotient 260/280 nm of 2.0 or higher and with high integrity was used (Fig. 4-14). RNaseA-treated RNA and isolated 16S ribosomal *Escherichia coli* RNA was validated the same way. All RNA preparations showed high integrity and the expected ribosomal RNA pattern. Smaller size of 23S rRNA of *Proteus mirabilis* is congruent to the published sequence (www.ncbi.nlm.nih.gov). Besides the ribosomal RNA molecules several fragments of smaller size were detected. These fragments are cleavage products of 23S ribosomal RNA as already described[189] and not unspecific degradation products. These cleavage products are species-specific and were always detected in the same pattern for a given species. Digestion with RNaseA showed a complete loss of the signal, proving complete digestion of the *Escherichia coli* total RNA. The presence of residual fragments of 25 nt in size or smaller cannot be ruled out due to the detection limit of the capillary electrophoresis. However, as it has been reported that immunorecognition

requires a minimum length of the RNA ligand of 19 nt length[190], RNase digestion was regarded as complete. Isolated *E.coli* 16S ribosomal RNA showed the expected size and no further residual RNA molecules.

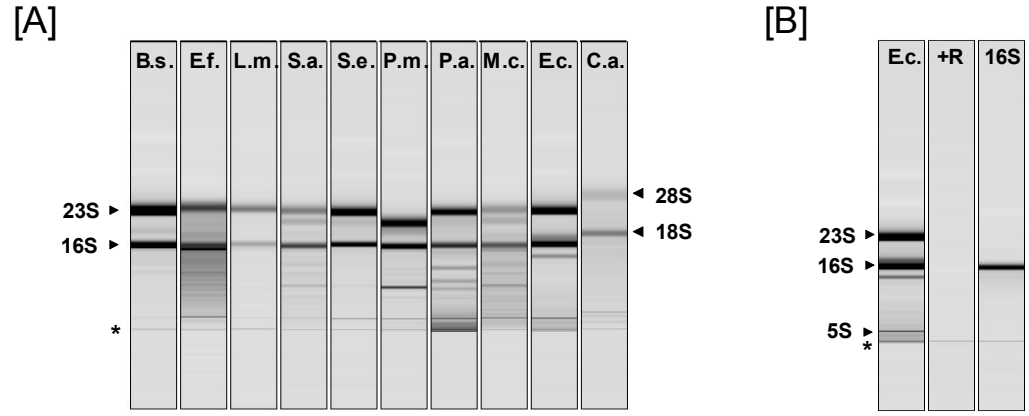

Fig. 4-14 Capillary electrophoresis image
[A] Total RNA preparations of *Bacillus subtilis* (B.s.), *Enterococcus faecalis* (E.f.), *Listeria monocytogenes* (L.m.), *Staphylococcus aureus* (S.a.), *Staphylococcus epidermidis* (S.e.), *Proteus mirabilis* (P.m.), *Pseudomonas aeruginosa* (P.a.), *Moraxella catharralis* (M.c.), *Escherichia coli* (E.c.) and the yeast *Candida albicans* (C.a.) were analyzed by capillary electrophoresis. The prokaryotic ribosomal 16S and 23S RNAs and the eukaryotic 18S and 28S ribosomal RNAs are depicted, *, indicates the 25 nt calibration marker. [B] RNase digested total E.coli RNA preparation (+R) and isolated *y* 16S ribosomal RNA (16S) were compared to total *E.coli* RNA preparation (E.c.). 5S, 16S and 23S ribosomal RNA are depicted, *, indicates the internal calibration marker.

4.2.2 Bacterial RNA induces a type-I interferon response in human PBMCs

4.2.2.1 Characterization of prokaryotic RNA-induced type-I interferon secretion

The total RNA preparations of five gram-positive bacterial species (*Bacillus subtilis*, *Enterococcus faecalis*, *Listeria monocytogenes*, *Staphylococcus aureus* and *Staphylococcus epidermidis*) and four gram-negative bacterial species (*Escherichia coli*, *Moraxella catharralis*, *Pseudomonas aeruginosa* and *Proteus mirabilis*) as well as RNA from *Candida albicans* as a eukaryotic control were formulated with DOTAP to increase endosomal delivery and tested for interferon-α (IFN-α) secretion of human PBMCs. IFN-α secretion in PBMCs is exclusively mediated by the activation of plasmacytoid dendritic cells, possibly via TLRs[24]. We observed a robust IFN-α secretion upon transfection of 1 µg/ml with all tested prokaryotic RNA preparations (Fig. 4-15 [A]). Transfection was performed in decreasing concentrations which reduced IFN-α secretion dose-dependently (data not shown). Species-specific IFN-α secretion varied between 700 and 1400 pg/ml. In contrast, *Candida albicans* RNA showed comparable weak immunostimulatory activity with secretion of 200 pg/ml IFN-α. Besides RNA, bacterial lysates contain a lot of different immunostimulatory molecules, such as LPS or CpG DNA. To exclude the possibility that immunostimulation was rather an effect of contaminations in the preparations than due to the RNA, all samples were digested by incubation with RNaseA. Digest efficiency was controlled by visualizing samples through automated capillary gel electrophoresis (shown for *E.coli* RNA in Fig. 4-14 [B]).

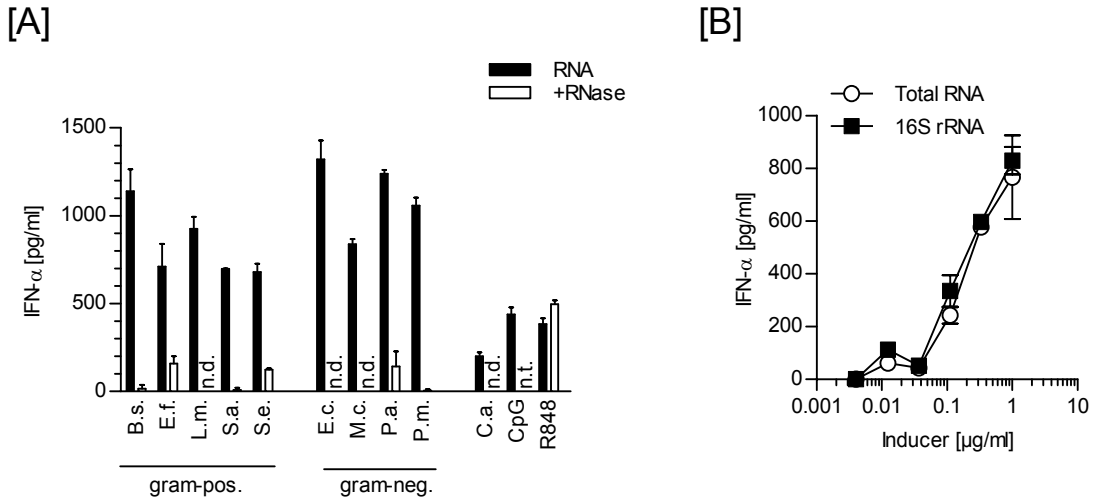

Fig. 4-15 Effects of bacterial RNA on IFN-α secretion in human PBMCs
[A] Human PBMCs were transfected with 1 µg/ml of total RNA preparations of *Bacillus subtilis* (B.s.), *Enterococcus faecalis* (E.f.), *Listeria monocytogenes* (L.m.), *Staphylococcus aureus* (S.a.), *Staphylococcus epidermidis* (S.e.), *Escherichia coli* (E.c.), *Moraxella catharralis* (M.c.), *Pseudomonas aeruginosa* (P.a.), *Proteus mirabilis* (P.m.) and the yeast *Candida albicans* (C.a.). RNAs were complexed with DOTAP prior to transfection. RNA was either untreated or digested with RNaseA. 1 µg/ml R848 and 1µM CpG DNA oligonucleotide 2216 (CpG) served as TLR7-specific and TLR9-specific positive controls for pDC activation. [B] Human PBMCs were transfected with either *Escherichia coli* total RNA or isolated 16S ribosomal RNA over the indicated concentration range. IFN-α secretion was measured by ELISA (n=3, mean ±SD). (n.d., not detected, n.t., not tested).

RNaseA treatment resulted in complete abrogation of IFN-α secretion (Fig. 4-15 [A]). Moreover, LPS a major and highly potent stimulus from gram-negative bacteria did not induce IFN-α which is consistent with the absence of TLR4 on plasmacytoid dendritic cells (pDCs)[191]. Next, we took into account that 80% of the total cellular RNA consists of the ribosomal RNA fraction[90] and isolated *E.coli* 16S ribosomal RNA (Fig. 4-14). Transfection with equal amounts of *E.coli* 16S ribosomal RNA and *E.coli* total RNA showed no alteration in IFN-α secretion over the tested concentration range. This indicates that ribosomal RNA represents the major immunostimulatory fraction within total bacterial RNA preparations (Fig. 4-15 [B]).

4.2.2.2 Interferon-α secretion in PBMCs depends on endosomal recognition

Next, we assessed whether bacterial RNA induces IFN-α in a manner dependent on TLR7 as it has been described for RNA oligonucleotides and viral RNAs[83,87,192]. Human PBMCs were transfected with different amounts of *Escherichia coli* and *Staphylococcus aureus* total RNA preparations as well as with RNA40 oligonucleotide, a well defined ligand for TLR7 activation[81]. For all RNAs a robust and dose-dependent IFN-α secretion was observed which was abrogated upon RNaseA treatment. Cotransfection with 2'-*O*-methyl-adenosine modified RNA oligonucleotide (2mA), which has been shown to act as a TLR7- and TLR8-specific inhibitor[167] (4.1.7) led to a complete abrogation of IFN-α secretion (Fig. 4-16 [A]). In contrast, cotransfection of 2mA with the TLR9-specific ligand CpG2216 did not alter IFN-α secretion, confirming the specificity of the inhibitor. Further, human PBMCs were incubated with increasing concentrations of chloroquine, which inhibits endosomal acidification and therefore inhibits signalling of the endosomally localized TLRs 3, 7 and 8. Chloroquine treatment resulted in a significant concentration-dependent reduction of IFN-α secretion upon transfection with bacterial RNA (Fig. 4-16 [B]) and CpG2216. These results indicate that bacterial RNA-mediated IFN-α secretion in human PBMCs depends on intact TLR7 signalling.

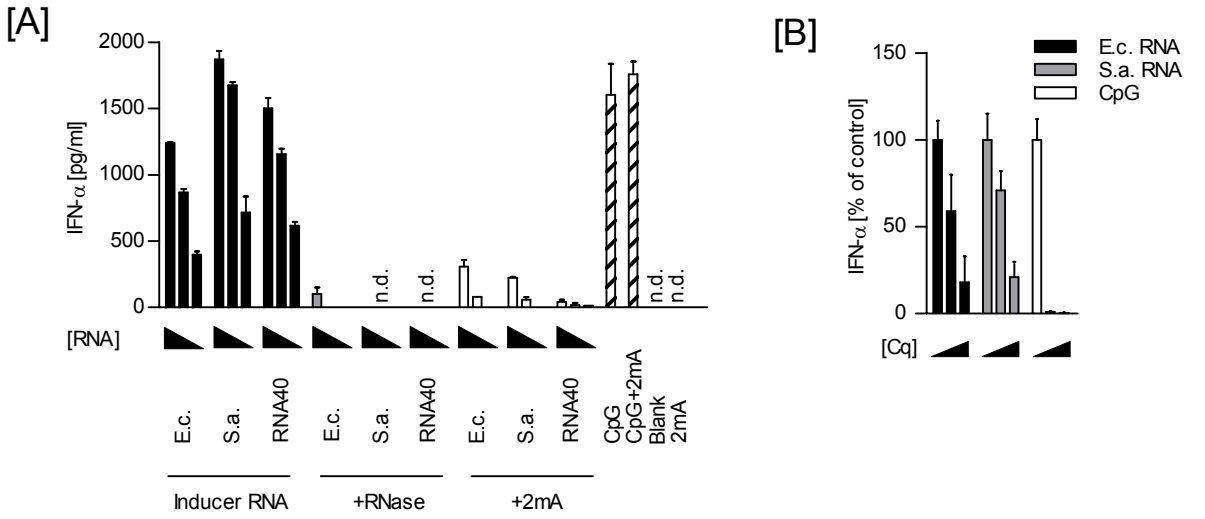

Fig. 4-16 TLR7-mediated IFN-α secretion upon bacterial RNA transfection
[A] Human PBMCs were transfected with *Escherichia coli* and *Staphylococcus aureus* total RNA or RNA40 oligonucleotide with decreasing concentrations from 1 µg/ml to 100 ng/ml. RNAs were either untreated, RNaseA-treated (+RNase) or cotransfected with inhibitory oligonucleotide 2mA (+2mA) at equal concentrations. 1 µM CpG2216 served as TLR9-specific positive control. [B] Human PBMCs were pre-incubated for two hours at 37°C with increasing concentrations (0 nM, 3 nM, and 30 nM) of chloroquine (Cq) and transfected with *Escherichia coli* and *Staphylococcus aureus* RNA. IFN-α secretion was detected by ELISA (n=2, mean +SD), values are depicted either in concentration [A] or depicted as compared to the untreated control [B]. (n.d., not detected).

4.2.2.3 Bacterial RNA triggers signalling pathways apart from TLR7

In addition to IFN-α secretion upon bacterial RNA transfection, we also observed a robust, dose-dependent TNF-α secretion in human PBMCs which is induced besides TLR7 by TLR8 which is strongly expressed in monocytes (Fig. 4-17). Cotransfection of 2mA and RNA40 led to a complete loss of TNF-α secretion, which again confirms the TLR7- and TLR8-dependent recognition of RNA oligonucleotides. Despite the complete reduction of secreted IFN-α, cotransfection of 2mA and bacterial RNA did not alter the amount of secreted TNF-α (Fig. 4-17 [A]). TNF-α secretion upon transfection with the TLR4-specific control LPS was not altered by cotransfection with the TLR7 inhibitor 2mA. RNaseA digestion proved that the major immunostimulatory fraction was bacterial RNA. Residual TNF-α secretion might be due to contaminations within the preparation, which trigger different pattern-recognition receptors expressed on the different cell-types within the human PBMC preparation. Additionally, chloroquine treatment did not alter bacterial RNA-induced TNF-α secretion similar to LPS which triggers the surface-located TLR4 (Fig. 4-17 [B]). These results implicate that TNF-α secretion upon transfection with bacterial RNA is independent of endosomal maturation and therefore independent of nucleic-acid sensing TLRs since all of them are endosomally localized[13-15]. Bacterial RNA recognition obviously differs from the recognition mechanisms described for RNA oligonucleotide with respect to TNF-α production in human PBMCs.

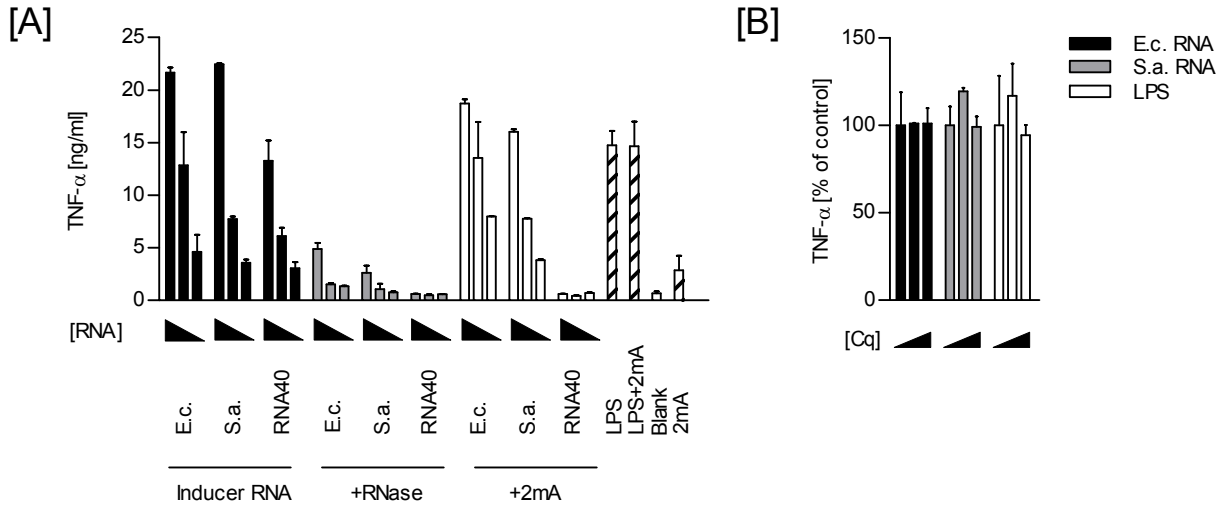

Fig. 4-17 Bacterial RNA-induced TNF-α secretion in human PBMCs
[A] Human PBMCs were transfected with *Escherichia coli* and *Staphylococcus aureus* total RNA or RNA40 oligonucleotide with decreasing concentrations from 1 µg/ml to 100 ng/ml. RNAs were either untreated, RNaseA-treated (+RNase) or cotransfected with inhibitory oligonucleotide 2mA (+2mA) at equal concentrations. 100 ng/ml LPS served as TLR4-specific positive control. [B] Human PBMCs were pre-incubated for two hours at 37°C with increasing concentrations (0 nM, 3 nM, and 30 nM) of chloroquine (Cq) and transfected with *Escherichia coli* and *Staphylococcus aureus* RNA. TNF-α secretion was detected by ELISA (n=2, mean +SD), values are depicted either in concentration [A] or depicted as compared to the untreated control [B].

4.2.3 Bacterial RNA induces IL-12p40 in murine dendritic cells

To further characterize the recognition mechanisms of bacterial RNA, it was necessary to study RNA stimulation in mice to make use of the published knockout mice. For this reason either FLT3L-derived pDC-like cells or GM-CSF-derived mDC-like cells were generated and either IFN-α or IL-12p40 as respective activation markers were detected. FLT3L-derived pDC-like dendritic cells are murine analogs to human pDCs characterized by TLR7 and TLR9 expression and enhanced endosomal trafficking. GM-CSF-derived mDC-like cells are regarded as analog to human myeloid dendritic cells. The generated cells showed a purity of 85% or higher as determined by flow cytometry (data not shown).

4.2.3.1 Bacterial species-specific recognition

GM-CSF-derived mDC-like cells showed a strong secretion of IL-12p40 upon transfection with *Escherichia coli* total RNA. IL-12p40 secretion was significantly reduced upon RNA digestion with RNaseA, indicating that the observed immunostimulation was mainly caused by the RNA itself. Eukaryotic RNA preparations from HEK293T cells and the yeast *Candida albicans* did not induce any detectable IL-12p40 (Fig. 4-18 [A]). Additionally, it was tested whether transfection procedure or RNase treatment altered the viability of the cells by MTT-assay. Neither RNA transfection nor RNaseA treatment changed the viability of the cells compared to the untreated cells (Fig. 4-18 [B]).

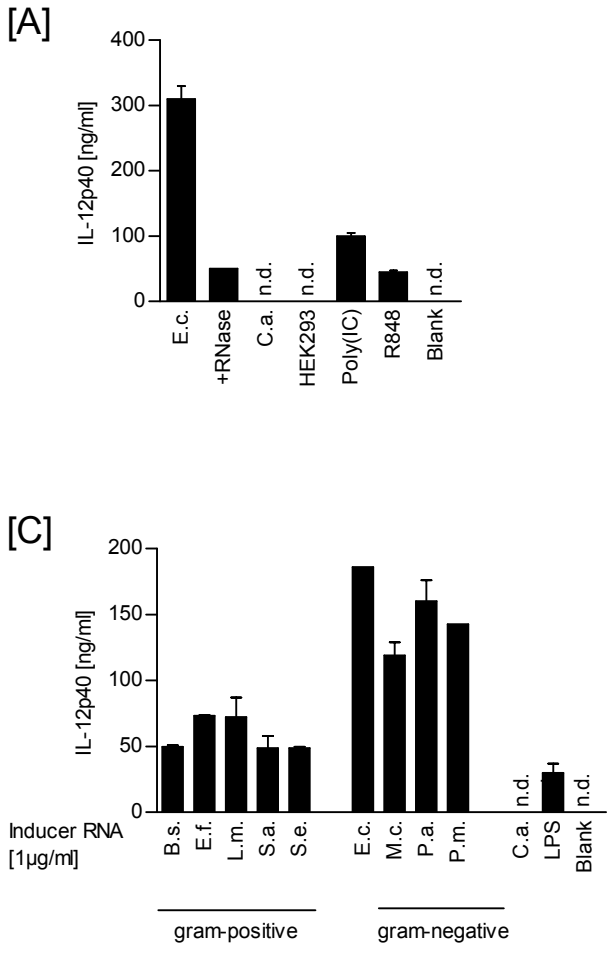

Fig. 4-18 Bacterial RNA-induced IL-12p40 secretion in GM-CSF-derived dendritic cells
[A] GM-CSF-derived dendritic cells were transfected with 1 µg/ml *Escherichia coli* total RNA (E.c.) encapsulated with DOTAP either untreated or RNaseA-digested. 1 µg/ml HEK293T total RNA and 1µg/ml *Candida albicans* total RNA served as eukaryotic RNA controls. Poly(IC) and R848 served as TLR3- and TLR7-specific ligand controls. IL-12p40 secretion was measured by ELISA (n=3, mean +SD, n.d., not detected). [B] Cells of the same experiment were tested 16 hours post-transfection for viability by MTT-assay. Values are displayed as compared to the untreated control. [C] 1 µg/ml of total RNA of *Bacillus subtilis* (B.s.), *Enterococcus faecalis* (E.f.), *Listeria monocytogenes* (L.m.), *Staphylococcus aureus* (S.a.), *Staphylococcus epidermidis* (S.e.), *Escherichia coli* (E.c.), *Moraxella catharralis* (M.c.), *Pseudomonas aeruginosa* (P.a.) and *Proteus mirabilis* (P.m.) was used for transfection of GM-CSF-derived dendritic cells. *Candida albicans* RNA served as eukaryotic RNA control. 100 ng/ml LPS served as TLR4-specific control. IL-12p40 secretion was measured by ELISA (n=3, mean +SD). (n.d., not detected).

Next, GM-CSF-derived dendritic cells were transfected with the same panel of bacterial total RNA preparations as already used above. Upon transfection with bacterial RNA, GM-CSF-derived dendritic cells secreted large amounts of IL-12p40 (Fig. 4-18 [C]). It was evident that all RNA preparations derived from gram-negative species showed a much higher immunostimulatory potential compared to the RNA preparations derived from gram-positive bacterial species. It is very likely that this observation is a synergistic effect of residual amounts of LPS within the preparations of gram-negative bacteria triggering additionally TLR4, which is highly expressed on GM-CSF-derived dendritic cells[193].

4.2.3.2 Recognition of bacterial RNA is TLR7-dependent in murine pDCs but independent of TLR7 in murine mDCs

To further investigate the different recognition mechanisms indicated by IFN-α and TNF-α secretion in human PBMCs, we generated FLT3L-derived dendritic cells from wild type and TLR7$^{-/-}$ mice, which can be regarded as *in vitro* analogs to human plasmacytoid dendritic cells[175,176]. We observed a strictly TLR7-dependent IFN-α secretion upon transfection with *Escherichia coli* total RNA, comparable to the immunostimulatory RNA oligonucleotide RNA40 (Fig. 4-19 [A]). Surprisingly and in sharp contrast to FLT3L-derived dendritic cells, *Escherichia coli* total RNA induced IL-12p40 was independent of TLR7 in GM-CSF-derived dendritic cells (Fig. 4-19 [B]). IFN-α could not be detected in GM-CSF-derived

dendritic cells (data not shown). Again, RNaseA digestion proved that secretion of IFN-α in pDCs and IL-12p40 in mDCs was dependent on RNA. These results confirmed the above findings in human PBMCs, showing that there are at least two different recognition mechanisms in bacterial RNA recognition. One is the TLR7-dependent induction of IFN-α in pDCs, the other one is a TLR7-independent induction of IL-12p40 in mDCs. The latter might be influenced by additional contaminants in the preparation, however, bacterial RNA is the major immunostimulatory component. Importantly, R848 induced IL-12p40 secretion was still TLR7-dependent, confirming the functionality of the TLR7$^{-/-}$ mice and further strengthening the different recognition principles of bacterial RNA.

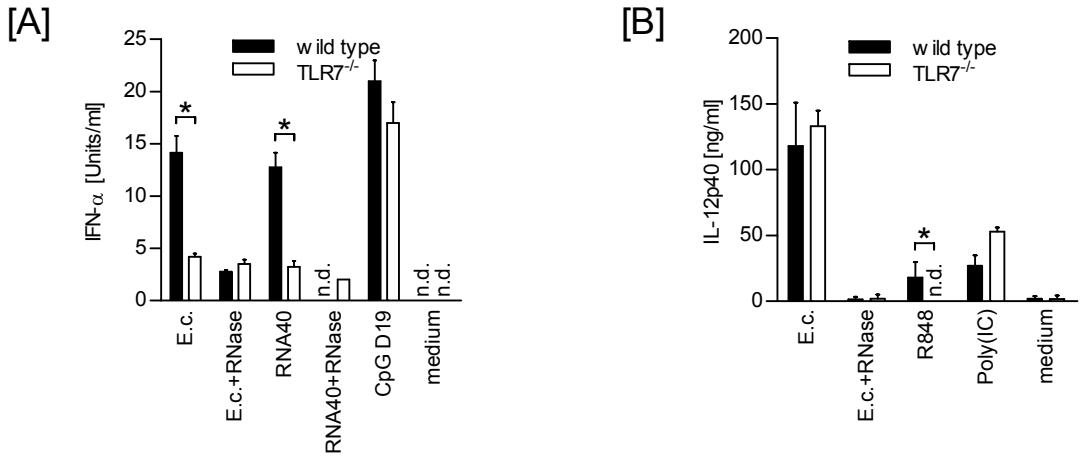

Fig. 4-19 Relevance of TLR7 for bacterial RNA recognition
[A] Murine FLT3L-derived dendritic cells or [B] GM-CSF-derived dendritic cells of wild type (black bars) or TLR7$^{-/-}$ (white bars) mice were transfected with 1 µg/ml of total *Escherichia coli* RNA. IFN-α and IL-12p40 were detected by ELISA, respectively. RNA40 and R848 served as TLR7-specificity controls. CpGD19 and Poly(IC) served as TLR9- and TLR3-specific ligands, respectively (n=3, mean +SD). (n.d., not detected, *, $p<0.05$ as compared to the wild type control).

4.2.3.3 Bacterial RNA mediated IL-12p40 secretion is TLR-independent

To investigate a possible influence of the remaining nucleic acid sensing TLRs on bacterial RNA recognition, we generated GM-CSF-derived dendritic cells from *lps2*-mice which harbor a point mutation in the TRIF molecule and can therefore be considered as deficient in TLR3-signalling, as well as cells from TLR9-knockout mice. Transfection with *Escherichia coli* total RNA showed no differences in IL-12p40 secretion between wild type and knockout cells. The controls Poly(IC), a specific TLR3-dependent ligand as well as CpG1668, a TLR9-specific ligand failed to induce IL-12p40 secretion in the respective knockout cells (Fig. 4-20 [A]+[B]). These findings further show that bacterial RNA is recognized independently of nucleic acid sensing TLRs in immune cells with the exception of plasmacytoid dendritic cells. Participation of murine TLR8 has not been addressed in this study since it has been shown that murine TLR8 does not respond to RNA stimulation and was therefore regarded as non-functional[81,194,195]. However, chloroquine treatment did not alter bacterial RNA-induced IL-12p40 secretion in GM-CSF-derived dendritic cells (Fig. 4-20 [C]). This observation excludes additionally the participation of nucleic-acid sensing TLRs in bacterial RNA recognition. In contrast to CpG1668 bacterial RNA-induced IL-12p40 secretion is induced independently of endosomal maturation or functionality.

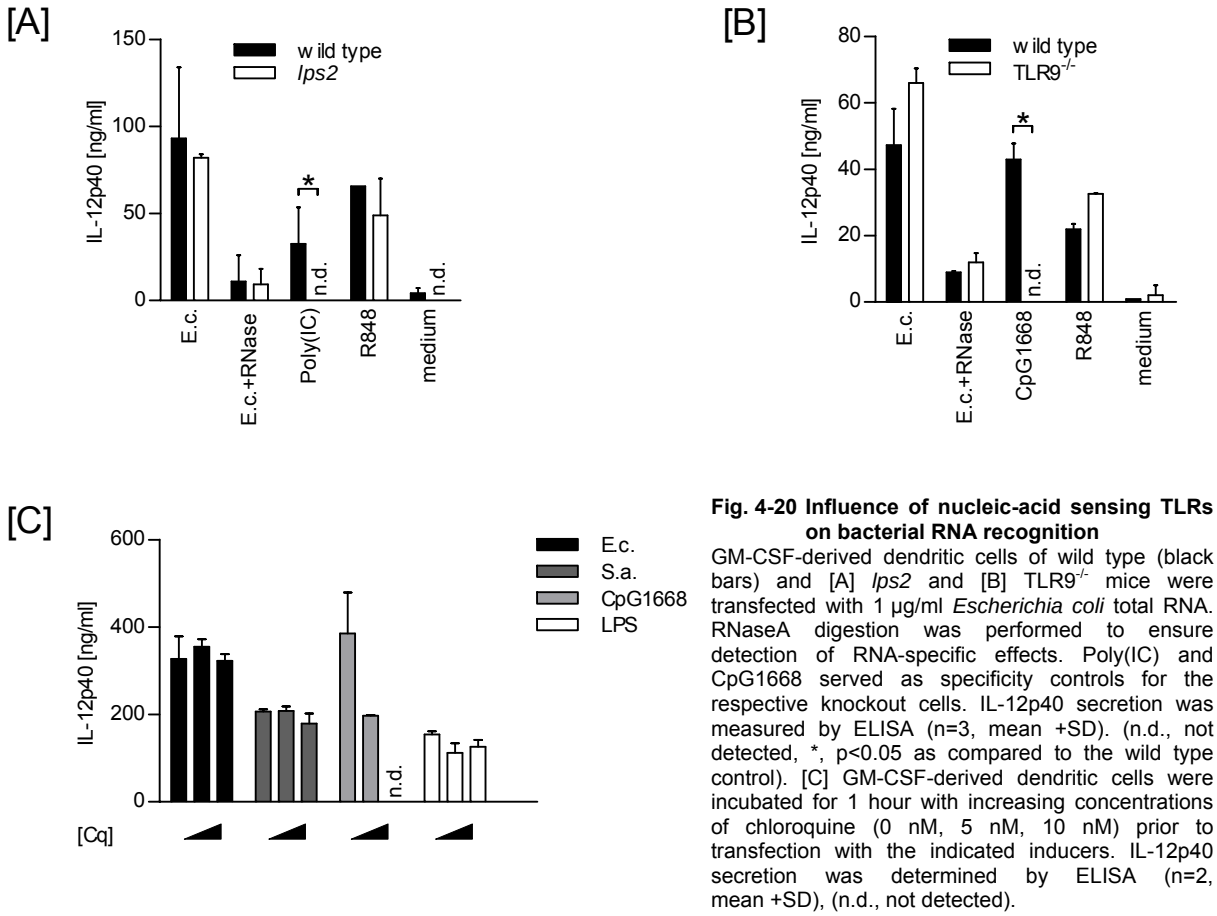

Fig. 4-20 Influence of nucleic-acid sensing TLRs on bacterial RNA recognition
GM-CSF-derived dendritic cells of wild type (black bars) and [A] *lps2* and [B] TLR9$^{-/-}$ mice were transfected with 1 µg/ml *Escherichia coli* total RNA. RNaseA digestion was performed to ensure detection of RNA-specific effects. Poly(IC) and CpG1668 served as specificity controls for the respective knockout cells. IL-12p40 secretion was measured by ELISA (n=3, mean +SD). (n.d., not detected, *, $p<0.05$ as compared to the wild type control). [C] GM-CSF-derived dendritic cells were incubated for 1 hour with increasing concentrations of chloroquine (0 nM, 5 nM, 10 nM) prior to transfection with the indicated inducers. IL-12p40 secretion was determined by ELISA (n=2, mean +SD), (n.d., not detected).

4.2.3.4 Viral RNA receptors are dispensable for bacterial RNA recognition

RIG-I and MDA5 recognize cytoplasmic viral RNAs by detecting 5'-triphosphorylated termini or short double-stranded RNAs in case of RIG-I or long double-stranded RNA molecules for MDA5[127,131]. Both structural features are present in bacterial total RNA preparations[187,196]. Therefore Huh7.5 based cell lines expressing functional RIG-I and MDA5 were analyzed[173]. Cells were transfected with an ISG56 reporter plasmid indicating IRF3 activation. Viral and bacterial RNA was encapsuled with Lipofectamine to ensure cytoplasmic translocation. RIG-I expressing Huh7.5 cells gained responsiveness to the RIG-I-specific viral RNA ligand vesicular stomatitis virus RNA (VSV RNA) (Fig.4-21). Furthermore, RIG-I and MDA5 expressing cells also showed sensitivity to a double-stranded hepatitis C virus transcript (HCV RNA). Both receptors responded to the RNA ligands as expected. The respective transfected receptors were therefore considered to be functional. The cell lines further displayed sensitivity to Poly(IC) which had a size distribution of 200-2000 nt as determined by capillary electrophoresis (data not shown). However, even when transfecting 500-fold higher amounts of *E.coli* RNA than the respective viral RNA we did not observe any detectable IRF3-activaton (Fig.4-21). Interestingly, RIG-I and MDA5 reconstituted cells did only activate the IRF3 reporter but not the NFκB reporter (data not shown) and this activation pattern does not fit to the strong NFκB response observed upon bacterial RNA stimulation. These results show that bacterial RNA, although sharing certain structural features with viral RNA, is not a ligand for the known viral RNA sensor proteins.

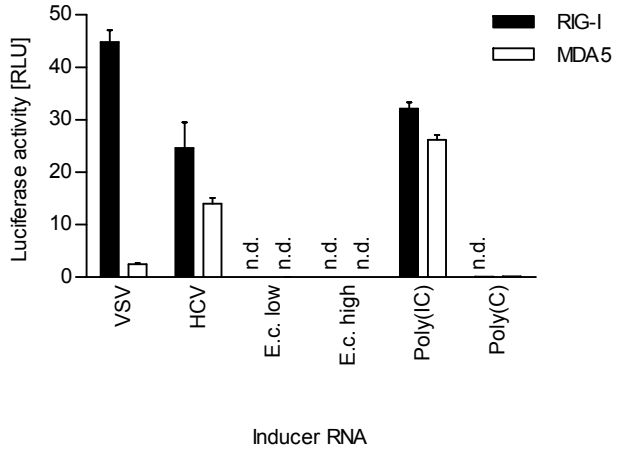

Fig.4-21 No influence of RIG-I and MDA5 on bacterial RNA recognition
Huh-7.5 cells expressing non-functional RIG-I were reconstituted with plasmids encoding RIG-I and MDA5, respectively. Cells were transfected with viral RNA (VSV, 0.1 µg/ml, HCV, 0.01 µg/ml), bacterial RNA (E.c.low, 1 µg/ml, E.c.high, 5 µg/ml) or 0.5 µg/ml Poly(IC). Poly(C) (5 µg/ml) served as the negative control. All RNAs were complexed with LF2000 prior to transfection. Huh-7.5 without RIG-I or MDA5 showed no detectable IRF3 activation upon transfection with the indicated RNAs. IRF3 activation was determined by Dual Luciferase Reporter Assay (n=3, mean+SD). (n.d., not detected).

4.2.3.5 ASC and interferon α/β receptor are required for bacterial RNA-induced IL-1β secretion but dispensable for IL-12p40 secretion

Besides uric acid and bacterial toxins, also bacterial RNA has been reported to be a ligand for NALP3 leading to inflammasome activation[65,66,135]. Inflammasome activation results in the processing of pro-IL-1β and pro-IL-18[55]. Further, it has been shown that NALP3 induces NFκB in a manner dependent on the ASC adaptor protein[68]. To investigate a possible influence of the inflammasome on the observed IL-12p40 secretion, GM-CSF-derived dendritic cells of wild type and ASC$^{-/-}$ mice were generated. ASC represents an essential adaptor molecule for inflammasome signalling[54]. ASC$^{-/-}$ cells can therefore be regarded as non-functional in terms of inflammasome signalling. As reported before, we observed a strict ASC-dependent IL-1β secretion in GM-CSF-derived dendritic cells upon stimulation with *Escherichia coli* and *Staphylococcus aureus* total RNA (Fig. 4-22 [A]). RNase digestion reduced IL-1β secretion, showing that the observed effects were dependent on bacterial RNA. However, bacterial RNA induced IL-12p40 secretion was independent of the ASC protein (Fig. 4-22 [B]), indicating that the ínflammasome does not participate in the observed IL-12p40 secretion. In contrast to bacterial RNA-induced IL-12p40 secretion, RNase treatment reduced IL-1β to a lower extent indicating that contaminations within the preparation induce IL-1β but not IL-12p40 secretion.

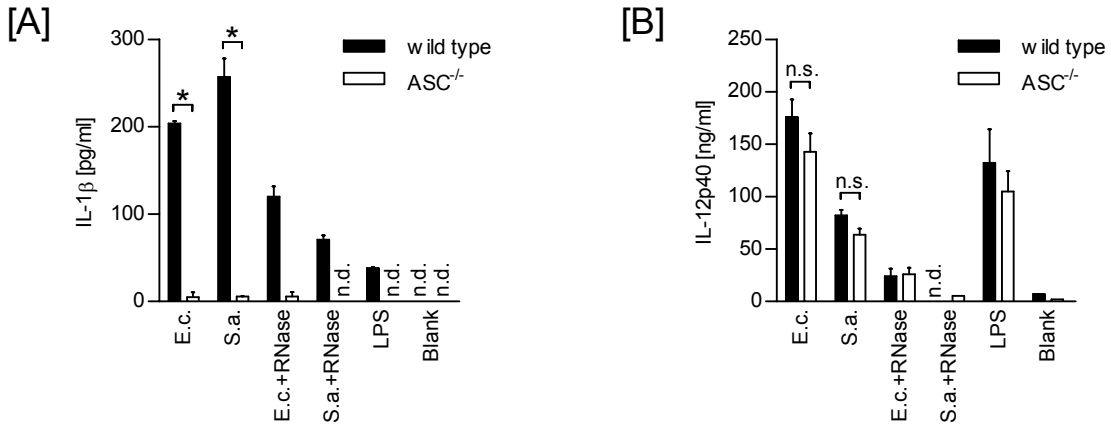

Fig. 4-22 Differential requirement for ASC in bacterial RNA-mediated IL-1β and IL-12p40 secretion
GM-CSF-derived dendritic cells were generated from wild type and ASC$^{-/-}$ mice. Cells were stimulated with 1 µg/ml *Escherichia coli* and *Staphylococcus aureus* total RNA. RNA was additionally digested with RNaseA. [A] IL-1β and [B] IL-12p40 secretion was measured by ELISA (n=2, mean +SD). (n.d., not detected, *, $p<0.05$ as compared to the wild type control, n.s., not significant as compared to the wild type control).

Activation of the inflammasome by cytosolic bacteria has been shown to be dependent on intact type-I IFN signalling[136]. To assess whether type-I IFN signalling is required for bacterial RNA-mediated IL-12p40 secretion, GM-CSF-derived dendritic cells of wild type and IFN α/β receptor-deficient (IFNAR1$^{-/-}$)-knockout mice were prepared. IL-1β secretion upon bacterial RNA transfection was dependent on IFNAR1 and therefore dependent on type-I-IFN signalling (Fig. 4-23 [A]). However, bacterial RNA-mediated IL-12p40 secretion was not altered in the absence of functional IFNAR1 (Fig. 4-23 [B]). Again, RNaseA digestion clearly demonstrated that the observed effects were attributable to RNA and not induced by residual contaminations.

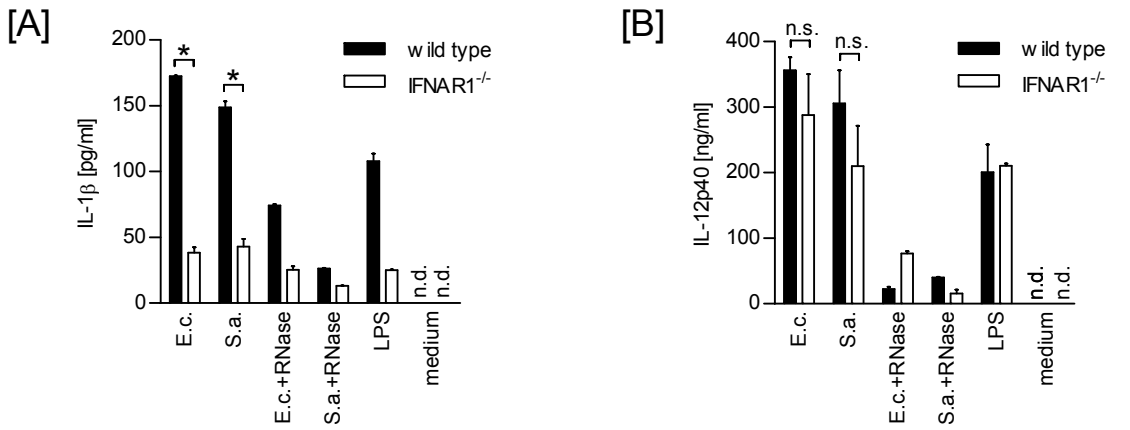

Fig. 4-23 Differential requirement for type-I IFN signalling in bacterial RNA-mediated IL-1β and IL-12p40 secretion
GM-CSF-derived dendritic cells were generated from wild type and IFNAR1$^{-/-}$ mice. Cells were stimulated with 1 µg/ml *Escherichia coli* (E.c.) and *Staphylococcus aureus* (S.a.) total RNA. RNA was additionally digested with RNaseA. IL-1β [A] and IL-12p40 [B] secretion was measured by ELISA (n=3, mean +SD). (n.d., not detected, *, $p<0.05$ as compared to the wild type control, n.s., not significant as compared to the wild type control).

4.2.4 Bacterial RNA induces an immune response in non-professional immune cells

To confirm the TLR-independent recognition described above, HEK293T cells which lack functional TLRs with the possible exception of TLR3 were transfected with plasmids encoding for TLR3, 7 and 8, respectively. Cells were transfected with *Escherichia coli* total RNA and NFκB activation was determined by Dual Luciferase Assay. Surprisingly, strong NFκB activation was already observed in control vector-transfected cells (Fig. 4-24 [A]). In contrast, NFκB activation was strongly enhanced upon transfection with the respective TLR-specific controls. Poly(IC) and R848 showed elevated levels of NFκB activation in TLR3 and TLR7/8 transfected cells, respectively. However, bacterial RNA-mediated NFκB activation was not further enhanced by transfection of any of the RNA-sensing TLRs 3, 7 or 8. Basal sensitivity of control vector-transfected upon Poly(IC) transfection could be mediated by basally expressed TLR3 or RIG-I in HEK293T cells (Fig. 4-24 [B]).

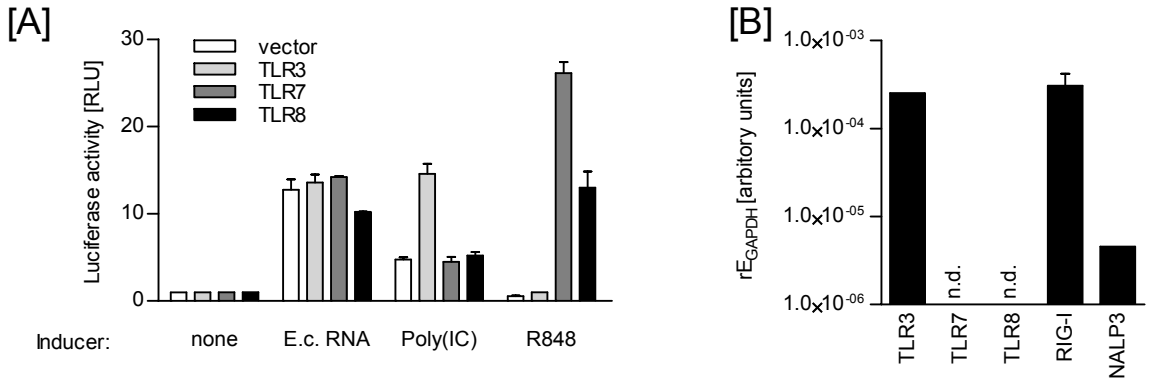

Fig. 4-24 TLR-mediated recognition of bacterial RNA
[A] HEK293T cells were transfected with plasmids encoding the indicated human TLRs or empty vector. 8 h post-transfection, cells were stimulated with 10 µg/ml *Escherichia coli* total RNA, 25 µg/ml Poly(IC) and 1 µg/ml R848, respectively. NFκB activation was determined by Dual Luciferase Assay (n=3, mean +SD). [B] RT-PCR of untreated HEK293T cells to determine endogenous expression of RNA-sensing receptors. Values were normalized to the house-keeping gene GAPDH (n=3, mean +SD). (n.d., not detected).

To exclude the participation of the basally expressed RNA-sensing receptors TLR3 and RIG-I, we used an experimental approach based on siRNAs targeting TLR3 and RIG-I, respectively. SiRNA-mediated gene-suppression was evaluated by quantitative RT-PCR and showed a reduction of at least 85% of messenger RNA transcription compared to non-genomic control siRNA-treated cells (Fig. 4-25 [A]). Transfection of siRNA-treated cells with bacterial RNA altered NFκB activation only marginally, excluding TLR3 and RIG-I as the responsible receptors for bacterial RNA. Thus, even non-professional immune cells are able to respond to bacterial RNA in a manner independent of any known RNA receptor.

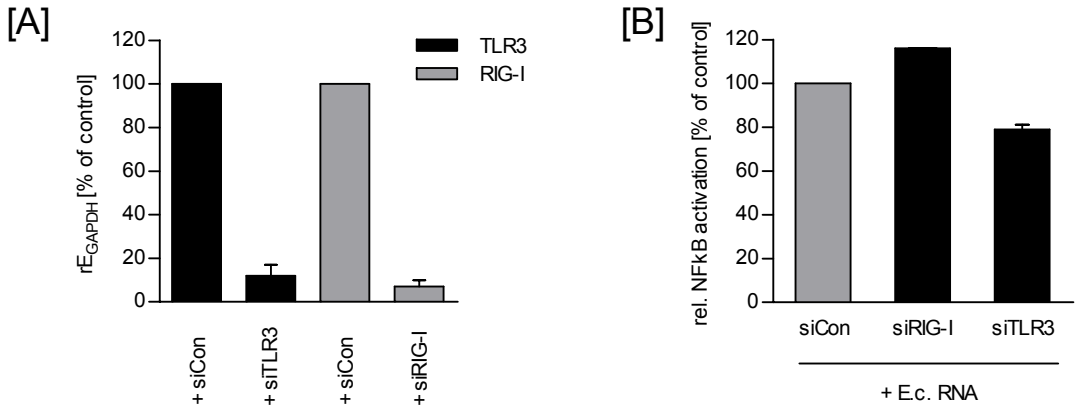

Fig. 4-25 Relevance of endogenously expressed RNA-sensors in HEK293T cells on bacterial RNA recognition
[A] HEK293T cells were transfected twice with 10 nM of the indicated siRNAs. Gene-silencing was validated 72 h post-transfection by RT-PCR. Gene expression is displayed as values normalized to siCon-treated gene expression (n=3, mean +SD). [B] HEK293T cells treated with the indicated siRNAs were transfected with 10 µg/ml *Escherichia coli* total RNA 72 h after the first siRNA transfection. NFκB activation was determined by Dual Luciferase Assay, values are normalized to NFκB activation of control siRNA-treated cells (n=3, mean +SD).

4.2.4.1 Species-specific recognition in HEK293T cells

Transfection with the whole panel of bacterial RNAs from the experiments above confirmed the immunorecognition of bacerial RNA in HEK293T cells. Surprisingly, only some transfected bacterial RNAs led to an activation of NFκB, whereas others were immunological silent (Fig. 4-26 [A]). NFκB activation was independent of the gram-type of the respective bacteria since *Bacillus subtilis* RNA

strongly induced NFκB, but *Moraxella catharralis* RNA led to no induction of NFκB. These findings exclude possible LPS contaminations as a source of activation. However, strong species-dependent effects indicated the participation of contaminants within the activating bacterial RNA preparations, although RNaseA treatment resulted in an abrogation of NFκB activation similar to the effects observed in immune cells (Fig. 4-26 [B]).

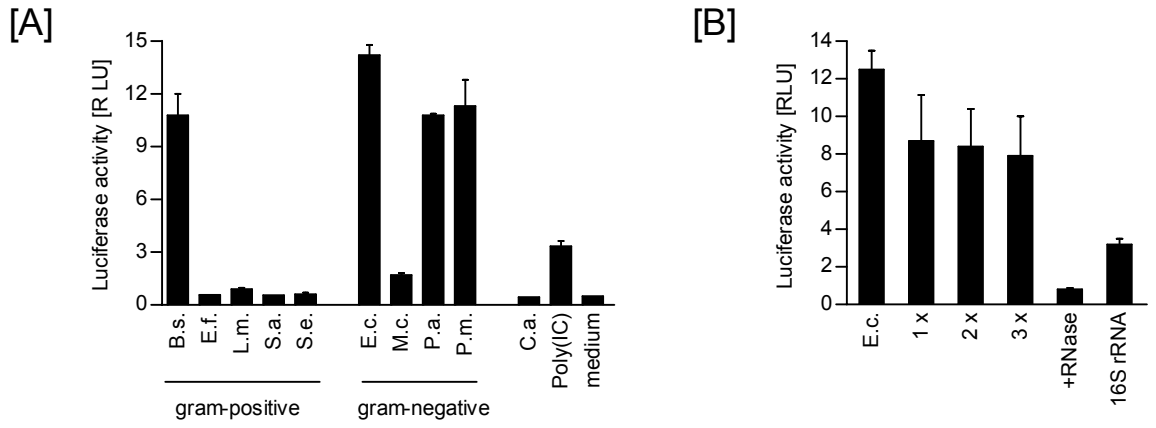

Fig. 4-26 Species-specific recognition of bacterial RNA in HEK293Tcells
[A] HEK293T cells were transfected with 10 µg/ml of the indicated bacterial RNA preparations. NFκB activation was determined by Dual Luciferase Assay. *Candida albicans* RNA preparation served as eukaryotic RNA control, Poly(IC) as specific ligand for TLR3 (n=3, mean +SD). [B] HEK293T cells were either transfected with 10 µg/ml E.c. RNA preparation or with equal amounts of further on-column purified *Escherichia coli* RNA preparations, number of purification steps is indicated. Additionally, cells were transfected with 10 µg/ml isolated 16S ribosomal RNA. RNaseA-treated *Escherichia coli* RNA served as a negative control (n=3, mean +SD).

This idea was further supported by the fact that, in contrast to human PBMCs (Fig. 4-15 [B]), 16S ribosomal RNA of *Escherichia coli* showed a much weaker potential to activate NFκB in HEK293T cells compared to the total RNA preparation (Fig. 4-26 [B]). Purification of the total RNA by one additional on-column washing step indeed reduced NFκB activation. However, additional washing steps did not reduce NFκB activation further showing still highly elevated activation levels compared to the 16S ribosomal RNA fraction (Fig. 4-26 [B]).

4.2.4.2 Analysis of possible contribution of contaminants to bacterial RNA stimulation

To investigate whether contaminants might contribute to the immunostimulation induced by bacterial RNA, HEK293T cells were tested for the expression of the NOD1 and NOD2 receptor which sense the components of bacterial cell walls diamino-pimelic acid (DAP)[197] and muramyl-dipeptide (MDP)[198], respectively. It had been reported before that NOD1 and NOD2 ligands show synergistic effects on TLR stimulation[70]. HEK293T cells showed a high transcription of NOD1 and still detectable levels of NOD2 transcription (Fig. 4-27).

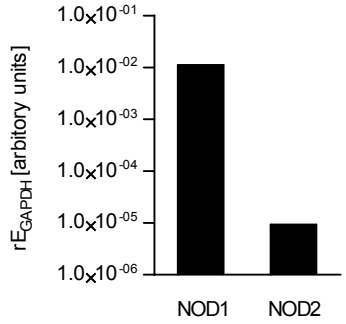

Fig. 4-27 Transcription of NOD1 and NOD2 in HEK293T
Expression of NOD1 and NOD2 transcription levels was determined by quantitative RT-PCR. Values were normalized to transcription of the house-keeping gene GAPDH (n=3, mean).

Costimulation of the weak NFκB inducer *Staphylococcus aureus* RNA with MDP-dpm which represents a ligand for both, NOD1 and NOD2, resulted in a slightly elevated NFκB activation. However, even transfection of such high amounts as 10 mg/ml MDP-dpm did not result in NFκB activation levels as high as detected for *Escherichia coli* RNA (Fig. 4-28 [A]). *Staphylococcus aureus* RNA substituted with RNaseA-treated and therefore non-active *Escherichia coli* RNA did not alter NFκB activation significantly (Fig. 4-28 [B]). These results show that residual NOD1 and NOD2 ligands within the RNA preparations are not responsible for the high levels of NFκB upon stimulation with bacterial RNA in HEK293T cells. Further, digested *Escherichia coli* RNA was not able to reconstitute high levels of NFκB activation if cotransfected with weak inducing *Staphylococcus aureus* RNA indicating that residual contaminants do not seem to play the major role for immunorecognition in HEK293T cells. Cotransfection of *Escherichia coli* RNA and digested *Escherichia coli* RNA did not alter the NFκB activation significantly, proving that residual RNAseA is not degrading the cotransfected bacterial RNA. Importantly, *Staphylococcus aureus* RNA-induced NFκB activation showed a reduction in activation upon RNaseA treatment.

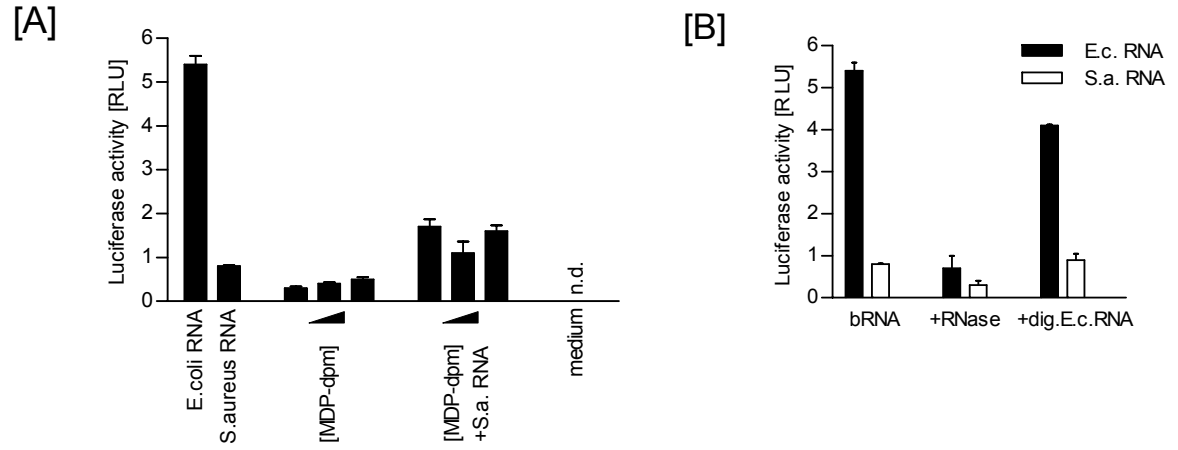

Fig. 4-28 Neglectable effects of contaminants on bacterial RNA-mediated NFκB activation in HEK293T cells
[A] HEK293T cells were transfected either with 10 µg/ml of the indicated bacterial RNA or with increasing amounts (0.1, 1.0, 10 mg/ml) of the NOD1 and NOD2 ligand MDP-dpm. *Staphylococcus aureus* RNA was cotransfected with the same amounts of MDP-dpm. NFκB activation was measured by Dual Luciferase Assay (n=3, mean +SD). [B] HEK293T cells were transfected with 10 µg/ml RNA of *Escherichia coli* (black bars) or *Staphylococcus aureus* (white bars). Bacterial RNA (bRNA) was either untreated, digested with RNaseA (+RNase) or digested *Escherichia coli* RNA (dig.E.c.) was added in equal concentration (n=3, mean +SD). (n.d., not detected).

4.2.5 Summary

In this study we could show that bacterial RNA represents an immunostimulatory pattern. Bacterial RNA strongly triggers a type-I interferon response in human PBMCs which was dependent on endosomal maturation and could be blocked by a TLR7-specific inhibitor. Surprisingly, TNF-α secretion in human PBMCs upon bacterial RNA transfection was independent of both. Murine FLT3L-derived pDC-like cells from TLR7-deficient mice were unresponsive to bacterial RNA. However, in GM-CSF-derived mDC-like cells TLR3, 7, 8 and 9 were dispensable for IL-12p40 induction by bacterial RNA. Even non-professional immune cells were able to mount a NFκB response upon stimulation with bacterial RNA. The viral RNA sensor proteins RIG-I and MDA5 were ruled out to be responsible for this reactivity. Whereas the inflammasome adaptor protein ASC and a functional type-I interferon receptor were necessary for IL-1β secretion in myeloid dendritic cells these proteins were dispensable for IL-12p40 induction by bacterial RNA. Further, possible immunostimulatory contaminants were shown to play only a minor role for bacterial RNA-mediated immunorecognition.

Our results show that besides the activation of TLR7 and the inflammasome, bacterial RNA activates additional receptors similarly as it has been reported for the recognition of bacterial DNA. Although the encapsulation of bacterial RNA was necessary for immunostimulation endosomal maturation was dispensable indicating that the receptors are located in the cytosol

4.3 Ligand specificity of RIG-I

RIG-I recognizes a wide variety of RNA viruses[44]. Sensing of viral RNA has been linked in several reports to the presence of double-stranded RNA (dsRNA) intermediates that occur during the process of viral replication[6,29,34,126]. Recently, it was further shown that RIG-I mainly recognizes dsRNA up to a maximum length of approximately 2000 bp[131]. However, the recognition of dsRNA by RIG-I was challenged by two reports showing that rather the terminal 5'-triphosphate of viral RNA molecules serves as the major target structure for RIG-I recognition[127,128]. In fact, one of the reports stated that any RNA lacking a 5'-triphosphate could not serve as a substrate for RIG-I[128]. The role of dsRNA recognition by RIG-I and the contribution of the 5'-triphosphate thus remains to be characterized in more detail. We addressed the question whether double-strandness and presence of a terminal 5'-triphosphate represent two independent target structures for RIG-I-mediated RNA recognition. If RIG-I is triggered by dsRNA independently of any 5'-triphosphate, we further hypothesized that signalling intensity would increase with the length of the dsRNA ligand due to a higher number of putative binding sites for RIG-I.

4.3.1 Characterization of RIG-I expressing Huh7.5 cells

To investigate RNA induced triggering of RIG-I we used the Huh7.5 cell line which carries a dominant negative mutation in the RIG-I protein[199]. Huh7.5 cells were reconstituted with wild type RIG-I (Huh7.5 RIG-I wt) (Marco Binder, Heidelberg) as previously described[173], resulting in functional RIG-I signalling. IRF3 activation was determined by measuring ISG56 reporter activity. Huh7.5 cells were *per-se* non-responsive to stimulation with Poly(IC) in ISG56 reporter assays. This indicated the absence of endogenously expressed TLR3 which was additionally confirmed by Microarray analysis (data not shown). Reconstitution with functional RIG-I resulted in 32-fold higher ISG56 reporter activity upon transfection with Poly(IC) (Fig. 4-29 [A]). There was no sensitivity towards the synthetic single-stranded RNA molecules Poly(C) and Poly(I). According to the manufacturer's informations Poly(C), Poly(I) and Poly(IC) are synthesized from nucleotide-diphosphates and are therefore not harboring any terminal 5'-triphosphate. Additionally, Poly(C) and Poly(I) are not capable to form any secondary structures and therefore do not produce any possible target structures for RIG-I. Further, we tested the sensitivity of Huh7.5 RIG-I wt cells towards the highly immunostimulatory component LPS and shrimp alkaline phosphatase (SAP) which we were going to use in future experiments. Huh7.5 cells showed no sensitivity to both (Fig. 4-29 [B]).

Due to the non-responsiveness to LPS, a contribution of TLR4 on ISG56 activity in Huh7.5 could be ruled out. To confirm that Poly(IC) stimulation is independent of any 5'-triphosphate we incubated Poly(IC) with SAP prior to transfection. Poly(IC)-induced ISG56 promoter activation was not altered by SAP pretreatment. Additionally, unaltered ISG56 activity upon SAP pre-treatment indicated that phosphatase treatment did not influence the integrity of Poly(IC) otherwise.

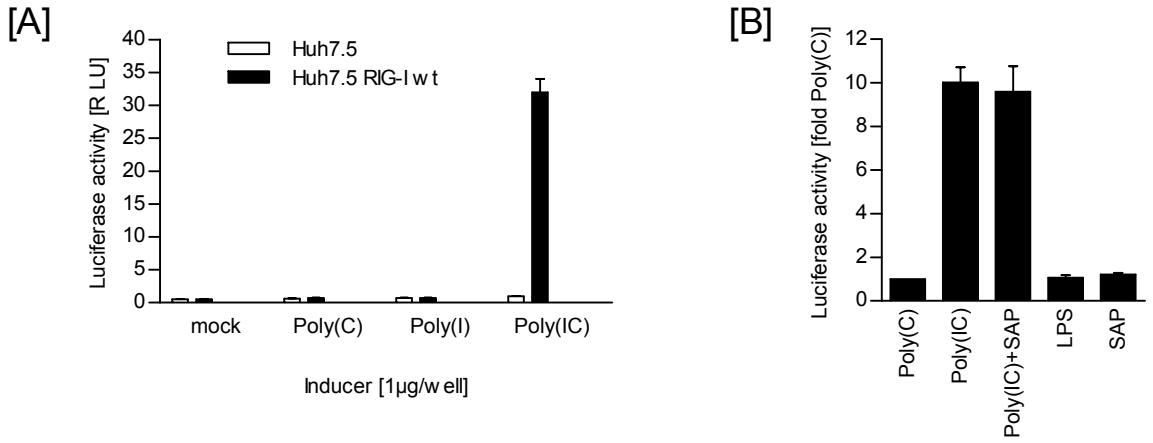

Fig. 4-29 Reconstituting RIG-I signalling in Huh7.5 cells
[A] Huh7.5 cells (white bars) and Huh7.5 reconstituted with wild type RIG-I (black bars) were transfected with 1 µg/well of the indicated inducers. ISG56 reporter activity was determined by Dual Luciferase Assay. (n=2, mean +SD). [B] Huh7.5 cells reconstituted with wild type RIG-I were transfected with 1 µg/well Poly(C), Poly(IC), Poly(IC) pretreated with 10 U SAP, 100 ng/well LPS or 10 U SAP. ISG56 reporter activity was determined by Dual Luciferase Assay. Values are expressed as multiples of Poly(C)-induced ISG56 activity. (n=2, mean +SD)

4.3.2 Recognition of different RNAs by RIG-I

4.3.2.1 Double-stranded RNA represents a target structure for RIG-I

The fact that Poly(IC) but neither Poly(I) nor Poly(C) triggered IRF3 signalling in Huh7.5 RIG-I wt cells indicated that double-stranded RNA conformation might serve as a target structure for RIG-I. We therefore tested 58 nucleotide long RNA *in vitro* transcripts corresponding to the Rabies Virus (RV) leader RNA (Karl-Klaus Conzelmann, Munich) or 9600 nucleotide long *in vitro* transcripts of replication-incompetent full-length genomes of HCV (Con1/ΔGDD) (Marco Binder, Heidelberg). RNA molecules were either single-stranded or annealed to the corresponding antisense strand prior to transfection. To exclude a differential influence of the terminal 5'-triphosphates on RIG-I mediated signalling, we used equal amounts of single- and double-stranded RNA molecules in terms of mass, respectively, to yield the same molarity of 5'-ends. When Huh7.5 RIG-I wt cells were transfected with the different RNA ligands we measured ISG56 reporter activity in every condition (Fig. 4-30).

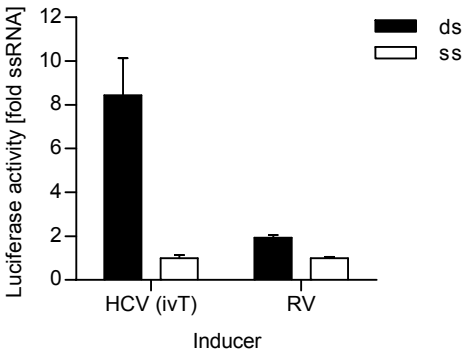

Fig. 4-30 Stimulation of RIG-I by single- and double-stranded RNA ligands
Huh7.5 RIG-I wt cells were either transfected with 10 ng/well HCV *in vitro* transcript (HCV(ivT)) or with 20 ng/well RV leader RNA (RV). RNA ligands were either single-stranded (white bars) or annealed with the respective antisense strands to duplexes (black bars) prior to transfection. ISG56 reporter activity was determined by Dual Luciferase Assay. For better comparability, values are expressed as multiples of ssRNA-induced ISG56 reporter activity. (n=2, mean +SD).

However, for both RNA ligands, RIG-I showed an increased sensitivity for the double-stranded conformation. As mentioned above, the respective single- and double-stranded RNA ligands harbored the same total number of terminal 5'-triphosphates since transfection was performed with equal

masses of RNA. A differential contribution of the 5'-triphosphate was therefore ruled out. Taken together, the results indicated that dsRNA represents a target structure for RIG-I on top of the recognition of the 5'-triphosphate. Further, the contribution of the double-strand seems to increase with the length of the ligand indicated by the differential activity of the 58 and 9600 nucleotide long RNAs.

However, comparability of the two RNA ligands is limited since both are completely different in terms of sequence and possible secondary structures. Although there is not much known about the influence of certain sequence motifs on RIG-I signalling, a recent report indicated that certain uridine-rich sequence stretches within the HCV genome are preferrentially detected by RIG-I[132].

4.3.2.2 Sensitivity to RIG-I increases with the ligand length

In order to address the issue of length-dependent recognition of dsRNA by RIG-I, we decided to generate a set of RNA ligands with overlapping sequences and increasing size. HCV *in vitro* transcripts were considered to be not favourable due to extensive secondary structure formations[200-202]. We therefore decided to use the coding sequence (CDS) of endogenous TLR3 as template for the generation of the *in vitro* transcripts. Extending from position 1271 of human TLR3 cDNA *in vitro* transcripts ranging from 40 nucleotides up to 1600 nucleotides in length were generated, gel purified and finally validated by capillary electrophoresis (Fig. 4-31). Additionally, the 40-mer was synthesized commercially to bear a hydroxyl-group at the 5'-end instead of a 5'-triphosphate.

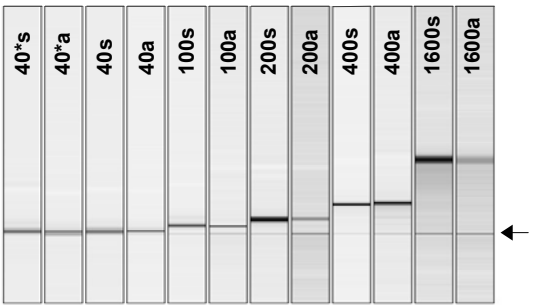

Fig. 4-31 Capillary electrophoresis image of *in vitro* transcripts
In vitro transcripts of 40, 100, 200, 400 and 1600 nucleotides in length were analyzed by capillary electrophoresis. RNA strands were transcribed in sense (s) and in antisense orientation (as). Commercially synthesized 40-mer RNA oligonucleotides are depicted as 40*. (Arrow indicates the 25 nt internal calibration marker).

Synthesized as well as *in vitro* transcribed RNA molecules were detected at the expected size and showed high integrity. Further side products from the *in vitro* transcription reaction were shown to be removed completely during the purification procedure.

To address substrate specificity of RIG-I in a quantitative fashion we decided to perform titration experiments with the generated *in vitro* transcripts after being annealed to form dsRNA. Since all *in vitro* transcripts harbor a triphosphate at each 5'-end, dsRNA was transfected in equal molarities to ensure that the extent of a possible contribution of the 5'-triphosphate was identical. In fact, sensitivity of RIG-I signalling to dsRNA was increased with increasing ligand length (Fig. 4-32 [A]). Surprisingly, maximum signalling was slightly reduced with increasing size of the dsRNA ligand. However, this fits to a recent report which showed that RIG-I mediated signalling decreases with increasing length of the dsRNA ligand at saturating ligand concentrations[131].

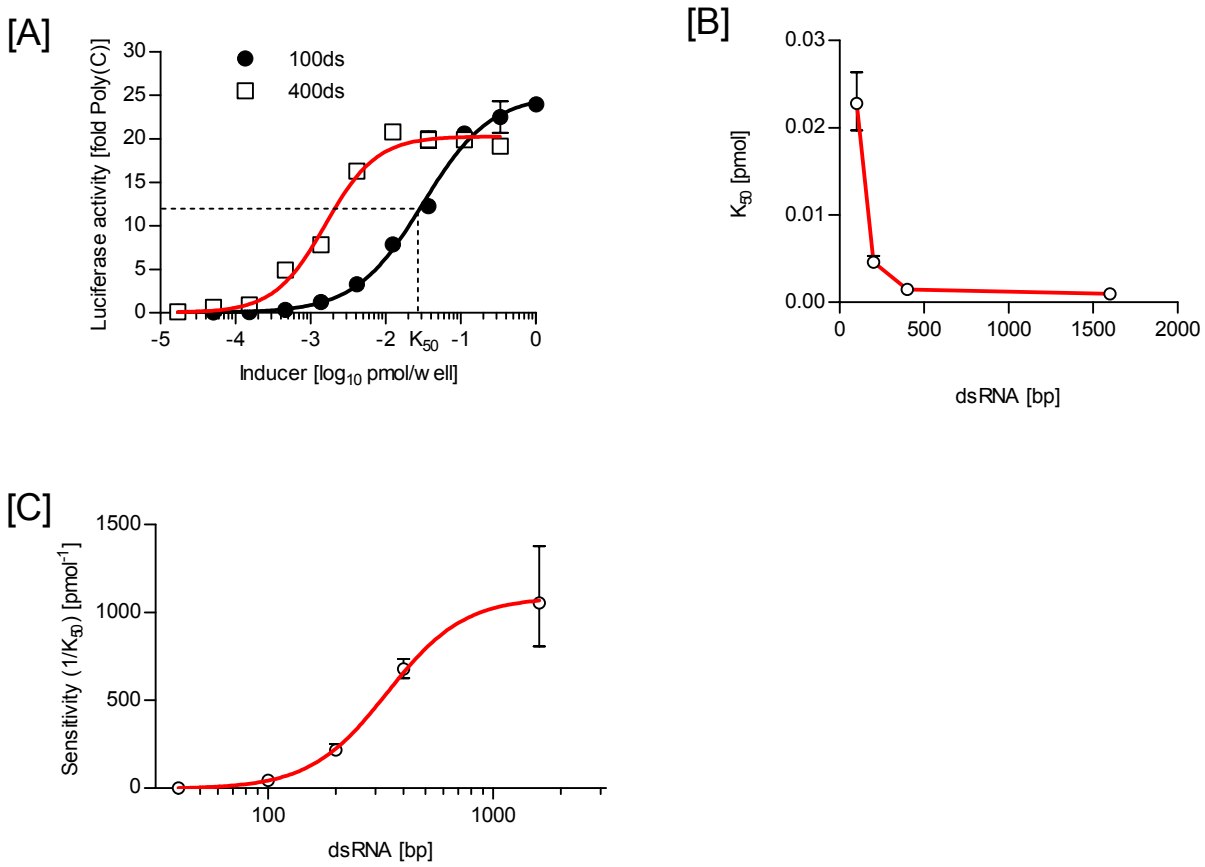

Fig. 4-32 Length-dependent recognition of dsRNA by RIG-I
[A] Huh7.5 RIG-I wt cells were transfected with dsRNA of the indicated sizes generated by *in vitro* transcription and annealed to complete dsRNA. Ligand concentration was titrated over the indicated concentration range. ISG56 reporter activity was determined by Dual Luciferase Assay. Values are shown for 100ds and 400ds *in vitro* transcripts and depicted as multiples of Poly(C)-induced ISG56 reporter activity. Determined substrate concentration for half-maximal signalling (K_{50}) for 100ds *in vitro* transcript is indicated (n=3, mean ± SD). [B] Substrate concentrations for half-maximal signalling were plotted versus the substrate length (n=3, mean ± SD). [C] Sensitivity of RIG-I to dsRNA was defined as $1/K_{50}$ and plotted versus the substrate length (n=3, mean ±.95% conf.).

However, despite the slight decrease of maximum signalling strength, ligand titration clearly showed that sensitivity of RIG-I to dsRNA was increased substantially with the length of the ligand. RIG-I was most sensitive to the 1600 nucleotide long dsRNA substrate. Half-maximal signalling for 400 nucleotide long RNA was measured at a substrate concentration (K_{50}) of about 1.5 fmol/well whereas the K_{50} of 100 nucleotide long dsRNA was at about 0.02 pmol/well, thus showing a 30-fold lower sensitivity of an only 4-fold smaller ligand to RIG-I. Plotting the determined K_{50} of the different dsRNA samples versus the length of the respective ligands again showed that signalling of RIG-I to dsRNA was drastically increasing with increasing ligand length (Fig. 4-32 [B]). The reciprocal of the determined K_{50} values was defined as sensitivity of RIG-I to its ligand. Highest sensitivity was reached from approximately 800 basepairs on. Half-maximal sensitivity was reached at 340 basepairs.
Importantly, the total number of 5'-triphosphates was identical among all transfected dsRNA ligands excluding the possibility that the observed differential signalling activity was generated by the 5'-ends. Taken together, these experiments extent the view on RIG-I substrate specificity. Besides the recognition of the terminal 5'-triphosphate, RIG-I detects the presence of dsRNA. Further, the disproportionately high increase in sensitivity towards longer dsRNA strongly indicates that ligand binding to RIG-I occurs rather in a cooperative than linear manner.

4.3.2.3 Contribution of the terminal 5'-triphosphate

Next, we wanted to investigate the influence of the terminal 5'-triphosphate in relation to the recognition of double-stranded conformation of the RNA ligands. The results from the experiments above showed that dsRNA is recognized length-dependently while keeping the number of 5'-triphosphates constant. Additionally, assuming that terminal 5'-triphosphates are recognized independently of the length of the ligand suggested that the fraction of the signal due to the terminal 5'-triphosphate would be higher for shorter dsRNA ligands.

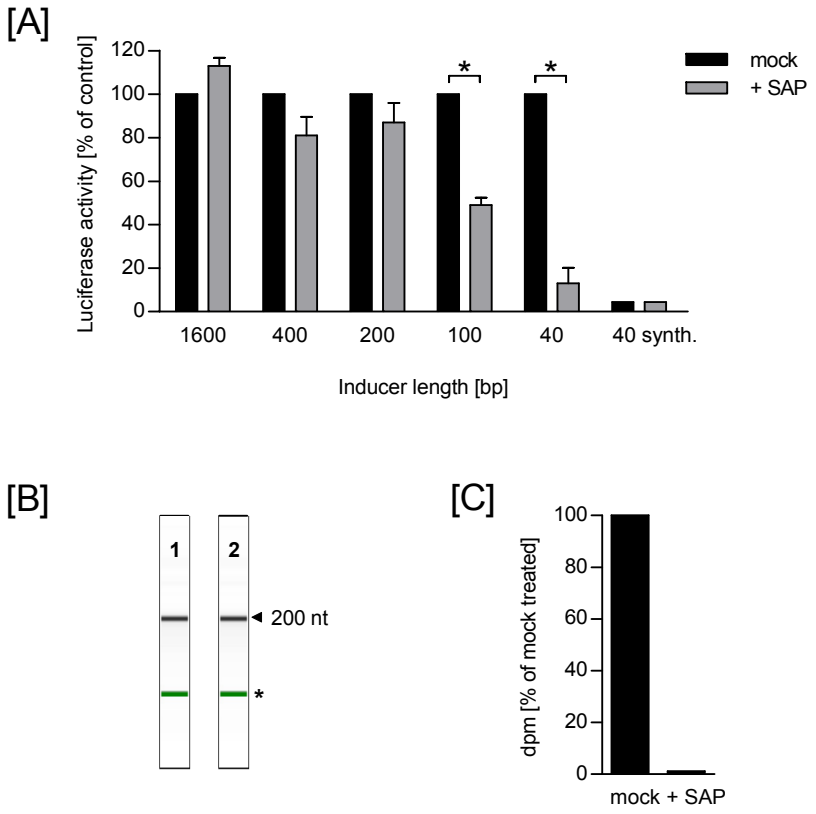

Fig. 4-33 Influence of the 5'-triphosphate on RIG-I signalling
[A] *In vitro* transcripts of the indicated length were either phosphatase (gray bars) or mock treated (black bars) prior to annealing. Concentrations for half-maximal signalling (K_{50}): 0.6, 1.5, 4.5, 20 and 10000 fmol/well for 1600, 400, 200, 100 and 40 bp dsRNA ligands, respectively. Synthetic double-stranded 40-mer served as positive control. ISG56 activity was determined by Dual Luciferase Assay. Values were normalized to the untreated control for better comparability. (n=2, mean +SD). (*, $p<0.05$, as compared to mock-treated RNA ligand). [B] The integrity of the RNA ligands was tested. 200 nt long single-stranded RNA was either phosphatase treated as above (1) or not (2) and applied to capillary gel electrophoresis. (*, indicates the internal calibration marker). [C] Efficiency of phosphatase treatment was determined by *in vitro* transcription with γ-^{32}P-labeled GTP and subsequent dephosphorylation. Residual radioactivity was measured and is depicted in disintegrations per minute (dpm). Values were normalized to the untreated control.

Therefore the dsRNA ligands from the experiments above were either incubated with shrimp alkaline phosphatase (SAP) or mock treated prior to transfection. Transfection was performed with the substrate concentrations for half-maximal signalling (K_{50}) which had been determined in the experiment above. Using K_{50} avoided that the signalling saturation level was passed and therefore the detection of quantitative signalling differences was ensured. In fact, the presence of a 5'-triphosphate showed a significant contribution to RIG-I signalling for shorter dsRNA. Dephosphorylation of double-stranded 40 bp and 100 bp *in vitro* transcripts reduced signalling by 87% and 51%, respectively. However, when ligands of 200 nucleotides or longer were used, the influence of the 5'-triphosphate became negligible (Fig. 4-33 [A]). Signalling of dephosphorylated double-stranded 40-mer was

comparable to the signalling activity of synthetic double-stranded 40-mer which harbors a hydroxyl-group instead of a triphosphate at the 5'-end. Using capillary gel electrophoresis we could show that the integrity of the dsRNA ligands was not compromised by the phosphatase treatment (Fig. 4-33 [B]). In order to check the efficiency of the phosphatase treatment we dephosphorylated 5'-γ-^{32}P radiolabeled *in vitro* transcribed RNA and determined residual incorporated radioactivity after purification. We observed a decrease of radioactivity by 98% compared to the untreated control (Fig. 4-33 [C]) showing that phosphatase treatment was highly efficient. These residual 5'-triphosphates might explain the slightly higher activity of dephosphorylated *in vitro* transcribed 40-mer compared to the synthetic RNA oligonucleotide (Fig. 4-33 [A]).

4.3.2.4 Recognition of single-stranded RNA by RIG-I

As already described, the recognition of single-stranded RNA (ssRNA) was proposed to require the presence of a terminal 5'-triphosphate[127,128]. In the previous experiments, ssRNA represented a weaker ligand than dsRNA (Fig. 4-30). To test the sensitivity of RIG-I to ssRNA we decided to perform titration experiments as with the dsRNA above. We transfected Huh7.5 RIG-I wt cells with either single-stranded or double-stranded 100 nucleotide *in vitro* transcribed RNA in equal molarities (Fig. 4-34). Double-stranded RNA reached signalling saturation at about 1 pmol/well whereas single-stranded RNA of the same length was barely active at this concentration. However, also single-stranded RNA induced comparable ISG56 reporter activity upon transfection at 1000-fold higher ligand concentration. Although transfected dsRNA harbors twice as many triphosphorylated 5'-ends compared to the ssRNA this could not explain the enormous difference in RIG-I mediated recognition.

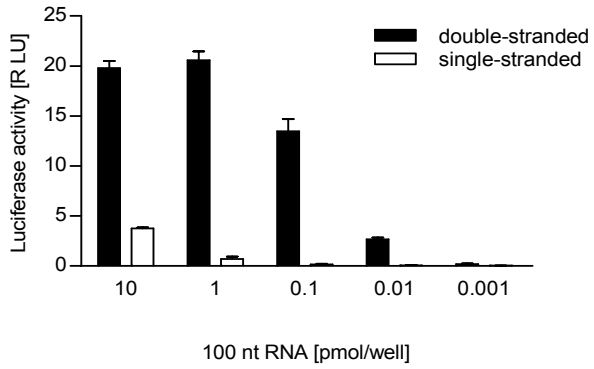

Fig. 4-34 Comparison of single-stranded and double-stranded RNA ligand recognition by RIG-I
100 nucleotide *in vitro* transcribed RNA was used for transfection at the indicated concentrations either in a single-stranded conformation (white bars) or in double-stranded conformation (black bars). ISG56 reporter activity was determined by Dual Luciferase Assay. (n=2, mean +SD).

To investigate the influence of the 5'-triphosphate and the length of ssRNA ligands on RIG-I recognition, ssRNA ranging from 100 to 1600 nucleotides was phosphatase-treated and used for transfection. Compared to the 100 nucleotide dsRNA all ssRNAs showed weaker induction of IRF3 signalling (Fig. 4-35). Dephosphorylation of the ssRNA resulted in a significant signal abrogation for ssRNA ligands up to a length of 200 nucleotides. Transfection with dephosphorylated ssRNA longer than 200 nucleotides resulted in a reduction but not significant abrogation of signalling indicating that also ssRNA represents a target structure for RIG-I. Importantly, as already observed for dsRNA ligands the recognition of ssRNA was length-dependent. Single-stranded RNA tends to form double-stranded stretches (4.1.8). Therefore the length-dependent signalling increase might be caused by a higher extent of double-stranded stretches in longer RNA molecules. In contrast to dsRNA recognition, the 5'-triphosphate contributes also to the recognition of RNA ligands longer than 200 basepairs.

Importantly, the influence of the 5'-triphosphate decreased with increasing substrate length comparable to the findings for the recognition of dsRNA. The stronger contribution of the 5'-triphosphate for ssRNA induced signalling is very likely to be caused by the lower extent of double-stranded target structures compared to dsRNA. The fact that signalling of dephosphorylated double-stranded 100 nt *in vitro* transcript was not altered compared to the untreated control was due to the applied ligand concentrations which were far in saturation for dsRNA (Fig. 4-32).

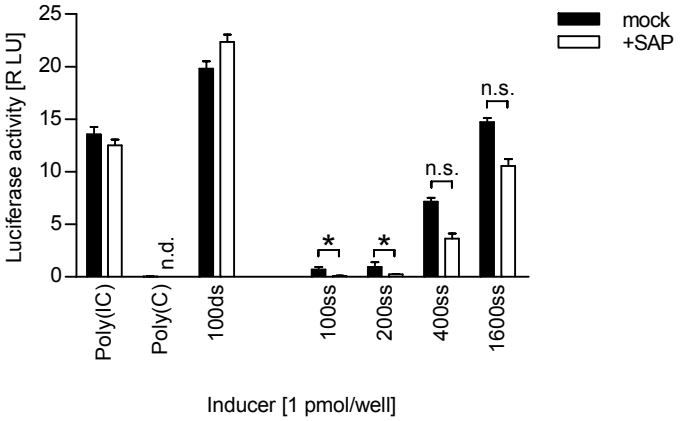

Fig. 4-35 Contribution of length and 5'-end on ssRNA recognition by RIG-I
1 pmol/well of *in vitro* transcribed ssRNA (ss) of the indicated lengths were used for transfection. ssRNA was either phosphatase treated (white bars) or not (black bars). 100 nucleotide dsRNA , 0.1 µg/well Poly(IC) and 1 µg/well Poly(C) were used as controls. ISG56 reporter activity was determined by Dual Luciferase Assay. (n=2, mean +SD). (n.d., not detected, n.s., not significant, *, $p<0.05$, as compared to the mock-treated RNA ligand).

Taken together, these reporter experiments clearly showed that RIG-I is triggered by 5'-triphosphorylated single- and double-stranded RNA ligands. Further, we could show that dsRNA is recognized also in the absence of a terminal 5'-triphosphate identifying double-strandness as a second target structure for RIG-I. Sensitivity of RIG-I to dsRNA was strictly length-dependent and the contribution of the 5'-triphosphate vanished if substrate length exceeded approximately 200 basepairs. Surprisingly, 400 nt or longer ssRNA also represented a ligand for RIG-I even in absence of a 5'-triphosphate. However the 5'-triphosphate contributed to RIG-I mediated signalling also for longer ssRNA ligands which contrasted the observation for dsRNA.

4.3.3 RIG-I-ligand interactions

The results from the ISG56 reporter assays showed that RIG-I possesses a higher sensitivity to longer dsRNA substrates indicating that RIG-I binds to dsRNA in a length-dependent manner due to a higher number of putative binding sites. In order to validate the results of the reporter studies and to prove quantitative binding of RIG-I to dsRNA, we aimed to study RIG-I:RNA interactions in biochemical assays.

4.3.3.1 Expression and purification of recombinant RIG-I protein

Recombinant RIG-I was expressed with a Glutathione-S-Transferase tag (GST) in *Sf9* cells and was affinity purified with glutathione 4B sepharose; finally wild type RIG-I was liberated by proteolytic cleavage and analyzed by SDS-PAGE (Fig. 4-36). Efficiency of RIG-I expression was tested by coomassie staining of the eluate fraction and verified by western blotting. The eluate fractions contained RIG-I in high purity and the protein showed the expected size. Uncleaved RIG-I_GST or degradation products of RIG-I were not detectable.

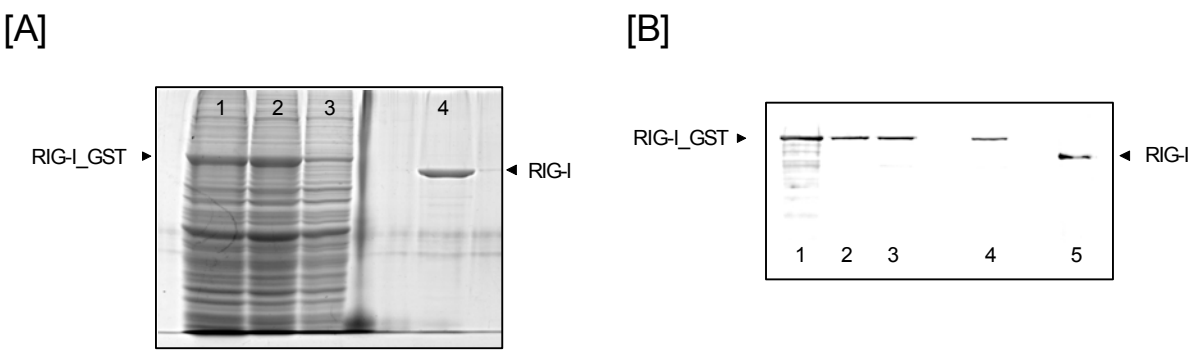

Fig. 4-36 Analysis of recombinantly expressed RIG-I
[A] Coomassie staining of selected fractions of the protein purification process: (1) total lysate, (2) soluble fraction, (3) post-binding supernatant and (4) cleaved eluate. [B] Western blot of selected fractions of the same protein purification: (1) total lysate, (2) soluble fraction, (3) insoluble fraction, (4) post-binding supernatant and (5) cleaved eluate. RIG-I_GST was detected at 132 kDa and cleaved RIG-I at 106 kDa.

4.3.3.2 Functionality of recombinant RIG-I

Functional RIG-I protein has been described to harbor a central domain with high homology to the DexD/H box and therefore to be capable to selectively unwind certain dsRNAs under consumption of ATP[129,130,133]. Recombinant RIG-I protein was therefore tested for ATPase activity upon incubation with different substrates (Fig. 4-37). We observed consumption of ATP when RIG-I was incubated with either Poly(IC) or double-stranded 400 basepair *in vitro* transcript. Non-responsiveness upon incubation without ATP ensured that no free pyrophosphate was present within the reaction mixture.

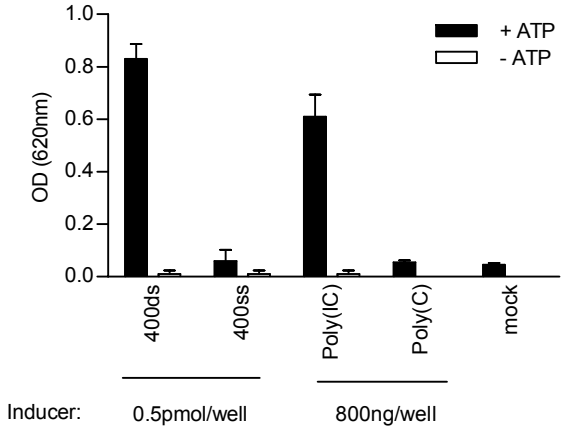

Fig. 4-37 ATPase activity of recombinant RIG-I
2 pmol of RIG-I were incubated for 30 minutes at 37oC with either 0.5 pmol in vitro transcript or 500 ng Poly(IC) and Poly(C), respectively. 1 mM ATP was either added to the reaction mixture (black bars) or not (white bars). ATPase activity was determined in a photometer at 620 nm wavelength. (mean +SD), (n.d., not detected, n.t., not tested).

Further, ATPase activity was low with single-stranded RNA substrates. Activity with the 400 nt single-stranded *in vitro* transcript was more than 10-fold lower compared to the respective double-stranded *in vitro* transcript. The ATPase activity was regarded as evidence for the functionality of the recombinant protein. To test whether same molarities of dsRNA of different lengths induces ATPase activity of RIG-I differently, we incubated RIG-I protein with different concentrations of double-stranded *in vitro* transcripts with increasing length (Fig. 4-38). We observed a length-dependent ATPase activity with dsRNA substrates over the tested concentration range. Paralleling the results of the ISG56 reporter assays, RIG-I showed a higher sensitivity to longer substrates resulting not only in more sensitive signalling but also in higher ATPase activity.

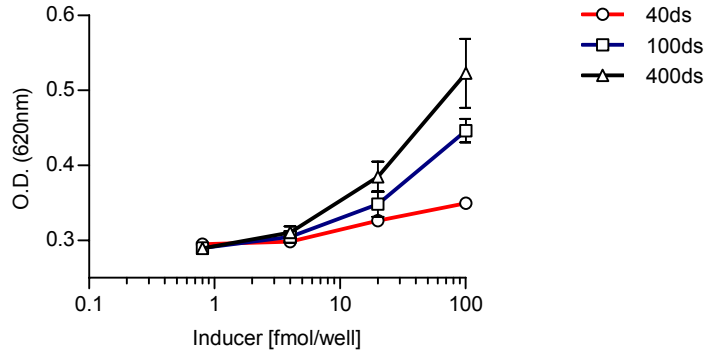

Fig. 4-38 Length-dependent ATPase activity
2 pmol of RIG-I were incubated with three double-stranded in vitro transcripts of 40, 100 and 400 basepairs in length over the indicated concentration range. ATPase activity was determined in a photometer at 620 nm wavelength. (mean ±SD).

4.3.4 Summary

In this study we could show that double-stranded conformation of RNA serves as a recognition motif sufficient to trigger RIG-I. In reporter based titration assays with well defined RNA ligands we detected a drastical increased sensitivity of RIG-I to longer dsRNA ligands. Further, the contribution of the 5'-triphosphate for signalling was shown to be relevant for shorter dsRNA molecules up to a length of approximately 200 basepairs. For longer dsRNA substrates the influence of the 5'-triphosphate reached non-significant levels indicating that the contribution of the 5'-triphosphate might be overestimated for the recognition of long viral RNA sensing. Taken together, these findings show that RIG-I binds besides the 5'-triphosphate also dsRNA in a putatively cooperative manner.

Besides the recognition of dsRNA, RIG-I also binds to ssRNA. Surprisingly we also observed RIG-I-mediated signalling with dephosphorylated ssRNA. However, sensitivity of RIG-I was far below the levels detected for dsRNA recognition. Similar to dsRNA, recognition of ssRNA was also length-dependent. A minimum length of approximately 400 nucleotides was required for efficient signalling indicating that ssRNA might form partial duplex structures which are sensed by RIG-I. Our observations identified dsRNA as a separate recognition motif for RIG-I and help to understand controversially discussed aspects of RNA recognition by RIG-I.

5 Discussion

5.1 siRNA-mediated immunostimulation

The discovery that synthetic short interfering RNA duplexes (siRNA) activate the RNA interference machinery without triggering an interferon response in mammalian cells was considered a breakthrough for the development of siRNA-based therapeutics[140,161]. Consequently, these findings were nominated “breakthrough of the year” by Science magazine[203]. Closer investigations revealed that naked siRNA does not necessarily induce an IFN response *in vivo*[96]. However, it became apparent that systemic application of siRNA in combination with delivery agents such as cationic lipids, under certain circumstances showed severe side-effects, such as the induction of a type-I interferon response. Certain, but not all, siRNAs induced a so far hardly predictable interferon response[97-99] which could be attributed to the activation of TLRs in plasmacytoid dendritic cells[83,85,99,186]. Of note, for the application of siRNAs in therapeutic trials the induction of an interferon response should be avoided or minimized. Otherwise siRNAs could share the fate of antisense oligonucleotides (asODNs) which mostly did not pass clinical trials despite of intriguing *in vitro* results[166]. One reason for the failure of asODNs was that it was not realized that CpG-containing asODNs induce activation of TLR9. Thus, CpG-mediated TLR9 activation, which can easily be avoided, led to failure of a whole class of substances.

It was hypothesized that recognition of siRNA by TLR7/8, TLR3 or PKR[83,98,204] are molecular processes that could be separated from RNA interference which in turn would allow to establish more specific pharmaceuticals. It is now clear that siRNAs induce immunostimulation in a sequence-dependent manner[83,85]. This issue has been investigated in detail for single-stranded RNA oligonucleotides. The exact mechanism of TLR7-mediated RNA recognition is unclear so far but it has been shown that immunoactivation is induced by certain immunostimulatory sequences. Although much effort has been undertaken to identify these immunostimulatory sequence motifs, similar to approaches already described for the recognition of DNA oligonucleotides[78], it became rapidly clear that in contrast to DNA the recognition of RNA did not rely on easily identifiable sequence motifs. So far, it has been suggested that certain GU-rich sequence motifs would induce the observed immunoactivation[81,83,85]. In contrast to these reports, others showed that rather the excessive presence of uridine residues was responsible for immunorecognition by TLR7[86]. It was further assumed that the avoidance of certain sequences, if better defined, would separate siRNA-mediated immunostimulation from RNA interference. However, so far it is barely possible to link the sequence to the immunostimulatory potential of siRNAs. The restriction of RNA-sensing TLRs to endosomal compartments is believed to be the reason that endogenous RNA molecules are not recognized. In addition to the existence of immunostimulatory sequences within RNA molecules and the compartimentalization of the receptors, the absence of nucleotide modifications which naturally occur very abundantly in endogenous RNA has been addressed as a motif for immunorecognition[89]. Various naturally occuring nucleotide modifications have been shown to suppress immunostimulation (e.g. pseudouridine) whereas others showed no significant influence (5’-methylcytidine)[89,90,182,205].

5.1.1 Sequence-dependent recognition of siRNAs

The here presented results confirm that siRNAs are able to induce an interferon response in human PBMCs. It could be shown that the siRNA-induced interferon-α secretion is mediated by TLR7 in plasmacytoid dendritic cells similar to the already described recognition of single-stranded RNA oligonucleotides[81]. TLR7 dependency was further validated using TLR7-knockout mice. Since it has been reported previously that siRNA duplexes do not separate when entering endosomal compartments but rather stay in a double-stranded conformation[101] it can be assumed that TLR7 binds not only single-stranded RNA ligands but is also triggered by short double-stranded RNA substrates as already described for TLR3[109]. Recent reports demonstrated that TLR3 forms dimeric structures upon binding of dsRNA which are required for activation[115,116]. Further, it became evident that the immunostimulatory potential of various siRNAs differed significantly suggesting a sequence-dependent recognition since all siRNAs were synthesized similarly and did not differ in length. Transfection with different RNA oligonucleotides, either avoiding or favouring previously suggested uridine or guanosine-uridine rich immunostimulatory motifs, indeed resulted in a differential induction of interferon-α secretion in human PBMCs.

RNA oligonucleotides with a low amount of either guanosine or uridine residues showed in general a low ability to induce interferon-α in contrast to oligonucleotides with a high content of the respective nucleotides. However, oligonucleotides EGFP1as and EGFP1s containing no more than the statistically expected number of guanosine and uridine residues in a random order surprisingly showed a high potential to induce interferon-α. These results indicated that the sequence of the transfected oligonucleotide might not be the only target structure for immunorecognition principles of TLR7.

5.1.2 Nucleotide modifications within the minor groove of RNA duplexes reduce immunostimulation

Within this work it could be shown that the introduction of modified nucleotides into RNA oligonucleotides resulted in an altered type-I interferon secretion. RNA oligonucleotides containing 2'-deoxy and 2'-*O*-methoxy residues revealed that the 2'-position of the ribose is very relevant for immunorecognition. 2'-deoxyuridine including thymidine but none of the other deoxy-modified nucleotides was identified to significantly reduce interferon-α secretion (4.1.4.1). In agreement with this observation 2'-*O*-methyl-uridine and, additionally, 2'-*O*-methyl-adenosine abolished immunostimulation. From the literature it is also known that 2'-*O*-methyl-guanosine reduces immunostimulation, thus our results now contribute to the notion that the 2'-position of the ribose is critical for TLR7-mediated recognition[91,92,206]. However, the 2'-*O*-methyl derivate of cytosine showed no effect in terms of altered interferon secretion. This confirms again that immunorecognition also depends on certain immunostimulatory sequence motifs which are very likely to comprise no cytosine residues.

The substraction as well as the methylation of the hydroxyl group at the 2'-position of the ribose removes a possible hydrogen bonding donor. Both modifications alter the minor groove within an RNA duplex. On the other hand, nucleotide modifications which alter the nucleobase and therefore the major groove of an RNA duplex did not influence the extent of immunorecognition. Neither

5’-methylcytidine-containing EGFP1as which harbors a sterically demanding methyl-group at the site of major groove recognition nor 7’-deazaguanosine-containing EGFP1as which omits a nitrogen as a possible H-bond acceptor showed any effect in terms of interferon-α secretion (Fig. 5-1).

Taken together, the results support the conclusion that immunorecognition of RNA depends on recognition within the minor groove whereas alterations of the major groove show only negligible effects assuming that siRNA forms a duplex structure. Thus, the minor groove of an RNA duplex seems to be the target structure for TLR7-mediated recognition in contrast to most DNA protein interactions which are mediated by major groove recognition. However, RNA duplexes can form A-type helices which in contrast to B-type DNA helices exhibit a larger minor groove, thus allowing for better protein interactions. The potential to reduce immunostimulation by 2’-deoxyuridine and thymidine residues was comparable and quite effective. Introduction of thymidine residues in two further functional siRNA molecules revealed that modification of uridine residues displays a universal strategy for the reduction of interferon-α secretion in human PBMCs. This observation is now confirmed by recent reports showing that 2’-deoxyuridine-containing RNA strands reduce immunostimulation[100,206].

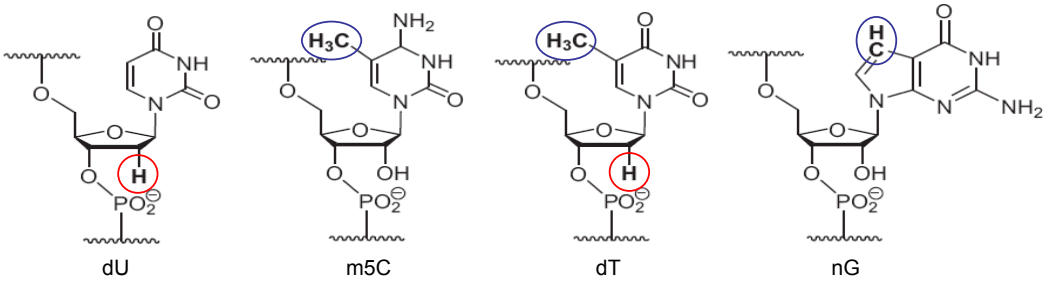

Fig. 5-1 Structures of 2’-deoxyuridine, 5’-methyl-cytosine, thymidine and 7’-deazaguanosine
Uridine was replaced by 2’-deoxyuridine (dU) or thymidine (dT) missing a hydroxylgroup at the 2’-position of the ribose affecting the recognition within the minor groove (encircled in red). Modifications facing the major groove as the methylgroup at the 5’-position of the uridine nucleobase (dT), an additional methylgroup at the 5’-position of the cytosine nucleobase (m5C) or missing nitrogen at the 7’-position of the guanosine nucleobase (nG) do not alter immunostimulation (encircled in blue).

Transfection of 2’-deoxyuridine- as well as thymidine-containing RNA oligonucleotides at high concentrations such as 1 µg/ml still induced residual interferon-α secretion in human PBMCs. In contrast to this observation, 2’-*O*-methyl-adenosine and 2’-*O*-methyl-uridine-containing RNA oligonucleotides were completely inactive even at the highest concentrations applied. This observation is in agreement with other reports showing that 2’-*O*-methyl-uridine residues convert RNA oligonucleotides to become antagonists in terms of TLR7-mediated signalling[91,92]. In contrast to the tested uridine and adenosine residues as well as contrasting reports investigating the influence of guanosine on immunostimulation, 2’-*O*-methyl-cytosine showed no significant effect on immunostimulation. In parallel 2’-deoxy-cytosine residues reduced immunostimulation to some extent but still to a much lower extent than 2’-deoxy-uridine residues. This indicates that cytosine residues are not part of any possible immunostimulatory motif.

5.1.3 2'-*O*-methyl-modifications inhibit TLR7 signalling

The differences between 2'-*O*-methyl-modifications and 2'-deoxy-modifications became more obvious when investigating the immunostimulatory potential of double-stranded RNA duplexes. 2'-*O*-methyl-adenosine modified RNA oligonucleotides were already completely silent in terms of interferon-α secretion if only the leading-strand of an siRNA duplex was modified. Thus, the immunostimulation of the unmodified passenger-strand was suppressed indicating that 2'-*O*-methyl-modifications act in a dominant-negative manner on TLR7 signalling. In contrast, 2'-*O*-methyl-uridine modifications showed only a reduction in interferon-α secretion comparable to 2'-deoxy-uridine-modified RNA if incorporated in the leading-strand of an siRNA. Additionally, it was reported that 2'-*O*-methyl-uridine also inhibits TLR9 activation by type A CpG-oligodeoxynucleotides in human and mice, thus lacking TLR7/8 specificity[91]. This identifies thymidine modifications as immunologically silent in contrast to 2'-*O*-methyl-adenosine-modifications. In agreement with this observation cotransfection of EGFP1as and dT-modified EGFP1as resulted in a reduction of interferon-α of about 50% showing that the dT-modified RNA oligonucleotide did not influence the triggering of TLR7 by the unmodified EGFP1as. In contrast, cotransfection with 2'-*O*-methyl-adenosine-modified EGFP1as completely abrogated immunostimulation of unmodified EGFP1as. Introduction of thymidine residues in both strands of an siRNA duplex further decreased interferon-α secretion in human PBMCs indicating that residual activity had indeed been induced by the unmodified passenger-strand of the duplex. Importantly, the residual immunological activity of the RNA duplex with thymidine in both strands was only observed in concentrations which were far above of those needed for RNA interference activity. Taken together, these results show that thymidine modifications represent silent modifications in terms of immunorecognition which contrasts findings for 2'-*O*-methyl-derivates that dominantly inhibit TLR7 signalling. Clinically, our findings might be important, since thymidine modifications would still allow intact TLR7 signalling and recognition of other ligands (e.g. viral ssRNA)[207]. Antagonistic activity on TLR7 signalling induced by 2'-*O*-methyl-adenosine would not be desirable in this context.

5.1.4 Nucleotide modifications influence RNAi differentially

Next, it had to be assessed whether the immunological relevant modifications influence RNA interference. Indeed, the tested modifications showed significant differences in terms of RNA interference. Whereas thymidine modifications in the leading-strand of an siRNA duplex showed only marginal reduction of gene-silencing activity compared to the unmodified siRNA duplex, 2'-deoxy-uridine substitutions were already less efficient. Introduction of thymidine residues into two further antisense strands of functional siRNA molecules also showed no significant reduction of gene-silencing activity suggesting a general principle. The lower ability of 2'-deoxy-uridine residues compared to thymidine residues in terms of gene-silencing might be explained by a higher stability of the thymidine-containing duplex. Even introduction of thymidine residues in the second strand of an siRNA duplex, which was necessary to completely block immunostimulation, did not alter the ability to suppress gene expression. In sharp contrast to these findings, 2'-*O*-methyl-uridine-modified and especially 2'-*O*-methyl-adenosine modifications showed a lower efficiency in gene silencing. Therefore, the introduction of 2'-*O*-methoxy derivates, although showing a strong reduction in terms of interferon secretion are not favourable for the introduction into siRNA molecules due to their lower

ability in gene-silencing activity. It has been reported that the 2'-hydroxyl-group of the ribose is not essential for RNA interference[208] with exception of sterically very demanding groups (e.g. methylation) which might influence the RNAi machinery. Especially modifications in the leading-strand of an siRNA duplex are well tolerated and even not naturally occuring modifications such as 2'-fluoro modifications are able to induce efficient gene-silencing[209]. The position of modified nucleotides for gene-silencing activity of the respective siRNA duplex depend on the kind of modification[210,211] but in general it is thought that modifications in the middle of a duplex are not well tolerated[212]. Our results suggested that thymidine residues are a valuable tool to design functional siRNA molecules and simultaneously inhibit unwanted side-effects like interferon-α secretion.

5.1.5 TLR7 might detect double-stranded structures

Ligand recognition of RNA in double-stranded conformation by TLR3[109] was also recently implicated for DNA recognition of TLR9. It was shown that CpG-containing DNA in forced double-stranded conformation is preferentially recognized by TLR9 due to higher ligand stability compared to single-stranded DNA ligands[213,214]. Further, a recent report demonstrated that similar to TLR9, N-terminal cleavage of TLR7 is required for ligand binding and activation. Additionally, TLR7 and TLR9 belong to the same subfamily of TLRs and show high sequence homology and the same number of LRRs with irregular insertions[215,216]. The high homology of TLR7 and TLR9 suggests the possibility that the same mechanisms of receptor activation are operative. In turn this would indicate that TLR7, similar to TLR9, might recognize RNA preferentially in double-stranded conformation.

The important role of uridine residues for immunorecognition was demonstrated by the significant reduction of type-I interferon secretion if modified at the 2'-position of the ribose. Further, the here presented results, in addition to several other reports, demonstrated that uridine plays a pivotal role for immunorecognition[86,92,100]. Uridine residues tend to the form duplex structures since they are not only able to bind to adenosine but also to guanosine residues[185]. Taken together, there is some indication that TLR7-mediated recognition is induced by the presence of uridine residues within double-stranded RNA stretches.

Indeed, hyperchromicity assays within this work confirmed that the immunostimulatory RNA oligonucleotide EGFP1as has the propensity to form secondary structures. We detected two different transition points for EGFP1as indicating secondary structure formation. The lower detected temperature transition was significantly reduced in dT-modified EGFP1as. This indicates indirectly that secondary structure formation could be critical for immunorecognition. Further indication for this conclusion resulted from the fact that RNA oligonucleotides with a low ability to induce interferon-α secretion displayed no or low formation of intramolecular duplex structures when analyzing the sequences by hyperchromicity assays or structure prediction programs. Investigations of intramolecular and intermolecular structure formation as well as uridine content confirmed that all RNA oligonucleotides with a high ability to induce interferon-α owned a high content of uridine residues within possible secondary stem-loop structures. Although the frequency of immunorelevant modifications was shown to influence the potential of type-I interferon secretion[89], partial substitution of uridine residues within two different immunostimulatory RNA oligonucleotides did not result in significant differences regarding interferon-α secretion. Neither thymidine insertions within predicted stem-loop structures nor within sequences predicted to form no secondary structures resulted in a

significant reduction of interferon-α secretion. These findings indicate that uridine residues in general might be detected by TLR7 rather than exclusively in stem-loop structures. On the other hand, the substitution of only some uridine residues might not be sufficient to suppress immunostimulation since alternative secondary structures, besides the predicted ones, might form.

Taken together, the here presented results show that immunorecognition of siRNA is induced in a very similar manner as already described for recognition of single-stranded RNA oligonucleotides[81]. It became evident that published immunostimulatory sequences contributed to the extent of interferon-α secretion but sequence motifs are not the only origin of immunostimulation. Additionally, nucleotide modifications at the 2'-position of the ribose, as they occur in high frequency in endogenous RNA (e.g. 2'-methoxy-modifications in messenger RNA)[90] are critical for TLR7-mediated recognition. This gives strong evidence that rather the minor groove than the major groove is the site of recognition. Thymidine residues were identified as favourable modifications within siRNA molecules since they altered RNA interference only slightly compared to all other tested immunorelevant modifications but reduced immunoactivity. In contrast to thymidine residues, 2'-*O*-methyl-adenosine substitutions completely inhibited TLR7 signalling. This modification showed a strong reduction in RNA interference efficiency and was therefore considered not useful for siRNA applications, but could be used for specific TLR7 inhibition. In parallel to the other nucleic acid sensing TLRs 3 and 9, evidence is presented that TLR7 also recognizes its ligand in double-stranded conformation.

5.2 Immunorecognition of prokaryotic RNA

Additionally to siRNA mediated immunorecognition, this work focused on the investigation of the mechanisms of prokaryotic RNA recognition. Prokaryotic DNA has been described in several reports as a target for immunorecognition principles. It has been demonstrated that prokaryotic DNA is sensed in a TLR9-dependent manner[78]. Additionally, strong evidence has been given for the presence of a cytosolic DNA receptor[78,137,217]. However, in contrast to the well-described recognition of viral RNA, the mechanisms of bacterial RNA recognition are barely understood. At the beginning it was even unclear whether prokaryotic RNA is active in terms of immunostimulation. Although bacterial RNA carries various non-self structures such as an altered nucleotide modification pattern[89], a 5'-triphosphate in the messenger RNA[187] and stretches of double-stranded conformation which allow for the interaction with different PRRs, the contribution of the respective receptors remained elusive. Further, species–dependent recognition as it has been described for the recognition of bacterial DNA[79] was not investigated so far.

Viral RNA has been shown to represent an immunostimulatory pattern which induces a type-I interferon response. Recognition has been associated with the sensing by receptors belonging to the TLR and RIG-like receptor class[44,192]. The principles to distinguish non-self RNA from host-derived RNA are structural differences found in the RNA molecules[127,131]. Recognition of viral RNA by professional immune cells has been shown to be mediated by the RNA-sensing TLRs 3, 7 and 8[109,192]. Recognition of endogenous RNA is limited by the restriction of these TLRs to endosomal compartments which get only into contact with RNA molecules that have been taken up via the endocytotic pathway. Besides this compartimentalization it has been shown that nucleotide

modifications as they occur in eukaryotic RNA are able to reduce immunostimulation[89,90]. Further structural differences such as a shorter poly-A tail of prokaryotic RNA have been identified as a target structure for TLR-mediated recognition[218]. Besides the recognition by TLRs, viral RNA has been shown to be sensed by the cytoplasmic RNA sensor proteins RIG-I and MDA5. These proteins target structures that are characteristic for viral RNA, such as double-stranded conformation[131] or the presence of an accessible 5'-triphosphate[127].

5.2.1 TLR7-mediated recognition of prokaryotic RNA

In this work, it could be shown that similar to viral RNA, bacterial RNA is also recognized in a TLR7-dependent manner by plasmacytoid dendritic cells (pDCs). It has been shown that this cell-type shows enhanced endosomal uptake and retains received molecules for a longer time within the endosomal compartment[28]. Further, pDCs show strong expression of the endosomal TLRs 7 and 9 making this cell-type to a predestinated sensor for non-self nucleic acids[191,219]. Additionally, these cells are strong producers of type-I interferons due to their constitutive expression of IRF7[24]. Bacterial RNA in this work now has been shown to be an inducer of IFN-α. Interestingly, the potential to induce IFN-α was rather similar between the different tested bacterial species. Immunostimulation did neither correlate with the gram-type of the tested bacteria nor with possible contaminants since RNAseA digestion resulted in a nearly complete abrogation of IFN-α secretion. Although there is indication that TLR7 recognizes certain sequence motifs within RNA oligonucleotides[81,83] this seems to play only a minor role for whole bacterial RNA preparations.

Sequence analysis of the ribosomal RNA (rRNA) of the different bacterial species did not show any superior abundance of immunostimulatory sequence motifs in any of the tested species when aligning bacterial rRNA sequences with published immunostimulatory sequence motifs.

This contrasts findings for the recognition of bacterial DNA by TLR9 which has been shown to correlate directly with the content of CpG dinucleotides within the sequence[79] indicating that RNA sensing is not limited to certain sequence motifs. Stimulation with non-self RNA of eukaryotic origin as for example *Candida albicans* resulted in a significant lower IFN-α secretion. This might be due to the higher content of nucleotide modifications within eukaryotic RNA[220] which has been described to be relevant for TLR-mediated RNA sensing[89]. Ribosomal RNA which represents approximately 80% of the total cellular RNA was isolated and tested for IFN-α secretion. Immunostimulation with 16S rRNA showed the same dose-dependent IFN-α secretion as the respective total RNA of *Escherichia coli* identifying ribosomal RNA as one of the major immunostimulatory component within bacterial RNA. TLR7-mediated recognition of bacterial RNA was proven by cotransfection with the TLR7-specific inhibitor 2mA[91,167] (4.1.7) which resulted in a complete abrogation of IFN-α secretion. TLR7-dependency of bacterial RNA induced IFN-α secretion was additionally validated by the use of TLR7 knockout mice and reduction of IFN-α by inhibition of endosomal maturation through chloroquine treatment.

5.2.2 Prokaryotic RNA triggers (a) receptor(s) apart from TLR7

Surprisingly, it could be observed that bacterial RNA is sensed by one or multiple further receptors apart from TLR7. Besides IFN-α, bacterial RNA induced the secretion of TNF-α in human PBMCs Inhibiton of TLR7 by cotransfection with 2mA abrogated RNA oligonucleotide induced TNF-α secretion

as expected but did not alter bacterial RNA induced TNF-α secretion. Further, a significant contribution of any possible contaminant was ruled out since TNF-α secretion vanished upon RNaseA digestion. This observation excluded TLR7 as the responsible receptor for bacterial RNA induced TNF-α secretion in human PBMCs. The responsible receptor system was identified to reside in the cytosol since endosomal maturation showed no influence on activation and bacterial RNA had to be delivered to the cytosol with appropriate transfection reagents (e.g. Lipofectamine). In a similar way, bacterial RNA also induced IL-12p40 in murine mDC-like cells. In contrast to IFN-α secretion in human PBMCs, RNA preparations of gram-negative bacteria showed an increased immunostimulatory potential compared to RNA of gram-positive origin which was possibly attributed to residual amounts of LPS within the RNA preparations of gram-negative bacteria. However, RNA digestion in any case resulted in a significant reduction of IL-12p40 secretion. Similar to TNF-α secretion in human PBMCs the IL-12p40 secretion in murine mDC-like cells was independent of TLR7. The remaining nucleic-acid detecting TLRs 3 and 9 were also ruled out by use of the respective knockout mice. Additionally, chloroquine treatment did not alter bacterial RNA induced IL-12p40 secretion indicating that the same cytosolic receptor system inducing TNF-α in human PBMCs might be responsible for IL-12p40 secretion in murine mDC-like cells. Although a participation of the endosomally located murine TLR8 in bacterial RNA sensing was not specifically investigated, it could be excluded since intact endosomal signalling was dispensable for bacterial RNA recognition.

5.2.3 Viral RNA receptors and NALP3 are dispensable for prokaryotic RNA – induced NFκB activation

Bacterial RNA shares some structural features with viral RNA. Bacterial messenger RNA harbors a terminal 5'-triphosphate which has been shown to be a target structure for RIG-I[127]. Also, partial double-stranded stretches could serve as target structures for RLR-mediated recognition. Transfection of Huh7.5 cells expressing either functional RIG-I or MDA5 with bacterial RNA did not result in any detectable ISG56 transcription although the respective viral RNA ligands resulted in the expected activation. Additionally, RLRs are known to trigger besides IRF3 also NFκB activation[6], however, NFκB activation was neither detectable upon transfection with bacterial RNA nor with viral RNA in Huh7.5 cells. These observations excluded the RIG-like receptors as being responsible for cytosolic bacterial RNA recognition.

The NALP3 inflammasome is known to induce caspase-1 activation which leads to the processing of pro-IL-1β to IL-1β[55]. Besides various other ligands, bacterial RNA has been described to activate the NALP3 inflammasome[135] supporting the idea of further RNA-sensing cytosolic receptor systems. In our experiments the inflammasome adaptor molecule ASC which has been shown to be essential for inflammasome-mediated signalling was necessary for bacterial RNA-mediated IL-1β secretion and, interestingly, this was additional dependent on functional IFNAR1 signalling. Similar observations have been reported for cytosolic *Francisella* induced secretion of IL-1β by activation of the inflammasome which was also dependent on IFNAR1[136]. In contrast to dependency of IL-1β secretion on ASC, the observed induction of IL-12p40 after bacterial RNA transfection was independent on ASC protein. Therefore a further cytosolic receptor system, besides the already described RLRs and the inflammasome has to reside in the cytosol mediating the recognition of bacterial RNA.

5.2.4 Bacterial RNA induces a general danger signal

In addition to the recognition of bacterial RNA by professional immune cells such as dendritic cells we observed that bacterial RNA induced a strong and robust NFκB response in the HEK293T cell line. In contrast to the tested immune cells above, the recognition of bacterial RNA by HEK293T cells was restricted to only some RNA preparations. RNA of gram-negative bacteria with the exception of *Moraxella catharralis* strongly induced NFκB whereas most RNAs of gram-positive origin with the exception of *Bacillus subtilis* induced NFκB only weakly. The observed effects were still attributed to the RNA since RNaseA digestion abrogated activation completely. Similar to the experiments with immune cells neither additionally transfected nucleic acid sensing TLRs nor endogenously expressed TLR3 and RIG-I could be linked to bacterial RNA recognition. It has been reported that bacterial contaminants activating TLRs and NLRs simultaneously could result in a synergistic activation[70]. We therefore tested a possible contribution of NOD1 and NOD2 receptors which are both expressed in HEK293T cells but could not detect a significant influence. Further phenol/chloroform purification of bacterial RNA showed only a minor reduction of the immunostimulatory potential indicating that putative residual contaminants did not play a pivotal role for recognition. Moreover, digested immunostimulatory *Escherichia coli* RNA could not reconstitute immunoactivation of the weak immunostimulatory *Staphylococcus aureus* RNA proving that the observed effects are indeed attributed to the RNA.

It is noteworthy that professional immune cells and especially pDCs make use of the TLRs to recognize microbial nucleic acids leading to a specific immune response. The recognition principles are highly specific and sense certain sequence motifs in RNA oligonucleotides as well as the content of nucleotide modifications. In contrast, cytosolic receptor systems are expressed much more broadly and less specific. The finding that bacterial RNA is detected by an unknown cytosolic receptor within a broad range of cell-types parallels previous findings of the cytosolic recognition of bacterial DNA. It was shown that independently of a specific sequence, DNA triggers a cytosolic receptor[221,222]. In fact, much attention has since then been focused on the identification of cytosolic recognition principles of nucleic acids. The discovery of the DNA-sensing receptor DNA-dependent activator of IFN-regulatory factors (DAI)[80] firstly showed that besides the TLRs additional cytosolic receptors are involved the recognition of non-self DNA. Additionally the Trex1 protein which was originally described to be involved in DNA repair was shown to sense single-stranded DNA retroelements leading to the induction of type-I interferons[217]. The identification of new cytosolic DNA-sensing receptor systems supports the idea of similar recognition systems for the sensing of non-self RNA. Double-stranded DNA has recently been shown to induce the secretion of IL-1β mediated by the newly identified receptor AIM2. Further, it has been demonstrated that AIM2 binds to the adaptor protein ASC forming an inflammasome which in turn activates caspase-1 similar to the well-described RNA sensing NALP3 inflammmasome[223]. Taking into account that the recognition of DNA and RNA follows comparable mechanisms and that there are several cytosolic receptor systems recognizing non-self DNA strongly suggests the existence of further RNA sensing receptors.

The biological relevance of the cytosolic nucleic acid recognition for host defense is not fully understood yet. The fact that bacterial RNA is sensed over a broad range of different cell-types including non-immune cells such as HEK293T cells suggests that cytosolic RNA sensing serves rather as a general danger signal than as a specific immune signal as it is induced by the TLR system.

Induction of the cytosolic recognition system could be a signal that the cells are already inevitable infected and lost. Type-I intererons in case of viral RNA or viral DNA and NFκB activation in case of bacterial RNA, followed by chemokine induction (e.g. IL-8), attracts further cells and alarms neighboring cells. This could be regarded as a general cell-autonomous defence response as it is currently discussed and which is also a topic that has been addressed by the "Sonderforschungsbereich 670" in Cologne.

5.3 Ligand specificity of RIG-I

In contrast to bacterial RNA recognition, viral RNA recognition has been investigated in more detail. RIG-I and MDA5 have been identified as the two major receptors for cytosolic viral RNA.

Two recent reports demonstrated that RIG-I is not detecting double-stranded RNA but instead RNA bearing a 5'-triphosphate, be it single- or double-stranded[127,128]. On the other hand, it has been shown that the C-terminal RD domain of RIG-I comprises a basic cleft which binds 5'-triphosphorylated RNA as well as double-stranded RNA. In contrast to ssRNA, binding of dsRNA was independent of a terminal 5'-triphosphate indicating that double-strandness might display a second target structure within vRNA recognition by RIG-I[129]. However, recognition and signalling of RIG-I upon dsRNA binding remained controversially discussed.

In order to characterize the role of dsRNA recognition by RIG-I and to analyze the influence of a 5'-triphosphate, we used an RIG-I signalling negative cell line (Huh7.5) overexpressing functional RIG-I protein (Huh7.5 RIG-I wt)[173] which proofed to be a highly sensitive tool for measuring RIG-I activity and to quantify RIG-I signalling. In ISG56 reporter assays Huh7.5 RIG-I wt cells showed high sensitivity to Poly(IC) stimulation. Since Poly(IC) is synthesized from nucleotide-diphosphates and therefore harbours no 5'-triphosphate there was a first indication that RIG-I is sensing also double-stranded RNA structures in the absence of a 5'-triphosphate. Further, no RIG-I-mediated signalling was detected upon transfection with Poly(C) or Poly(I) which are due to their sequence unable to form secondary structures. A possible participation of TLR3 had been ruled out because microarray analysis revealed no endogenous expression. Additionally, LPS which is known to be a highly potent ligand of TLR4 and to be a very present contamination even at concentrations as high as 100 ng/well showed no activity in the reporter assays.

5.3.1 Double-stranded RNA is recognized by RIG-I

Transfection of Huh7.5 RIG wt cells with either short (58 nt) or long (9600 nt) *in vitro* transcripts of Rabies Virus leader sequence (RV) and Hepatitis C Virus (HCV), respectively, resulted in ISG56 activation. ISG activation by the single-stranded transcripts could nicely be explained with the presence of terminal 5'-triphosphates. Signalling activity upon transfection with double-stranded RV RNA was not significantly elevated compared to the single-stranded RV RNA. In contrast to the short RV duplex (58 bp), we observed a strongly increased signalling of the HCV RNA duplex (9600 bp) compared to the single strand. These results indicated that double-stranded RNA conformation indeed represents a second target structure for RIG-I besides the terminal 5'-triphosphate. Assuming that dsRNA is recognized by RIG-I regardless of any 5'-triphosphate, it appears plausible that the length of the double-strand is crucial for the extent of signalling activity leading to the hypothesis that double-

strand recognition by RIG-I depends on the length of the ligand. Although signalling was drastically increased by transfection with longer dsRNA, comparability was limited since both ligands differ in sequence. Sequence-dependent recognition by RIG-I is not well investigated. However a recent report showed that RIG-I activity of viral ssRNA is determined by the presence of uridine (U)- or adenosine (A)-rich sequences that can be hundreds of bases apart from the 5'-end[132]. Additionally uridine-rich sequence stretches within the HCV genome were identified of being preferentially recognized by RIG-I[132]. On the other hand, an increasing number of guanosine (G) residues were shown to reduce 5'-triphosphate induced signalling[224]. However recognition of certain sequences by RIG-I might have only a minor influence since the 5'-triphosphate was shown to be sufficient for signalling activity.

In order to investigate length-dependent dsRNA recognition by RIG-I in detail, we decided to generate *in vitro* transcripts increasing in size with overlapping sequence to minimize sequence-specific effects on signalling. Further, we purified the *in vitro* transcripts by gel excision to ensure the absence of otherwise frequent side-products of the *in vitro* transcription reaction. Thus, the generated RNA substrates possessed a defined size, high purity and were controlled for integrity.

5.3.2 Sensitivity of RIG-I to dsRNA is length-dependent

Transfection of Huh7.5 RIG-I wt cells with dsRNA ligands ranging from 40 to 1600 basepairs showed no significant increase in maximal signal strength. The final levels of signalling activity were rather slightly decreased upon transfection with longer dsRNA ligands. These results were in agreement with a recent report showing that RIG-I detects shorter dsRNA substrates whereas MDA5 is the major sensor for long dsRNA[131]. Notably, mainly Poly(IC) was used the cited work which was digested for different amounts of time resulting in dsRNA analogs of different length. Digested Poly(IC) was validated by gel electrophoresis but it was not ensured that residual side products were present within the sample and this should be considered when interpreting the reported results. Further, Poly(IC) of different length was transfected in equal mass and not molarity resulting in an increasing number of shorter Poly(IC) molecules and thereby limiting the comparison of the ligand length. Finally, ligands were transfected in saturated concentrations and only maximal signalling was measured instead of sensitiviy of RIG-I to the ligand. The slight decrease in maximal signalling upon transfection in saturated concentrations might rather be caused by the fact that the adaptor molecule IPS-1 is attached to the mitochondrial membrane and is therefore not fully accessible for all RIG-I molecules bound to a very long RNA molecule. Shorter RNA molecules would not bind as many RIG-I proteins, resulting in lower sensitivity, but all of them could bind to the respective adaptor IPS-1 due to smaller complex size.

Carefully, performing titration experiments with clearly defined transcripts here showed that sensitivity of RIG-I to dsRNA increasing in size was dramatically enhanced. Assuming that RIG-I binds to dsRNA structures, it appears feasible that longer dsRNA stretches would offer more accessible receptor binding sites resulting in the observed increase in sensitivity. Moreover, we determined the substrate concentration for half-maximal signalling (K_{50}) for the respective dsRNA molecules and defined the reciprocal ($1/K_{50}$) as sensitivity of RIG-I to its ligand. Sensitivity of a 400 basepair duplex compared to a 100 basepair duplex was increased 15-fold although ligand length was only 4-fold higer. These results strongly indicated that RIG-I might in fact bind to dsRNA in a cooperative manner. This suggests that the affinity of RIG-I to bind to dsRNA increases with the presence of already bound RIG-

I. In support to the results from the reporter assays, we observed enhanced ATPase activity of recombinantly expressed RIG-I upon incubation with dsRNA ligands of increasing size. The role of the RIG-I-owned ATPase activity for immunorecognition has been discussed controversially. However, mutations of the ATP-binding site resulted in a complete loss of signalling but ligand binding of dsRNA and 5'-triphosphorylated RNA was not influenced[6,133]. However, the current opinion is that ligand binding and ATPase activity are both required for the formation of an active RIG-I complex.

Importantly, the total number of 5'-triphosphates was identical among all transfected dsRNA ligands excluding the possibility that the observed differential signalling activity was generated by the 5'-ends. Taken together, double-stranded conformation of RNA was identified as a recognition motif for RIG-I-induced signalling activity. Further, these findings indicate cooperative binding of RIG-I to dsRNA as concluded from the observed disproportional increase in sensitivity of RIG-I towards longer dsRNA ligands. For half-maximal sensitivity a minimum ligand length of approximately 340 basepairs is required suggesting that the biological function of RIG-I is in fact the sensing of long dsRNA molecules. The detection of terminal 5'-triphosphorylated structures might support the recognition but is very likely to play a minor role for signalling in response to longer dsRNA. The 5'-triphosphate might be the initial motif which is recognized when viral RNA genomes enter the cell. During viral replication, the double-stranded RNA replication intermediate might present the second motif for RIG-I leading to an increase of signalling and thereby reducing the relevance of the 5'-triphosphate.

5.3.3 Contribution of the terminal 5'-triphosphate to RIG-I signalling

Length-dependent binding of RIG-I to double-stranded RNA implicated that this binding would diminish the relative contribution of the 5'-end with increasing ligand length. We hypothesized that the relevance of the 5'-end would be important for short dsRNA ligands, as confirmed by several reports but would vanish with increasing substrate length. To investigate the role of the 5'-end we dephosphorylated the RNA strands before annealing. Dephosphorylation was shown to be highly efficient and not to affect ligand integrity. Transfection was performed with dsRNA substrates either mock- or phosphatase-treated with the determined concentrations for half-maximal signalling. We observed that the contribution of 5'-triphosphate-mediated signalling decreased with the substrate length, reaching non-significant levels from about 200-400 basepairs on.

These results show that double-stranded conformation and the 5'-triphosphate display two independent target structures for RIG-I-mediated signalling. Double-stranded ligands shorter than 100 basepairs are preferentially detected by the presence of the 5'-triphosphate whereas longer ligands are detected mainly by the double-strand configuration which offers more putative binding sites and therefore making the 5'-end dispensable (Fig. 5-2). Again, dsRNA substrates, being 200 basepairs or longer in size, present sufficient double-stranded conformation for full signalling activity at ligand concentrations for half-maximal signalling. These results implicate that the role of the 5'-triphosphate might be overestimated and the recognition of double-stranded RNA underestimated. On the other hand, several reports showed that RIG-I-mediated recognition of viral RNA genomes (e.g. influenza) strictly depends on the presence of a terminal 5'-triphosphate[127,128]. In fact, recognition of the 5'-triphosphate might be the initial cellular response upon entering viral RNA, whereas double-strand recognition by RIG-I represents a response to replicating virus. Therefore, both recognition motifs would be relevant for cellular defence during different steps of viral infection.

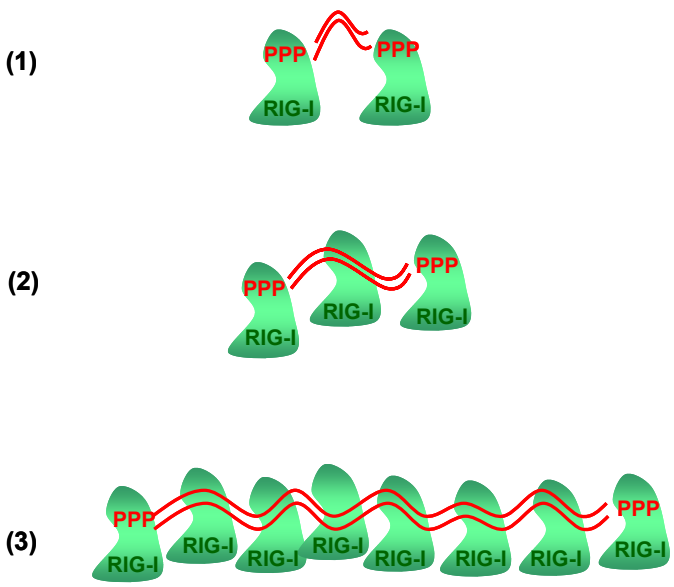

Fig. 5-2 Model for dsRNA recognition by RIG-I
(1) Small dsRNA is recognized by RIG-I in the presence of 5'-triphosphates (PPP). (2) Longer dsRNA molecules (approximately 100 bp) enable RIG-I to bind also to double-stranded stretches leading to a partially 5'-triphosphate-independent signalling. (3) dsRNA molecules from 200-400 bp on provide binding sites for more RIG-I molecules and thereby reduce the relative contribution of the 5'-triphosphorylate-induced signalling.

5.3.4 Single-stranded RNA is a ligand for RIG-I

Several reports showed that 5'-triphosphorylated and double-stranded RNA binds to the C-terminal domain (CTD) of RIG-I[129,130]. A basic cleft within the CTD was identified to be responsible for binding. In fact, single-stranded RNA without a terminal triphosphate was shown not to bind within this cleft excluding non-phosphorylated single-stranded RNA as a possible ligand for RIG-I. However, all reports dealt with RNA *in vitro* transcripts far below 100 nucleotides in length. In fact, in our experiments reporter activity upon transfection with 100 nucleotide *in vitro* transcript resulted in an approximately 1000-fold lower activity of the single-strand compared to the duplex. Still, also the single-stranded *in vitro* transcript showed dose-dependent signalling indicating a specific recognition. Regarding the length-dependent recognition of double-stranded RNA substrates, we suggest a similar mechanism for the recognition of single-stranded RNA. Indeed, upon transfection with ssRNA in equimolar concentrations but increasing in size we observed a length-dependent signalling activity. Importantly, the total number of 5'-triphosphates was identical indicating that also ssRNA harbors possible recognition sites for RIG-I binding apart from the 5'-end. Dephosphorylation resulted in signalling abrogation for ssRNA ligands shorter than 400 nucleotides. Transfection with dephosphorylated ssRNA of 400 nucleotides and larger reduced signalling activity but only to a non-significant extent, compared to the phosphorylated control.

Although these observations strongly indicate that ssRNA harbors additional target structures, ssRNA binding to the CTD of RIG-I was never demonstrated. Additionally, the propensity of single-stranded RNA to form partial double-stranded structures which is enhanced by unconventional wobble base-pairing is well-described[185]. Thus, it appears very likely that *in vitro* transcribed ssRNA tends to form partial double-stranded structures length-dependently which might be recognized by RIG-I even in the absence of a terminal 5'-triphosphate (Fig. 5-3).

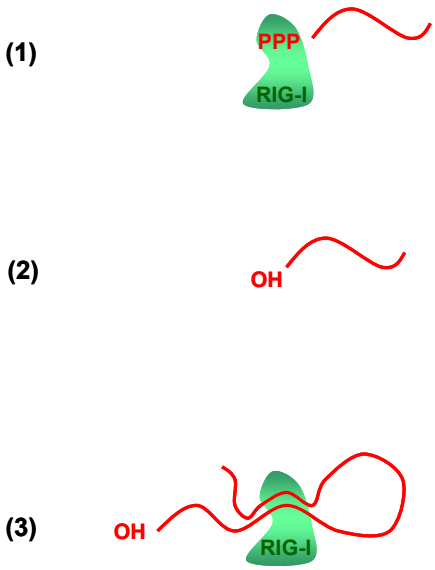

Fig. 5-3 Model for ssRNA recognition by RIG-I
(1) RIG-I binds to the 5'-triphosphate (PPP) of short ssRNA molecules. (2) Upon dephosphorylation, RIG-I does not bind to ssRNA leading to signal abrogation. (3) ssRNA exceeding 400 nucleotides in length tends to form double-stranded structures which serve as binding sites for RIG-I restoring signalling activity.

The biological role of ssRNA recognition has to be regarded critically since in contrast to a 5'-triphosphate or double-stranded conformation, endogenous RNA (e.g. messenger RNA) would also act as a target for RIG-I-mediated recognition. Although not much is known about the influence of naturally occurring modifications on RIG-I recognition, it has been shown that uridine modifications, such as pseudouridine or 2'-*O*-methyl-uridine reduce RIG-I-induced type-I interferon secretion significantly[127]. This suggests that discrimination between self and non-self RNA is not only determined by the presence of double-stranded or 5'-triphosphorylated molecular structures but also by the content of nucleotide RNA modifications similar to the recognition of RNA by TLR7[89].

Additionally, it is known that ssRNA inside a cell is covered by different RNA-binding proteins preventing the formation of duplex structures. Thus, the relevance of ssRNA recognition by RIG-I remains elusive.

Substrate specificity of the cytosolic vRNA sensor RIG-I has attracted much attention in the course of the last few years. Our results show that in contrast to recent reports[127,128], RIG-I RNA recognition is not restricted to RNA substrates bearing a terminal 5'-triphosphate but that also unphosphorylated dsRNA is sensed by RIG-I. Both target structures, double-stranded conformation and 5'-triphosphate, rather complement each other and both contribute to RIG-I-mediated signalling. Further, sensitivity of RIG-I to dsRNA enhances with the length of the ligand reducing the relative contribution of the 5'-end. From a substrate length of 200-400 basepairs on, the double-stranded conformation represents the major RNA motif making the contribution of the 5'-end negligible.

This might also help to understand why RIG-I affects susceptibility of mice to japanese encephalitis virus (JEV)[44], a flavivirus whose genome carries a cap at its 5'-end. Additionally, the identification of double-stranded conformation as an independent target structure for RIG-I is supported by the fact that also ssRNA from a length of 400 nucleotides on is sensed by RIG-I in the absence of a 5'-triphosphate which is very likely caused by intramolecular folding of the ligand RNA. Viral RNA genomes can be several thousands of nucleotides in length are detected by the 5'-triphosphate. However, during replication the generated long double-stranded replication intermediate might be sensed predominantly giving the 5'-end only a minor role for signalling. Both, the 5'-end and the

double-stranded conformation, represent distinct recognition motifs for RIG-I, but might act at different stages of the infection.

5.3.5 Outlook

Regarding siRNA-mediated immunostimulation, it could be shown within this work that TLR7 is the responsible receptor for the observed off-target effects in terms of type-I interferon secretion. Further, it was demonstrated that the 2'-position of the ribose is of crucial importance for immunostimulation. As this position would face the minor groove of an RNA duplex and because further evidence is given that stimulating RNA indeed adopts a duplex structure, the results give hints towards a possible mechanism of receptor ligand interaction. Interestingly, substitution of uridine residues to thymidine resulted in a significant reduction of type-I interferon in human PBMCs without affecting RNAi. Thus, this substitution was identified as a suitable tool for the design of immunological silent siRNAs.
However, there was indication that RNA molecules with uridine residues within stem-loop structures as they occur by intra- and intermolecular folding might be preferentially recognized by TLR7. Further investigation of the positional influence of the thymidine residues would allow for a more precise design of immunologically silenced siRNA molecules. The requirement of RNA duplex formation for receptor ligand interaction could further be investigated by the introduction of modifications that interfere with base-pairing (e.g. 3'-N-methyl-thymidine) and therefore inhibit the formation of duplex structures. Followed by the *in vitro* experiments, it would be highly interesting whether thymidine substitutions show the same effects in *in vivo* experiments giving the possibility to apply siRNA without severe side-effects.

Besides TLR7-mediated recognition of RNA, it could be demonstrated that bacterial RNA recognition differs from so far described recognition principles. On the one hand, bacterial RNA is sensed similar to RNA oligonucleotides by TLR7 in pDCs leading to the induction of type-I interferons. On the other hand, it could be shown that bacterial RNA is sensed by a further cytosolic receptor leading to strong NFκB activation. All so far described RNA sensors could be ruled out, including the recently described viral RNA receptors RIG-I and MDA5. Recognition of bacterial RNA by NALP3 leading to the induction of IL-1β could be confirmed but was shown to be dispensable for secretion of IL-12p40. These results indicate that similar to DNA, further cytosolic receptor systems have to be operative also for bacterial RNA. Pull-down approaches with immobilized bacterial RNA would possibly lead to the identification of the responsible receptor or of involved adaptor molecules. This would allow to describe a new signalling pathway for bacterial RNA recognition. Alternatively, a genome-wide siRNA approach using reliable NFκB reporters could lead to the identification of the receptor including involved signalling molecules. The diverse nucleotide modifications occurring in different frequency and abundance in prokaryotic RNA compared to eukaryotic RNA could be examined regarding their potential to mediate or inhibit immunostimulation. This would allow for a molecular explanation of recognition of bacterial RNA.

Substrate specificity of RIG-I has been in the focus over the last few years. Within this work, it could be demonstrated that the described 5'-triphosphate is not the only target structure for RIG-I but that RNA in double-stranded conformation represents a second independent target structure. The sensitivity to dsRNA of increasing size is significantly enhanced, indicating that the biological role of RIG-I is rather the sensing of long dsRNA than of the terminal 5'-end. Further, the performed reporter

assays implicate that RIG-I might bind in a cooperative manner to double-stranded RNA structures explaining the significant length-dependency. To fully elucidate the ligand requirements of RIG-I, the experiments could be validated by biochemical approaches. Gel filtration experiments with the recombinantly expressed RIG-I protein and different RNA ligands could allow to determine the number of RIG-I proteins binding to a certain dsRNA substrate. Alternatively, RIG-I ligand interaction could be studied using atomic force microscopy as recently performed to study the differential ligand requirements of RIG-I and MDA5, respectively[131]. The relevance of ATPase hydrolysis by RIG-I for signalling activity remains not fully understood although a recent report showed that a terminal 5'-triphosphate is required for translocation of RIG-I on dsRNA[225]. Experiments with RIG-I carrying a mutation in the ATP-binding site (K270A) would elucidate the role of the ATPase activity for signalling activity upon transfection with different RNA ligands.

6 Bibliography

1. Janeway, C.A., Jr. & Medzhitov, R. Innate immune recognition. *Annu Rev Immunol* **20**, 197-216 (2002).

2. Janeway, C.A., Jr. How the immune system recognizes invaders. *Sci Am* **269**, 72-79 (1993).

3. Janeway, C.A., Jr. Approaching the asymptote? Evolution and revolution in immunology. *Cold Spring Harb Symp Quant Biol* **54 Pt 1**, 1-13 (1989).

4. Matzinger, P. The danger model: a renewed sense of self. *Science* **296**, 301-305 (2002).

5. Takeda, K. Evolution and integration of innate immune recognition systems: the Toll-like receptors. *J Endotoxin Res* **11**, 51-55 (2005).

6. Yoneyama, M. *et al.* The RNA helicase RIG-I has an essential function in double-stranded RNA-induced innate antiviral responses. *Nat Immunol* **5**, 730-737 (2004).

7. Martinon, F. & Tschopp, J. NLRs join TLRs as innate sensors of pathogens. *Trends Immunol* **26**, 447-454 (2005).

8. Tschopp, J., Martinon, F. & Burns, K. NALPs: a novel protein family involved in inflammation. *Nat Rev Mol Cell Biol* **4**, 95-104 (2003).

9. Willment, J.A. & Brown, G.D. C-type lectin receptors in antifungal immunity. *Trends Microbiol* **16**, 27-32 (2008).

10. Hashimoto, C., Hudson, K.L. & Anderson, K.V. The Toll gene of Drosophila, required for dorsal-ventral embryonic polarity, appears to encode a transmembrane protein. *Cell* **52**, 269-279 (1988).

11. Lemaitre, B., Nicolas, E., Michaut, L., Reichhart, J.M. & Hoffmann, J.A. The dorsoventral regulatory gene cassette spatzle/Toll/cactus controls the potent antifungal response in Drosophila adults. *Cell* **86**, 973-983 (1996).

12. Rutschmann, S., Kilinc, A. & Ferrandon, D. Cutting edge: the toll pathway is required for resistance to gram-positive bacterial infections in Drosophila. *J Immunol* **168**, 1542-1546 (2002).

13. de Bouteiller, O. *et al.* Recognition of double-stranded RNA by human toll-like receptor 3 and downstream receptor signaling requires multimerization and an acidic pH. *J Biol Chem* **280**, 38133-38145 (2005).

14. Lee, J. *et al.* Molecular basis for the immunostimulatory activity of guanine nucleoside analogs: activation of Toll-like receptor 7. *Proc Natl Acad Sci U S A* **100**, 6646-6651 (2003).

15. Latz, E. *et al.* TLR9 signals after translocating from the ER to CpG DNA in the lysosome. *Nat Immunol* **5**, 190-198 (2004).

16. Nishiya, T., Kajita, E., Miwa, S. & Defranco, A.L. TLR3 and TLR7 are targeted to the same intracellular compartments by distinct regulatory elements. *J Biol Chem* **280**, 37107-37117 (2005).

17. Medzhitov, R. & Janeway, C., Jr. The Toll receptor family and microbial recognition. *Trends Microbiol* **8**, 452-456 (2000).

18. Akira, S. & Takeda, K. Toll-like receptor signalling. *Nat Rev Immunol* **4**, 499-511 (2004).

19. Medzhitov, R. *et al.* MyD88 is an adaptor protein in the hToll/IL-1 receptor family signaling pathways. *Mol Cell* **2**, 253-258 (1998).

20. O'Neill, L.A. & Bowie, A.G. The family of five: TIR-domain-containing adaptors in Toll-like receptor signalling. *Nat Rev Immunol* **7**, 353-364 (2007).

21. Kawai, T. & Akira, S. TLR signaling. *Cell Death Differ* **13**, 816-825 (2006).

22. Li, S., Strelow, A., Fontana, E.J. & Wesche, H. IRAK-4: a novel member of the IRAK family with the properties of an IRAK-kinase. *Proc Natl Acad Sci U S A* **99**, 5567-5572 (2002).

23. Deng, L. *et al.* Activation of the IkappaB kinase complex by TRAF6 requires a dimeric ubiquitin-conjugating enzyme complex and a unique polyubiquitin chain. *Cell* **103**, 351-361 (2000).

24. Colonna, M., Trinchieri, G. & Liu, Y.J. Plasmacytoid dendritic cells in immunity. *Nat Immunol* **5**, 1219-1226 (2004).

25. Krug, A. *et al.* Identification of CpG oligonucleotide sequences with high induction of IFN-alpha/beta in plasmacytoid dendritic cells. *Eur J Immunol* **31**, 2154-2163 (2001).

26. Rothenfusser, S., Tuma, E., Endres, S. & Hartmann, G. Plasmacytoid dendritic cells: the key to CpG. *Hum Immunol* **63**, 1111-1119 (2002).

27. Moynagh, P.N. TLR signalling and activation of IRFs: revisiting old friends from the NF-kappaB pathway. *Trends Immunol* **26**, 469-476 (2005).

28. Honda, K. *et al.* Spatiotemporal regulation of MyD88-IRF-7 signalling for robust type-I interferon induction. *Nature* **434**, 1035-1040 (2005).

29. Yoneyama, M. *et al.* Shared and unique functions of the DExD/H-box helicases RIG-I, MDA5, and LGP2 in antiviral innate immunity. *J Immunol* **175**, 2851-2858 (2005).

30. Takeuchi, O. & Akira, S. MDA5/RIG-I and virus recognition. *Curr Opin Immunol* **20**, 17-22 (2008).

31. Yoneyama, M. & Fujita, T. [Non-self RNA-sensing mechanism of RIG-I RNA helicase]. *Seikagaku* **80**, 838-843 (2008).

32. Loo, Y.M. *et al.* Distinct RIG-I and MDA5 signaling by RNA viruses in innate immunity. *J Virol* **82**, 335-345 (2008).

33. Bowie, A.G. & Fitzgerald, K.A. RIG-I: tri-ing to discriminate between self and non-self RNA. *Trends Immunol* **28**, 147-150 (2007).

34. Rothenfusser, S. *et al.* The RNA helicase Lgp2 inhibits TLR-independent sensing of viral replication by retinoic acid-inducible gene-I. *J Immunol* **175**, 5260-5268 (2005).

35. Komuro, A. & Horvath, C.M. RNA- and virus-independent inhibition of antiviral signaling by RNA helicase LGP2. *J Virol* **80**, 12332-12342 (2006).

36. Murali, A. *et al.* Structure and function of LGP2, a DEX(D/H) helicase that regulates the innate immunity response. *J Biol Chem* **283**, 15825-15833 (2008).

37. Saito, T. *et al.* Regulation of innate antiviral defenses through a shared repressor domain in RIG-I and LGP2. *Proc Natl Acad Sci U S A* **104**, 582-587 (2007).

38. Venkataraman, T. *et al.* Loss of DExD/H box RNA helicase LGP2 manifests disparate antiviral responses. *J Immunol* **178**, 6444-6455 (2007).

39. Cordin, O., Banroques, J., Tanner, N.K. & Linder, P. The DEAD-box protein family of RNA helicases. *Gene* **367**, 17-37 (2006).

40. Kawai, T. *et al.* IPS-1, an adaptor triggering RIG-I- and Mda5-mediated type I interferon induction. *Nat Immunol* **6**, 981-988 (2005).

41. Seth, R.B., Sun, L., Ea, C.K. & Chen, Z.J. Identification and characterization of MAVS, a mitochondrial antiviral signaling protein that activates NF-kappaB and IRF 3. *Cell* **122**, 669-682 (2005).

42. Xu, L.G. *et al.* VISA is an adapter protein required for virus-triggered IFN-beta signaling. *Mol Cell* **19**, 727-740 (2005).

43. Meylan, E. *et al.* Cardif is an adaptor protein in the RIG-I antiviral pathway and is targeted by hepatitis C virus. *Nature* **437**, 1167-1172 (2005).

44. Kato, H. *et al.* Differential roles of MDA5 and RIG-I helicases in the recognition of RNA viruses. *Nature* **441**, 101-105 (2006).

45. Ting, J.P. & Davis, B.K. CATERPILLER: a novel gene family important in immunity, cell death, and diseases. *Annu Rev Immunol* **23**, 387-414 (2005).

46. Inohara, Chamaillard, McDonald, C. & Nunez, G. NOD-LRR proteins: role in host-microbial interactions and inflammatory disease. *Annu Rev Biochem* **74**, 355-383 (2005).

47. Aravind, L., Dixit, V.M. & Koonin, E.V. Apoptotic molecular machinery: vastly increased complexity in vertebrates revealed by genome comparisons. *Science* **291**, 1279-1284 (2001).

48. Maeda, S. *et al.* Nod2 mutation in Crohn's disease potentiates NF-kappaB activity and IL-1beta processing. *Science* **307**, 734-738 (2005).

49. Seth, R.B., Sun, L. & Chen, Z.J. Antiviral innate immunity pathways. *Cell Res* **16**, 141-147 (2006).

50. Netea, M.G. *et al.* The frameshift mutation in Nod2 results in unresponsiveness not only to Nod2- but also Nod1-activating peptidoglycan agonists. *J Biol Chem* **280**, 35859-35867 (2005).

51. van Heel, D.A. *et al.* Muramyl dipeptide and toll-like receptor sensitivity in NOD2-associated Crohn's disease. *Lancet* **365**, 1794-1796 (2005).

52. Martinon, F., Burns, K. & Tschopp, J. The inflammasome: a molecular platform triggering activation of inflammatory caspases and processing of proIL-beta. *Mol Cell* **10**, 417-426 (2002).

53. Martinon, F. & Tschopp, J. Inflammatory caspases: linking an intracellular innate immune system to autoinflammatory diseases. *Cell* **117**, 561-574 (2004).

54. Mariathasan, S. *et al.* Differential activation of the inflammasome by caspase-1 adaptors ASC and Ipaf. *Nature* **430**, 213-218 (2004).

55. Agostini, L. *et al.* NALP3 forms an IL-1beta-processing inflammasome with increased activity in Muckle-Wells autoinflammatory disorder. *Immunity* **20**, 319-325 (2004).

56. Thornberry, N.A. *et al.* A novel heterodimeric cysteine protease is required for interleukin-1 beta processing in monocytes. *Nature* **356**, 768-774 (1992).

57. Cerretti, D.P. *et al.* Molecular cloning of the interleukin-1 beta converting enzyme. *Science* **256**, 97-100 (1992).

58. Hoffman, H.M., Mueller, J.L., Broide, D.H., Wanderer, A.A. & Kolodner, R.D. Mutation of a new gene encoding a putative pyrin-like protein causes familial cold autoinflammatory syndrome and Muckle-Wells syndrome. *Nat Genet* **29**, 301-305 (2001).

59. Aganna, E. *et al.* Association of mutations in the NALP3/CIAS1/PYPAF1 gene with a broad phenotype including recurrent fever, cold sensitivity, sensorineural deafness, and AA amyloidosis. *Arthritis Rheum* **46**, 2445-2452 (2002).

60. Feldmann, J. *et al.* Chronic infantile neurological cutaneous and articular syndrome is caused by mutations in CIAS1, a gene highly expressed in polymorphonuclear cells and chondrocytes. *Am J Hum Genet* **71**, 198-203 (2002).

61. Dode, C. *et al.* New mutations of CIAS1 that are responsible for Muckle-Wells syndrome and familial cold urticaria: a novel mutation underlies both syndromes. *Am J Hum Genet* **70**, 1498-1506 (2002).

62. Willingham, S.B. *et al.* Microbial pathogen-induced necrotic cell death mediated by the inflammasome components CIAS1/cryopyrin/NLRP3 and ASC. *Cell Host Microbe* **2**, 147-159 (2007).

63. Creagh, E.M. & O'Neill, L.A. TLRs, NLRs and RLRs: a trinity of pathogen sensors that co-operate in innate immunity. *Trends Immunol* **27**, 352-357 (2006).

64. Kanneganti, T.D. *et al.* Bacterial RNA and small antiviral compounds activate caspase-1 through cryopyrin/Nalp3. *Nature* **440**, 233-236 (2006).

65. Mariathasan, S. *et al.* Cryopyrin activates the inflammasome in response to toxins and ATP. *Nature* **440**, 228-232 (2006).

66. Martinon, F., Petrilli, V., Mayor, A., Tardivel, A. & Tschopp, J. Gout-associated uric acid crystals activate the NALP3 inflammasome. *Nature* **440**, 237-241 (2006).

67. Kahlenberg, J.M., Lundberg, K.C., Kertesy, S.B., Qu, Y. & Dubyak, G.R. Potentiation of caspase-1 activation by the P2X7 receptor is dependent on TLR signals and requires NF-kappaB-driven protein synthesis. *J Immunol* **175**, 7611-7622 (2005).

68. Hasegawa, M. *et al.* ASC-mediated NF-kappaB activation leading to interleukin-8 production requires caspase-8 and is inhibited by CLARP. *J Biol Chem* **280**, 15122-15130 (2005).

69. Muruve, D.A. *et al.* The inflammasome recognizes cytosolic microbial and host DNA and triggers an innate immune response. *Nature* **452**, 103-107 (2008).

70. Uehara, A. *et al.* Muramyldipeptide and diaminopimelic acid-containing desmuramylpeptides in combination with chemically synthesized Toll-like receptor agonists synergistically induced production of interleukin-8 in a NOD2- and NOD1-dependent manner, respectively, in human monocytic cells in culture. *Cell Microbiol* **7**, 53-61 (2005).

71. Kato, H. *et al.* Cell type-specific involvement of RIG-I in antiviral response. *Immunity* **23**, 19-28 (2005).

72. Takeda, K., Kaisho, T. & Akira, S. Toll-like receptors. *Annu Rev Immunol* **21**, 335-376 (2003).

73. Echchannaoui, H. *et al.* Toll-like receptor 2-deficient mice are highly susceptible to Streptococcus pneumoniae meningitis because of reduced bacterial clearing and enhanced inflammation. *J Infect Dis* **186**, 798-806 (2002).

74. Poltorak, A. *et al.* Defective LPS signaling in C3H/HeJ and C57BL/10ScCr mice: mutations in Tlr4 gene. *Science* **282**, 2085-2088 (1998).

75. Hoshino, K. *et al.* Cutting edge: Toll-like receptor 4 (TLR4)-deficient mice are hyporesponsive to lipopolysaccharide: evidence for TLR4 as the Lps gene product. *J Immunol* **162**, 3749-3752 (1999).

76. Hornung, V. *et al.* Silica crystals and aluminum salts activate the NALP3 inflammasome through phagosomal destabilization. *Nat Immunol* **9**, 847-856 (2008).

77. Halle, A. *et al.* The NALP3 inflammasome is involved in the innate immune response to amyloid-beta. *Nat Immunol* **9**, 857-865 (2008).

78. Hemmi, H. *et al.* A Toll-like receptor recognizes bacterial DNA. *Nature* **408**, 740-745 (2000).

79. Dalpke, A., Frank, J., Peter, M. & Heeg, K. Activation of toll-like receptor 9 by DNA from different bacterial species. *Infect Immun* **74**, 940-946 (2006).

80. Takaoka, A. *et al.* DAI (DLM-1/ZBP1) is a cytosolic DNA sensor and an activator of innate immune response. *Nature* **448**, 501-505 (2007).

81. Heil, F. *et al.* Species-specific recognition of single-stranded RNA via toll-like receptor 7 and 8. *Science* **303**, 1526-1529 (2004).

82. Gorden, K.K., Qiu, X.X., Binsfeld, C.C., Vasilakos, J.P. & Alkan, S.S. Cutting Edge: Activation of Murine TLR8 by a Combination of Imidazoquinoline Immune Response Modifiers and PolyT Oligodeoxynucleotides. *J Immunol* **177**, 6584-6587 (2006).

83. Hornung, V. *et al.* Sequence-specific potent induction of IFN-alpha by short interfering RNA in plasmacytoid dendritic cells through TLR7. *Nat Med* **11**, 263-270 (2005).

84. Sioud, M. Induction of inflammatory cytokines and interferon responses by double-stranded and single-stranded siRNAs is sequence-dependent and requires endosomal localization. *J Mol Biol* **348**, 1079-1090 (2005).

85. Judge, A.D. *et al.* Sequence-dependent stimulation of the mammalian innate immune response by synthetic siRNA. *Nat Biotechnol* **23**, 457-462 (2005).

86. Diebold, S.S. *et al.* Nucleic acid agonists for Toll-like receptor 7 are defined by the presence of uridine ribonucleotides. *Eur J Immunol* **36**, 3256-3267 (2006).

87. Heil, F. *et al.* The Toll-like receptor 7 (TLR7)-specific stimulus loxoribine uncovers a strong relationship within the TLR7, 8 and 9 subfamily. *Eur J Immunol* **33**, 2987-2997 (2003).

88. Gorden, K.K. *et al.* Oligodeoxynucleotides differentially modulate activation of TLR7 and TLR8 by imidazoquinolines. *J Immunol* **177**, 8164-8170 (2006).

89. Kariko, K., Buckstein, M., Ni, H. & Weissman, D. Suppression of RNA recognition by Toll-like receptors: the impact of nucleoside modification and the evolutionary origin of RNA. *Immunity* **23**, 165-175 (2005).

90. Kariko, K. & Weissman, D. Naturally occurring nucleoside modifications suppress the immunostimulatory activity of RNA: implication for therapeutic RNA development. *Curr Opin Drug Discov Devel* **10**, 523-532 (2007).

91. Robbins, M. *et al.* 2'-O-methyl-modified RNAs act as TLR7 antagonists. *Mol Ther* **15**, 1663-1669 (2007).

92. Sioud, M., Furset, G. & Cekaite, L. Suppression of immunostimulatory siRNA-driven innate immune activation by 2'-modified RNAs. *Biochem Biophys Res Commun* **361**, 122-126 (2007).

93. Cekaite, L., Furset, G., Hovig, E. & Sioud, M. Gene expression analysis in blood cells in response to unmodified and 2'-modified siRNAs reveals TLR-dependent and independent effects. *J Mol Biol* **365**, 90-108 (2007).

94. Diebold, S.S. *et al.* Viral infection switches non-plasmacytoid dendritic cells into high interferon producers. *Nature* **424**, 324-328 (2003).

95. Persengiev, S.P., Zhu, X. & Green, M.R. Nonspecific, concentration-dependent stimulation and repression of mammalian gene expression by small interfering RNAs (siRNAs). *Rna* **10**, 12-18 (2004).

96. Heidel, J.D., Hu, S., Liu, X.F., Triche, T.J. & Davis, M.E. Lack of interferon response in animals to naked siRNAs. *Nat Biotechnol* **22**, 1579-1582 (2004).

97. Bridge, A.J., Pebernard, S., Ducraux, A., Nicoulaz, A.L. & Iggo, R. Induction of an interferon response by RNAi vectors in mammalian cells. *Nat Genet* **34**, 263-264 (2003).

98. Sledz, C.A., Holko, M., de Veer, M.J., Silverman, R.H. & Williams, B.R. Activation of the interferon system by short-interfering RNAs. *Nat Cell Biol* **5**, 834-839 (2003).

99. Marques, J.T. & Williams, B.R. Activation of the mammalian immune system by siRNAs. *Nat Biotechnol* **23**, 1399-1405 (2005).

100. Sioud, M. Single-stranded small interfering RNA are more immunostimulatory than their double-stranded counterparts: A central role for 2'-hydroxyl uridines in immune responses. *Eur J Immunol* **36**, 1222-1230 (2006).

101. Jarve, A. *et al.* Surveillance of siRNA integrity by FRET imaging. *Nucleic Acids Res* **35**, e124 (2007).

102. Liu, Y.J. IPC: professional type 1 interferon-producing cells and plasmacytoid dendritic cell precursors. *Annu Rev Immunol* **23**, 275-306 (2005).

103. Ewald, S.E. *et al.* The ectodomain of Toll-like receptor 9 is cleaved to generate a functional receptor. *Nature* **456**, 658-662 (2008).

104. Park, B. *et al.* Proteolytic cleavage in an endolysosomal compartment is required for activation of Toll-like receptor 9. *Nat Immunol* **9**, 1407-1414 (2008).

105. Matsushima, N. *et al.* Comparative sequence analysis of leucine-rich repeats (LRRs) within vertebrate toll-like receptors. *BMC Genomics* **8**, 124 (2007).

106. Lopez, C.B. *et al.* TLR-independent induction of dendritic cell maturation and adaptive immunity by negative-strand RNA viruses. *J Immunol* **173**, 6882-6889 (2004).

107. Kalali, B.N. *et al.* Double-stranded RNA induces an antiviral defense status in epidermal keratinocytes through TLR3-, PKR-, and MDA5/RIG-I-mediated differential signaling. *J Immunol* **181**, 2694-2704 (2008).

108. Jiang, Z. *et al.* Poly(I-C)-induced Toll-like receptor 3 (TLR3)-mediated activation of NFkappa B and MAP kinase is through an interleukin-1 receptor-associated kinase (IRAK)-independent pathway employing the signaling components TLR3-TRAF6-TAK1-TAB2-PKR. *J Biol Chem* **278**, 16713-16719 (2003).

109. Alexopoulou, L., Holt, A.C., Medzhitov, R. & Flavell, R.A. Recognition of double-stranded RNA and activation of NF-kappaB by Toll-like receptor 3. *Nature* **413**, 732-738 (2001).

110. Schroder, M. & Bowie, A.G. TLR3 in antiviral immunity: key player or bystander? *Trends Immunol* **26**, 462-468 (2005).

111. Edelmann, K.H. *et al.* Does Toll-like receptor 3 play a biological role in virus infections? *Virology* **322**, 231-238 (2004).

112. Melchjorsen, J. *et al.* Activation of innate defense against a paramyxovirus is mediated by RIG-I and TLR7 and TLR8 in a cell-type-specific manner. *J Virol* **79**, 12944-12951 (2005).

113. Daffis, S., Samuel, M.A., Suthar, M.S., Gale, M., Jr. & Diamond, M.S. Toll-like receptor 3 has a protective role against West Nile virus infection. *J Virol* **82**, 10349-10358 (2008).

114. Kariko, K., Ni, H., Capodici, J., Lamphier, M. & Weissman, D. mRNA is an endogenous ligand for Toll-like receptor 3. *J Biol Chem* **279**, 12542-12550 (2004).

115. Kleinman, M.E. *et al.* Sequence- and target-independent angiogenesis suppression by siRNA via TLR3. *Nature* **452**, 591-597 (2008).

116. Liu, L. *et al.* Structural basis of toll-like receptor 3 signaling with double-stranded RNA. *Science* **320**, 379-381 (2008).

117. Lee, H.K., Dunzendorfer, S., Soldau, K. & Tobias, P.S. Double-stranded RNA-mediated TLR3 activation is enhanced by CD14. *Immunity* **24**, 153-163 (2006).

118. Sun, J. *et al.* Structural and Functional Analyses of the Human Toll-like Receptor 3: ROLE OF GLYCOSYLATION. *J Biol Chem* **281**, 11144-11151 (2006).

119. Bell, J.K. *et al.* The molecular structure of the Toll-like receptor 3 ligand-binding domain. *Proc Natl Acad Sci U S A* **102**, 10976-10980 (2005).

120. Choe, J., Kelker, M.S. & Wilson, I.A. Crystal structure of human toll-like receptor 3 (TLR3) ectodomain. *Science* **309**, 581-585 (2005).

121. Takahashi, N., Takahashi, Y. & Putnam, F.W. Periodicity of leucine and tandem repetition of a 24-amino acid segment in the primary structure of leucine-rich alpha 2-glycoprotein of human serum. *Proc Natl Acad Sci U S A* **82**, 1906-1910 (1985).

122. Bell, J.K. *et al.* Leucine-rich repeats and pathogen recognition in Toll-like receptors. *Trends Immunol* **24**, 528-533 (2003).

123. Bell, J.K., Askins, J., Hall, P.R., Davies, D.R. & Segal, D.M. The dsRNA binding site of human Toll-like receptor 3. *Proc Natl Acad Sci U S A* **103**, 8792-8797 (2006).

124. Akira, S., Uematsu, S. & Takeuchi, O. Pathogen recognition and innate immunity. *Cell* **124**, 783-801 (2006).

125. Samuel, C.E. Antiviral actions of interferons. *Clin Microbiol Rev* **14**, 778-809, table of contents (2001).

126. Gitlin, L. *et al.* Essential role of mda-5 in type I IFN responses to polyriboinosinic:polyribocytidylic acid and encephalomyocarditis picornavirus. *Proc Natl Acad Sci U S A* **103**, 8459-8464 (2006).

127. Hornung, V. *et al.* 5'-Triphosphate RNA is the ligand for RIG-I. *Science* **314**, 994-997 (2006).

128. Pichlmair, A. *et al.* RIG-I-mediated antiviral responses to single-stranded RNA bearing 5'-phosphates. *Science* **314**, 997-1001 (2006).

129. Takahasi, K. *et al.* Nonself RNA-sensing mechanism of RIG-I helicase and activation of antiviral immune responses. *Mol Cell* **29**, 428-440 (2008).

130. Cui, S. *et al.* The C-Terminal Regulatory Domain Is the RNA 5'-Triphosphate Sensor of RIG-I. *Mol Cell* **29**, 169-179 (2008).

131. Kato, H. *et al.* Length-dependent recognition of double-stranded ribonucleic acids by retinoic acid-inducible gene-I and melanoma differentiation-associated gene 5. *J Exp Med* **205**, 1601-1610 (2008).

132. Saito, T., Owen, D.M., Jiang, F., Marcotrigiano, J. & Gale, M., Jr. Innate immunity induced by composition-dependent RIG-I recognition of hepatitis C virus RNA. *Nature* **454**, 523-527 (2008).

133. Gee, P. *et al.* Essential role of the N-terminal domain in the regulation of RIG-I ATPase activity. *J Biol Chem* **283**, 9488-9496 (2008).

134. Yoneyama, M. & Fujita, T. Structural Mechanism of RNA Recognition by the RIG-I-like Receptors. *Immunity* **29**, 178-181 (2008).

135. Kanneganti, T.D. *et al.* Bacterial RNA and small antiviral compounds activate caspase-1 through cryopyrin/Nalp3. *Nature* (2006).

136. Henry, T., Brotcke, A., Weiss, D.S., Thompson, L.J. & Monack, D.M. Type I interferon signaling is required for activation of the inflammasome during Francisella infection. *J Exp Med* **204**, 987-994 (2007).

137. Stockinger, S. *et al.* IFN regulatory factor 3-dependent induction of type I IFNs by intracellular bacteria is mediated by a TLR- and Nod2-independent mechanism. *J Immunol* **173**, 7416-7425 (2004).

138. Zamore, P.D. RNA interference: listening to the sound of silence. *Nat Struct Biol* **8**, 746-750 (2001).

139. Tuschl, T. RNA interference and small interfering RNAs. *Chembiochem* **2**, 239-245 (2001).

140. McManus, M.T. & Sharp, P.A. Gene silencing in mammals by small interfering RNAs. *Nat Rev Genet* **3**, 737-747 (2002).

141. Jorgensen, R. Altered gene expression in plants due to trans interactions between homologous genes. *Trends Biotechnol* **8**, 340-344 (1990).

142. Fire, A. *et al.* Potent and specific genetic interference by double-stranded RNA in Caenorhabditis elegans. *Nature* **391**, 806-811 (1998).

143. Svoboda, P., Stein, P., Hayashi, H. & Schultz, R.M. Selective reduction of dormant maternal mRNAs in mouse oocytes by RNA interference. *Development* **127**, 4147-4156 (2000).

144. Wianny, F. & Zernicka-Goetz, M. Specific interference with gene function by double-stranded RNA in early mouse development. *Nat Cell Biol* **2**, 70-75 (2000).

145. Lee, R.C. & Ambros, V. An extensive class of small RNAs in Caenorhabditis elegans. *Science* **294**, 862-864 (2001).

146. Lee, Y., Jeon, K., Lee, J.T., Kim, S. & Kim, V.N. MicroRNA maturation: stepwise processing and subcellular localization. *Embo J* **21**, 4663-4670 (2002).

147. Lee, Y. *et al.* The nuclear RNase III Drosha initiates microRNA processing. *Nature* **425**, 415-419 (2003).

148. Elbashir, S.M., Lendeckel, W. & Tuschl, T. RNA interference is mediated by 21- and 22-nucleotide RNAs. *Genes Dev* **15**, 188-200 (2001).

149. Elbashir, S.M., Martinez, J., Patkaniowska, A., Lendeckel, W. & Tuschl, T. Functional anatomy of siRNAs for mediating efficient RNAi in Drosophila melanogaster embryo lysate. *Embo J* **20**, 6877-6888 (2001).

150. Bernstein, E., Caudy, A.A., Hammond, S.M. & Hannon, G.J. Role for a bidentate ribonuclease in the initiation step of RNA interference. *Nature* **409**, 363-366 (2001).

151. Caudy, A.A., Myers, M., Hannon, G.J. & Hammond, S.M. Fragile X-related protein and VIG associate with the RNA interference machinery. *Genes Dev* **16**, 2491-2496 (2002).

152. Hammond, S.M., Boettcher, S., Caudy, A.A., Kobayashi, R. & Hannon, G.J. Argonaute2, a link between genetic and biochemical analyses of RNAi. *Science* **293**, 1146-1150 (2001).

153. Caudy, A.A. *et al.* A micrococcal nuclease homolog in RNAi effector complexes. *Nature* **425**, 411-414 (2003).

154. Hutvagner, G. & Zamore, P.D. A microRNA in a multiple-turnover RNAi enzyme complex. *Science* **297**, 2056-2060 (2002).

155. Zamore, P.D. Ancient pathways programmed by small RNAs. *Science* **296**, 1265-1269 (2002).

156. Zhao, Z., Cao, Y., Li, M. & Meng, A. Double-stranded RNA injection produces nonspecific defects in zebrafish. *Dev Biol* **229**, 215-223 (2001).

157. Caplen, N.J., Fleenor, J., Fire, A. & Morgan, R.A. dsRNA-mediated gene silencing in cultured Drosophila cells: a tissue culture model for the analysis of RNA interference. *Gene* **252**, 95-105 (2000).

158. Baglioni, C. *et al.* Interferon-induced enzymes: activation and role in te antiviral state. *Ann N Y Acad Sci* **350**, 497-509 (1980).

159. Minks, M.A., West, D.K., Benvin, S. & Baglioni, C. Structural requirements of double-stranded RNA for the activation of 2',5'-oligo(A) polymerase and protein kinase of interferon-treated HeLa cells. *J Biol Chem* **254**, 10180-10183 (1979).

160. Kumar, A., Haque, J., Lacoste, J., Hiscott, J. & Williams, B.R. Double-stranded RNA-dependent protein kinase activates transcription factor NF-kappa B by phosphorylating I kappa B. *Proc Natl Acad Sci U S A* **91**, 6288-6292 (1994).

161. Elbashir, S.M. *et al.* Duplexes of 21-nucleotide RNAs mediate RNA interference in cultured mammalian cells. *Nature* **411**, 494-498 (2001).

162. Miyagishi, M., Hayashi, M. & Taira, K. Comparison of the suppressive effects of antisense oligonucleotides and siRNAs directed against the same targets in mammalian cells. *Antisense Nucleic Acid Drug Dev* **13**, 1-7 (2003).

163. Grunweller, A. *et al.* Comparison of different antisense strategies in mammalian cells using locked nucleic acids, 2'-O-methyl RNA, phosphorothioates and small interfering RNA. *Nucleic Acids Res* **31**, 3185-3193 (2003).

164. Bertrand, J.R. *et al.* Comparison of antisense oligonucleotides and siRNAs in cell culture and in vivo. *Biochem Biophys Res Commun* **296**, 1000-1004 (2002).

165. Soutschek, J. *et al.* Therapeutic silencing of an endogenous gene by systemic administration of modified siRNAs. *Nature* **432**, 173-178 (2004).

166. Corey, D.R. RNA learns from antisense. *Nat Chem Biol* **3**, 8-11 (2007).

167. Eberle, F. *et al.* Modifications in Small Interfering RNA That Separate Immunostimulation from RNA Interference. *J Immunol* **180**, 3229-3237 (2008).

168. Cullen, B.R. Enhancing and confirming the specificity of RNAi experiments. *Nat Methods* **3**, 677-681 (2006).

169. Pei, Y. & Tuschl, T. On the art of identifying effective and specific siRNAs. *Nat Methods* **3**, 670-676 (2006).

170. Wiznerowicz, M., Szulc, J. & Trono, D. Tuning silence: conditional systems for RNA interference. *Nat Methods* **3**, 682-688 (2006).

171. Graham, F.L., Smiley, J., Russell, W.C. & Nairn, R. Characteristics of a human cell line transformed by DNA from human adenovirus type 5. *J Gen Virol* **36**, 59-74 (1977).

172. Blight, K.J., McKeating, J.A. & Rice, C.M. Highly permissive cell lines for subgenomic and genomic hepatitis C virus RNA replication. *J Virol* **76**, 13001-13014 (2002).

173. Binder, M., Kochs, G., Bartenschlager, R. & Lohmann, V. Hepatitis C virus escape from the interferon regulatory factor 3 pathway by a passive and active evasion strategy. *Hepatology* **46**, 1365-1374 (2007).

174. Brasel, K., De Smedt, T., Smith, J.L. & Maliszewski, C.R. Generation of murine dendritic cells from flt3-ligand-supplemented bone marrow cultures. *Blood* **96**, 3029-3039 (2000).

175. Brawand, P. *et al.* Murine plasmacytoid pre-dendritic cells generated from Flt3 ligand-supplemented bone marrow cultures are immature APCs. *J Immunol* **169**, 6711-6719 (2002).

176. Gilliet, M. *et al.* The development of murine plasmacytoid dendritic cell precursors is differentially regulated by FLT3-ligand and granulocyte/macrophage colony-stimulating factor. *J Exp Med* **195**, 953-958 (2002).

177. Inaba, K. *et al.* Identification of proliferating dendritic cell precursors in mouse blood. *J Exp Med* **175**, 1157-1167 (1992).

178. Richards, O.W. & Jahn, T.L. A Photoelectric Nephelometer for Estimating the Population Density of Microorganisms. *J Bacteriol* **26**, 385-391 (1933).

179. Zuker, M. Mfold web server for nucleic acid folding and hybridization prediction. *Nucleic Acids Res* **31**, 3406-3415 (2003).

180. Agrawal, S. & Kandimalla, E.R. Role of Toll-like receptors in antisense and siRNA [corrected]. *Nat Biotechnol* **22**, 1533-1537 (2004).

181. Dalpke, A.H., Zimmermann, S., Albrecht, I. & Heeg, K. Phosphodiester CpG oligonucleotides as adjuvants: polyguanosine runs enhance cellular uptake and improve immunostimulative activity of phosphodiester CpG oligonucleotides in vitro and in vivo. *Immunology* **106**, 102-112 (2002).

182. Chiu, Y.L. & Rana, T.M. siRNA function in RNAi: a chemical modification analysis. *Rna* **9**, 1034-1048 (2003).

183. Schlee, M., Hornung, V. & Hartmann, G. siRNA and isRNA: two edges of one sword. *Mol Ther* **14**, 463-470 (2006).

184. Robbins, M. *et al.* 2'-O-methyl-modified RNAs Act as TLR7 Antagonists. *Mol Ther* (2007).

185. Crick, F.H. Codon--anticodon pairing: the wobble hypothesis. *J Mol Biol* **19**, 548-555 (1966).

186. Sioud, M. Innate sensing of self and non-self RNAs by Toll-like receptors. *Trends Mol Med* **12**, 167-176 (2006).

187. Schoenberg, D.R. The end defines the means in bacterial mRNA decay. *Nat Chem Biol* **3**, 535-536 (2007).

188. Gutell, R.R. Collection of small subunit (16S- and 16S-like) ribosomal RNA structures: 1994. *Nucleic Acids Res* **22**, 3502-3507 (1994).

189. Evguenieva-Hackenberg, E. Bacterial ribosomal RNA in pieces. *Mol Microbiol* **57**, 318-325 (2005).

190. Marques, J.T. *et al.* A structural basis for discriminating between self and nonself double-stranded RNAs in mammalian cells. *Nat Biotechnol* **24**, 559-565 (2006).

191. Krug, A. *et al.* Toll-like receptor expression reveals CpG DNA as a unique microbial stimulus for plasmacytoid dendritic cells which synergizes with CD40 ligand to induce high amounts of IL-12. *Eur J Immunol* **31**, 3026-3037 (2001).

192. Diebold, S.S., Kaisho, T., Hemmi, H., Akira, S. & Reis e Sousa, C. Innate antiviral responses by means of TLR7-mediated recognition of single-stranded RNA. *Science* **303**, 1529-1531 (2004).

193. Wagner, H. The immunobiology of the TLR9 subfamily. *Trends Immunol* **25**, 381-386 (2004).

194. Hemmi, H. *et al.* Small anti-viral compounds activate immune cells via the TLR7 MyD88-dependent signaling pathway. *Nat Immunol* **3**, 196-200 (2002).

195. Jurk, M. *et al.* Human TLR7 or TLR8 independently confer responsiveness to the antiviral compound R-848. *Nat Immunol* **3**, 499 (2002).

196. Decatur, W.A. & Fournier, M.J. rRNA modifications and ribosome function. *Trends Biochem Sci* **27**, 344-351 (2002).

197. Girardin, S.E. *et al.* Nod1 detects a unique muropeptide from gram-negative bacterial peptidoglycan. *Science* **300**, 1584-1587 (2003).

198. Tanabe, T. *et al.* Regulatory regions and critical residues of NOD2 involved in muramyl dipeptide recognition. *Embo J* **23**, 1587-1597 (2004).

199. Sumpter, R., Jr. *et al.* Regulating intracellular antiviral defense and permissiveness to hepatitis C virus RNA replication through a cellular RNA helicase, RIG-I. *J Virol* **79**, 2689-2699 (2005).

200. Brown, E.A., Zhang, H., Ping, L.H. & Lemon, S.M. Secondary structure of the 5' nontranslated regions of hepatitis C virus and pestivirus genomic RNAs. *Nucleic Acids Res* **20**, 5041-5045 (1992).

201. Blight, K.J. & Rice, C.M. Secondary structure determination of the conserved 98-base sequence at the 3' terminus of hepatitis C virus genome RNA. *J Virol* **71**, 7345-7352 (1997).

202. Tanaka, T., Kato, N., Cho, M.J., Sugiyama, K. & Shimotohno, K. Structure of the 3' terminus of the hepatitis C virus genome. *J Virol* **70**, 3307-3312 (1996).

203. Couzin, J. Breakthrough of the year. Small RNAs make big splash. *Science* **298**, 2296-2297 (2002).

204. Kariko, K., Bhuyan, P., Capodici, J. & Weissman, D. Small interfering RNAs mediate sequence-independent gene suppression and induce immune activation by signaling through toll-like receptor 3. *J Immunol* **172**, 6545-6549 (2004).

205. Furset, G. & Sioud, M. Design of bifunctional siRNAs: Combining immunostimulation and gene-silencing in one single siRNA molecule. *Biochem Biophys Res Commun* **352**, 642-649 (2007).

206. Judge, A.D., Bola, G., Lee, A.C. & MacLachlan, I. Design of noninflammatory synthetic siRNA mediating potent gene silencing in vivo. *Mol Ther* **13**, 494-505 (2006).

207. Lund, J.M. *et al.* Recognition of single-stranded RNA viruses by Toll-like receptor 7. *Proc Natl Acad Sci U S A* **101**, 5598-5603 (2004).

208. Chiu, Y.L. & Rana, T.M. RNAi in human cells: basic structural and functional features of small interfering RNA. *Mol Cell* **10**, 549-561 (2002).

209. Prakash, T.P. *et al.* Positional effect of chemical modifications on short interference RNA activity in mammalian cells. *J Med Chem* **48**, 4247-4253 (2005).

210. Amarzguioui, M., Holen, T., Babaie, E. & Prydz, H. Tolerance for mutations and chemical modifications in a siRNA. *Nucleic Acids Res* **31**, 589-595 (2003).

211. Braasch, D.A. *et al.* RNA interference in mammalian cells by chemically-modified RNA. *Biochemistry* **42**, 7967-7975 (2003).

212. Somoza, A., Chelliserrykattil, J. & Kool, E.T. The Roles of Hydrogen Bonding and Sterics in RNA Interference. *Angew Chem Int Ed Engl* (2006).

213. Narayanan, S., Dalpke, A.H., Siegmund, K., Heeg, K. & Richert, C. CpG oligonucleotides with modified termini and nicked dumbbell structure show enhanced immunostimulatory activity. *J Med Chem* **46**, 5031-5044 (2003).

214. He, G. *et al.* Immunostimulatory CpG oligonucleotides form defined three-dimensional structures: results from an NMR study. *ChemMedChem* **2**, 549-560 (2007).

215. Hughes, A.L. & Piontkivska, H. Functional diversification of the toll-like receptor gene family. *Immunogenetics* **60**, 249-256 (2008).

216. Dolan, J. *et al.* The extracellular leucine-rich repeat superfamily; a comparative survey and analysis of evolutionary relationships and expression patterns. *BMC Genomics* **8**, 320 (2007).

217. Stetson, D.B., Ko, J.S., Heidmann, T. & Medzhitov, R. Trex1 prevents cell-intrinsic initiation of autoimmunity. *Cell* **134**, 587-598 (2008).

218. Koski, G.K. *et al.* Cutting edge: innate immune system discriminates between RNA containing bacterial versus eukaryotic structural features that prime for high-level IL-12 secretion by dendritic cells. *J Immunol* **172**, 3989-3993 (2004).

219. Hornung, V. *et al.* Quantitative expression of toll-like receptor 1-10 mRNA in cellular subsets of human peripheral blood mononuclear cells and sensitivity to CpG oligodeoxynucleotides. *J Immunol* **168**, 4531-4537 (2002).

220. Rozenski, J., Crain, P.F. & McCloskey, J.A. The RNA Modification Database: 1999 update. *Nucleic Acids Res* **27**, 196-197 (1999).

221. Yasuda, K. *et al.* Endosomal translocation of vertebrate DNA activates dendritic cells via TLR9-dependent and -independent pathways. *J Immunol* **174**, 6129-6136 (2005).

222. Stetson, D.B. & Medzhitov, R. Recognition of cytosolic DNA activates an IRF3-dependent innate immune response. *Immunity* **24**, 93-103 (2006).

223. Hornung, V. *et al.* AIM2 recognizes cytosolic dsDNA and forms a caspase-1-activating inflammasome with ASC. *Nature* (2009).

224. Gondai, T., Yamaguchi, K., Miyano-Kurosaki, N., Habu, Y. & Takaku, H. Short-hairpin RNAs synthesized by T7 phage polymerase do not induce interferon. *Nucleic Acids Res* **36**, e18 (2008).

225. Myong, S. *et al.* Cytosolic Viral Sensor RIG-I Is a 5'-Triphosphate-Dependent Translocase on Double-Stranded RNA. *Science* (2009).

7 Publications and Presentations

7.1 Publications

Eberle F, Sirin M, Binder M, Dalpke AH.

Bacterial RNA is recognized by different sets of immunoreceptors.

Eur. J Immunol. in revision

Eberle F, Giessler K, Deck C, Heeg K, Peter M, Richert C, Dalpke AH.

Modifications in small interfering RNA that separate immunostimulation from RNA interference.

J Immunol. 2008 Mar 1;180(5):3229-37.

Peter M, Bode K, Lipford GB, **Eberle F**, Heeg K, Dalpke AH.

Characterization of suppressive oligodeoxynucleotides that inhibit Toll-like receptor-9-mediated activation of innate immunity.

Immunology. 2008 Jan;123(1):118-28.

Järve A, Müller J, Kim IH, Rohr K, MacLean C, Fricker G, Massing U, **Eberle F**, Dalpke A, Fischer R, Trendelenburg MF, Helm M.

Surveillance of siRNA integrity by FRET imaging.

Nucleic Acids Res. 2007;35(18):e124.

Hellwage J, **Eberle F**, Babuke T, Seeberger H, Richter H, Kunert A, Härtl A, Zipfel PF, Jokiranta TS, Józsi M.

Two factor H-related proteins from the mouse: expression analysis and functional characterization.

Immunogenetics. 2006 Nov;58(11):883-93.

7.2 Presentations

Poster: Relevance of RNA-mediated immunostimulation for RNA-Interference

Florian Eberle, Kerstin Giessler, Klaus Heeg, Clemens Richert and Alexander Dalpke.

4th meeting of the society of therapeutic oligonucleotides, Boston, USA, September 2008

Talk: Defining Substrate Specificities of RIG-I and MDA5

Florian Eberle, Marco Binder, Ralf Bartenschlager and Alexander Dalpke.12. Symposium "Infektion und Immunabwehr" ; Burg Rothenfels, Germany; March 2008

Poster: Relevance of RNA-mediated immunostimulation for RNA-Interference

Florian Eberle, Kerstin Giessler, Klaus Heeg, Clemens Richert and Alexander Dalpke.

3rd meeting of the society of therapeutic oligonucleotides, Berlin, Germany, October 2007

Talk: Relevance of RNA-mediated immunostimulation for RNA-Interference (RNAi)Florian Eberle, Clemens Richert, Klaus Heeg, Kerstin Giessler and Alexander Dalpke.

Congress of the Society of Innate Immunity on Integration of Innate Immunity and Biological Systems“; Ankara, Turkey, May 2007

Poster: Relevance of RNA-mediated immunostimulation for RNA-Interference

Florian Eberle, Mehtap Sirin, Clemens Richert and Alexander Dalpke.

Spring School of Immunology, Ettal, Germany, February 2007

8 Acknowledgment

Für die außerordentlich gute Betreuung während meiner Doktorarbeit geht ganz besonderer Dank an **Prof. Dr. Alexander Dalpke**, der mir mit wissenschaftlichen Ratschlägen und bei Problemen wirklich immer zur Seite stand. Außerdem danke ich für seinen entspannten Umgang gegenüber unkonventionellen Ideen und Arbeitszeiten, die das Arbeiten nach eigenen Vorstellungen erst ermöglicht haben. Kurz gesagt, er war ein toller Chef.

Herrn **Prof. Dr. Klaus Heeg** danke ich für die Aufnahme in seine Abteilung. Außerdem für die extrem guten Arbeitsbedingungen und die Möglichkeit an zahlreichen Kongressen und Fortbildungen teilzunehmen.

Herrn **Prof. Dr. Ralf Bartenschlager** danke ich für die Begutachtung meiner Arbeit sowie seine Teilnahme an meinem PhD-Komitee. An **Prof. Dr. Rüdiger Hell** und **PD Dr. Mark Helm** geht herzlicher Dank für ihre Funktion als Prüfer im Rahmen meiner Disputation.

Danken möchte ich außerdem allen Personen, die entweder wissenschaftlich oder technisch an meiner Arbeit mitgewirkt haben:

Prof. Dr. Clemens Richert und **Kerstin Giessler** für die Synthese von modifizierten RNA oligonukleotiden.

Mehtap Sirin, **Alena Grebe**, **Paulina Paszkiewicz**, und **Ole Wicht,** die durch ihre medizinische Doktorarbeit, Bachelorarbeit oder Praktika massgeblich an dem Projekt der bakteriellen RNA Erkennung mitgewirkt haben.

Dr. Marco Binder für die gute Zusammenarbeit am Projekt der Ligandenerkennung von RIG-I. Das gemeinsame Arbeiten hat neben dem wissenschaftlichen Erfolg auch sehr viel Spaß gemacht. Außerdem danke ich **Stefan Seitz** und **Dr. Norbert Mücke** für die Unterstützung des Projekts und die gute Einführung in neue Arbeitstechniken.

Und natürlich geht Dank an alle **Mitarbeiterinnen und Mitarbeiter der Abteilung für Hygiene und Medizinische Mikrobiologie** für die gute und chillige Atmosphäre in und außerhalb des Labors. Besonders hervorheben möchte ich dabei **Dr. Konrad Bode** und **Dr. Mirjam Peter** für die gute gemeinsame Zeit und dafür, dass sie mir immer mit Hilfe zur Seite standen. Außerdem danke ich **Julia Strebovsky** für das Korrekturlesen meiner Arbeit und **Adelina Dillmann** ohne deren Hilfe ich im Labor wahrscheinlich deutlich weniger hätte leisten können.